A DISSERTATION FOR THE DEGREE OF DOCTOR OF PHILOSOPHY

The Role of Cellulose Nanofibrils in Structure Formation and Drying Stress Development of Pigment Coating Layer

종이 도공층 구조형성 및 건조응력 발현에 미치는 셀룰로오스 나노피브릴의 역할

Advisor Professor: Dr. Hak Lae Lee

by Kyudeok Oh

PROGRAM IN ENVIRONMENTAL MATERIALS SCIENCE
DEPARTMENT OF FOREST SCIENCES
GRADUATE SCHOOL
SEOUL NATIONAL UNIVERSITY

February, 2017

ABSTRACT

The Role of Cellulose Nanofibrils in Structure Formation and Drying Stress Development of Pigment Coating Layer

Kyudeok Oh

Program in Environmental Materials Science

Department of Forest Sciences

Graduate School

Seoul National University

Coating structure is one of the important factors determining pigment coated paper quality including printability. The structure is influenced by the type or composition of pigment, binder, and additives. Even though the pigment and binder determine the structure of the coating layer most significantly, a small amount of additives can also influence the structure. In this study, cellulose nanofibrils (CNF) were used as an additive of the coating color. CNF was selected as an additive because it is a potential material to thicken the coating color. The effect of CNF on the coating color and coating layer was suggested compared to carboxymethyl cellulose (CMC) that has been used as a traditional thickener. Initially, the rheological properties of the coating color were investigated to understand the effect of CNF on the microstructure of the

coating color. Drying kinetics was evaluated using the multispeckle-diffusing wave spectroscopy (MS-DWS) technique to suggest structure formation in the coating layer. Stress development was evaluated to investigate the effect of CNF on shrinkage of the coating layer. In addition, surface characteristics of the coating containing CNF were evaluated. Finally, CNF was applied to coated paper to investigate the change of in the optical, structural, and absorption properties of the coated paper.

CNF coating showed lower elastic behavior than CMC coating because there was no interaction between the particles in the coating color containing CNF. The microstructure of the coating color influenced the drying process. The particles in the CNF coating color moved freely because CNF did not form a structural network and increase the viscosity of the aqueous phase. The movement of the coating components, however, was greatly restricted by CMC because it created a network structure and increased the viscosity of the aqueous phase. CNF made the coating layer porous in a different manner than CMC. The voluminous characteristics of CNF made the coating layer porous.

CNF coating showed different stress development behavior compared to CMC. The drying stress of the coating layer increased with the addition of CMC because of the loosely packed structure of CMC coating, which increased the total shrinkage of the coating layer after the solidification point and the shrinkage of the precipitated CMC during drying. The stress of the CNF coating, however, was lower than that of the CMC coating because of the less structured CNF coating and the low shrinkage characteristics of

cellulose. The CNF coating showed much lower gloss than the CMC coating due to its water absorbing characteristics. The swollen CNF caused a rough surface because the shrinkage of CNF proceeded until the end of the drying process.

The CNF coating gave lower coated paper gloss than that of the CMC coating due to non-uniform shrinkage, which came from the gel-like structure of CNF. To improve the gloss of the coated paper, the coated paper was made with a low coat weight and under high shear rate. The gloss and roughness of the coated paper were similar for the CNF and CMC coatings. In addition, the surface defects in the coated paper diminished. The CNF coating greatly improved ink absorption compared to CMC coating in the ink absorption test and the modified Vandercook press test by forming a porous coating layer due to its low shrinkage characteristics. The small amount of CNF addition can promote the absorption rate and uniformity of coated paper without changing the material properties.

Keywords: Pore structure, drying stress, ink absorption, rheological properties, cellulose nanofibrils, carboxymethyl cellulose

Student number : 2012-30314

CONTENTS

Chapter 3

Chapter 4

Effect of Cellulose Nanofibrils on Surface and Absorption Characteristics of Coated Paper ····· 105

List of Tables

List of Figures

Chapter 1

Introduction

1. Introduction

Suspensions composed of particles and binders are widely used in various industries to manufacture diverse products such as papers, paints, batteries, and solar cells. In the case of the paper coating industry, the suspension composed of the pigment and binder commonly called coating color, is applied to the surface of dried base paper to manufacture coated paper. The application of a coating color onto base paper improves the appearance and printability of paper. The paper coating industry uses many mineral pigments including kaolin clay and ground calcium carbonate (GCC) as main pigments. Other minor pigments such as precipitated calcium carbonate (PCC), plastic pigment, and titanium dioxide, which occupy less than 10% of the total amount of the pigment, are being used. Since the pigments lack adhesion, several types of binding materials are used to make the pigment adhere each other or to the base paper. Styrene-butadiene or acrylate latex and starch are widely used binders in the paper coating industry because they have good binding power and economic advantages.

The prime purpose of paper coating is to improve the printability and visual appearance of paper. This is possible because the size of the coating pigment and binder is far less than the papermaking fibers. The printability of coated paper depends on the structure of the coating layer and the structure is determined by the type and ratio of the pigment and binder used; this is because these are the main ingredients of the coating suspension (Table 1-1).

When the pigment volume concentration is higher than the critical pigment volume concentration (CPVC), void spaces are present for light scattering, and decrease as binder faction increases since the binder fills up the interparticular voids. The size, size distribution, and shape of the pigments influence the structure of the porous coating layer because these properties affect pigment packing in the coating layer. The film forming behavior of the latex binder varies by the type and glass transition temperature (Tg) of the latex, which in turn changes the structure of the coating layer.

Table 1-1. Typical formulation of coating color

Formulation of coating color		
Main component	Pigment, pph	100
	Binder, pph	5 – 20
Minor component	Additive, pph	Less than 1 pph (each components)

Even though pigments and binders are the major components of the coating formulation, some additives that must be used have critical impact in coating runnability and coated paper properties. Thickener is one of the essential minor components because it controls the rheological properties and water retention of the coating color, which are two critical properties to control coating runnability. Several studies have reported the effect of thickeners such as carboxymethyl cellulose (CMC), polyvinyl alcohol (PVA), and hydroxyethyl cellulose (HEC) on the rheological properties of the coating

color (Fadat et al. 1988; Mcgenity et al. 1992; Husband 1998; Wallström and Järnström 2004; Choi et al. 2015). These conventional rheology modifiers are water-soluble polymers that increase the viscosity of the aqueous phase. It is also known that some thickeners change the coating structure since they can change the colloidal interactions of the coating components.

There are recent attempts to use cellulose nanofibrils (CNF) as a thickener of the coating color because it forms a gel-like structure in the suspension and shows high shear thinning behavior. Even though CNF is not a water-soluble polymer and may not have adsorption propensity onto other coating components, it can influence the water retention property and the low and high shear viscosity, which are useful properties as a coating additive. The effect of CNF on coating color rheology and coated paper has been reported in several studies (Dimic-Misic et al. 2013; Salo et al. 2015; Nazari and Bousfield 2016). The studies indicate that CNF influences the rheological properties of coating color in a different manner than the traditional thickeners like CMC. CNF coatings showed better leveling characteristics because of high flow mobility compared to the CMC coatings (Dimic-Misic et al. 2013), and this is identified by the gloss of the coated paper (Salo et al. 2015).

The influence of the thickener on the structure of the coating layer has not received much attention because the amount of thickener in the coating color is usually less than 1 pph. Few studies were performed to elucidate the effect of the dissolved thickener such as CMC and PVA on the consolidation process

of the coating layer (Du et al. 2014; Zang et al. 2010). The effect of thickener on the structure of the coating layer, drying stress development, and printing properties has not been investigated yet.

If we can change the coating structure with the use of a small amount of thickener, it will be useful for fine-tuning the coating structure and thereby the properties of coated paper. This is very advantageous if we can change the coating layer properties without changing the main component in a coating formulation. This is especially true if there is a new material like CNF that can be used as a coating additive.

2. Objectives

The objective of this study is to understand the effect of CNF on the rheological properties of coating color, drying stress development in the coating layer, and final structure of the coating layer. Finally, an attempt was made to elucidate the effect of CNF on the properties of coated paper including printing properties and print mottle. To understand the role of CNF as an additive in pigment coating, CMC was used as reference additive. A comparative study on rheology, structure forming, drying stress development, and final coating structure and property was performed with these two additives.

Effects of CNF and CMC on the rheological properties of coating color were evaluated using a stress-controlled rheometer. Multispeckle-diffusing wave spectroscopy and beam deflection method were used to investigate particle diffusion in the wet coating layer and stress development during drying, respectively. The porosity and pore size distribution of the coating layer were analyzed using mercury porosimetry.

In this thesis, coating structure formation, drying stress development, and coating structure and printing properties were investigated. In the first part of this study, the effect of CNF on the formation of the coating layer structure was examined and compared with CMC. This was achieved by analyzing the rheological properties of coating color, particle diffusivity in the wet coating

layer, and structure of the dried coating layer.

In the second part, stress development in the coating layer during ambient drying was investigated. The aim of the second part is to understand the relationship between stress development and shrinkage of the coating layer during drying. The change in surface characteristics was evaluated to elucidate the effect of CNF on the coating layer surface.

The aim of the last part was to investigate the effect of CNF on the surface and absorption characteristics of the coated paper with a novel technique developed herein.

3. Literature reviews

3.1 Rheological properties of coating color

The rheological properties of the coating color affect the runnability of the coating process and quality of the coated paper. The rheological properties of the coating color depend on a number of different factors such as the shape and size distribution of pigments, type and content of binders and thickeners, etc. Plate-shaped particles have a larger volume than round particles when rotating in suspension; therefore, incorporation of plate pigments increases the viscosity of the coating color (Roper 2000). A narrow particle size distribution also increases the viscosity (Roper 2000), because it is not possible to pack pigments that have a narrow particle size distribution compactly. Water-soluble binders such as starch and protein increase the viscosity of the coating color more than a latex binder (Bruun 2000) because they occupy more volume in the aqueous coating.

Water-soluble polymers such as CMC, PVA, and HEC have been used to control the rheological properties of the coating color. Non-absorbing (partly absorbed on clay) CMC, which has been used as a traditional thickener, can flocculate the coating components increasing the viscosity and elastic component of the coating color (Fadat et al. 1988; Mcgenity et al. 1992; Whalen-Shaw and Gautam 1995; Husband 1998; Wallström and Järnström 2004; Choi et al. 2015). PVA, which is a nonionic polymer, changes the

rheological properties of the coating color in a different way. Unlike CMC, PVA adsorbs onto pigment particles via hydrogen bonding and gives steric hindrance stabilization to the pigment particles. When the amount of PVA addition exceeds the adsorption capacity of the coating pigments, flocculation of the particles results from the bridging mechanism of PVA (Choi et al. 2015).

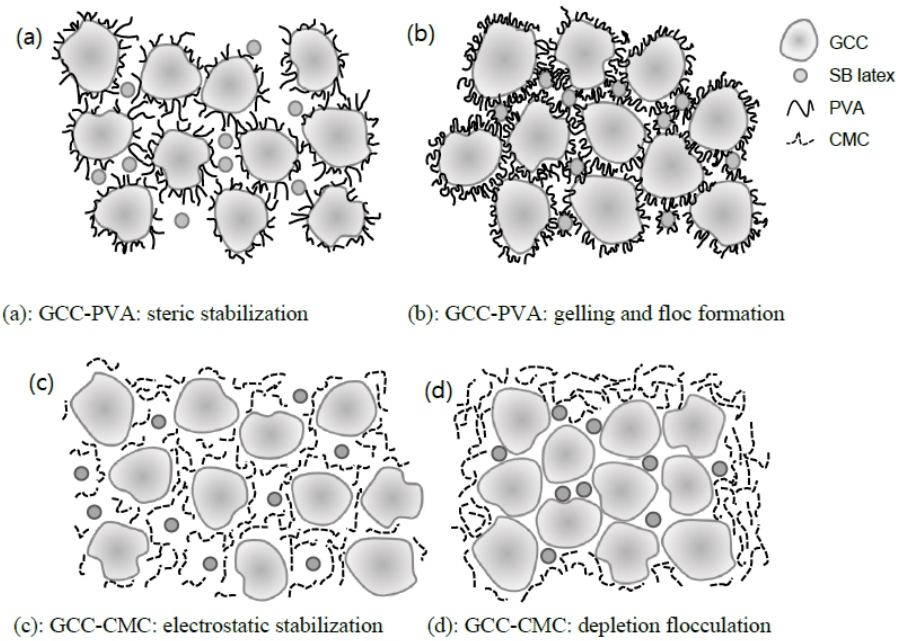

Fig. 1-1. Particles interaction depending on types and amount of soluble polymer (Choi et al. 2015).

CNF is one of the potential thickeners for the coating color due to its highly water absorbing property, i.e. gel-like structure, and shear thinning behavior in the suspension. Gel-like structure and water absorbing property of CNF may be helpful in improving the water retention of coating colors, and shear-thinning property improves runnability for high-speed coating. CNF coating showed lower elastic component and higher leveling characteristics than CMC coating because it does not cause flocculation of the coating components (Dimic-Misic et al. 2013; Salo et al. 2015). This leveling property may be helpful to obtain a smoother surface after coating.

The water retention of the coating color is one of the most important factors affecting the runnability and coated paper quality. For example, a coating color that shows poor water retention often gives coating defects such as streaks on the coated paper. Several factors like pigment shape and the use of water-soluble polymers affect the water retention property of coating colors. The plate-shaped pigment can improve water retention because platy pigments provide flow resistance to the aqueous phase (Lehtinen 2000) due to their tendency to align horizontal to the base paper surface. Water retention also increases with the addition of water-soluble polymers such as CMC, PVA, and starch because they tend to increase the viscosity of the aqueous phase (Lehtinen 2000).

3.2 Consolidation of coating layer

Consolidation of the coating layer has been investigated by measuring the change in the gloss and reflectance of the wet coating layer during drying (Watanabe and Lepoutre 1982; Lepoutre 1989; Larrondo and Lepoutre 1992; Al-Turaif and Lepoutre 2000; Zang et al. 2010; Du et al, 2014). Watanabe and Lepoutre (1982). Watanabe and Lepoutre (1982) showed that there were two distinct optical property changes due to two important changes occurring in the coating layer during drying (Fig. 1-2). The first important point is the moment when a sudden drop of gloss occurs. They called this the first critical concentration (FCC). After the application of a color, a continuous water film was present on the wet coating surface and this provided high reflection. The gloss of the wet coating layer slowly increased until the first critical concentration (FCC) because the reflective index of the pigment and latex is higher than that of water. After that, a sudden drop in the gloss occurred because the surface of the wet coating is no longer continuous. In other words, menisci start to form on the coating surface at FCC.

The reflectance of the coating layer decreased first because the gaps between the particles (pigment and latex) are closed and become less efficient in scattering light by the evaporation of water. At the second critical concentration (SCC), a sudden increase in reflectance occurs because the water-filled space is replaced with air, which creates a large difference in reflective index. Furthermore, SCC was characterized by the change in the

gloss of the wet coating layer. The point at which the gloss of the wet coating reaches a nearly constant value corresponds with SCC, and this indicates that the surface structure no longer changes after SCC. In other words, air replaces interparticular water in the coating layer after SCC.

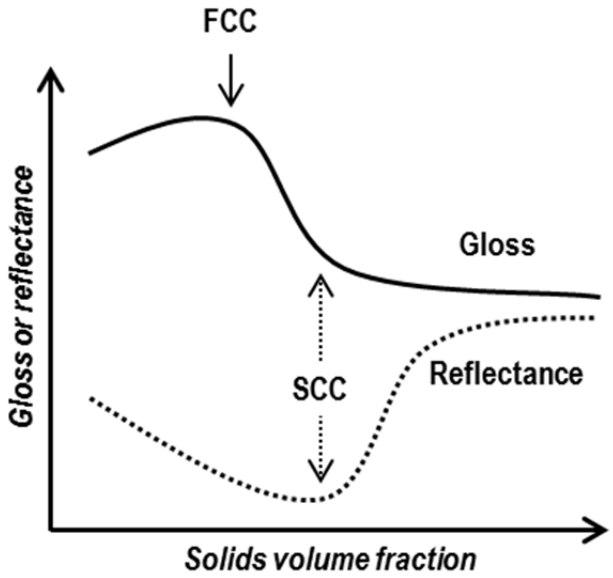

Fig. 1-2. Optical changes of coating layer during drying.

The critical concentrations of wet coating change based on the properties of the coating components like binder type, amount, and colloidal interaction. The effects of the binder conditions on the critical concentrations are shown in Table 1-2. Obviously, starch gives a higher shrinkage and lower void fraction in the coating, which can be attributed to the shrinking property of the water-soluble starch binder. In addition, non-filming latex gives higher porosity and lower shrinkage during drying, which results in higher gloss. Non-filming latex also shows a smaller difference between SCC and FCC when compared to filming latex.

Table 1-2. Coating composition at the critical concentrations (Watanabe and Lepoutre 1982)

Binder (20 pph)	Critical concentration, vol%		Void fraction of clay coatings	Shrinkage, %	75º Gloss, %
	FCC	SCC			
S/B nonfilming latex	58.0	64.0	0.37	11.9	75.0
S/B filming latex	61.5	79.0	0.21	45.5	46.5
Vinylacetate latex	57.0	75.0	0.26	39.5	36.0
Polyacrylic latex	62.0	77.0	0.24	36.8	42.0
S/B filming latex / oxidized starch (1:1)	58.0	77.0	0.22	47.6	30.5
Oxidized starch	53.5	74.0	0.20	57.0	26.5

Water-soluble polymers such as CMC, PVA, and oxidized starch affect consolidation of the coating layer. Du et al. (2014) reported that the volume fraction of the coating layer at the FCC decreased; they attributed this to the slow water evaporation rate by the polymers and the formation of a strong three-dimensional structure with pigment in the coating suspension and ionic crosslinks between the negative carboxylic chains. At the same polymer concentration, CMC shows the lowest volume fraction at the FCC because CMC solution evaporates less water than PVA and starch solutions (Du et al. 2014). However, it is not logical enough to correlate the water evaporation rate to the structure-forming property. For instance, starch binder has a lower evaporation rate than latex binder but it has a lower FCC than latex. This suggests that some other structure-forming property plays a major role in FCC change.

Larrondo and Lepoutre (1992) report consolidation of the coating layer in various latex binder types and fractions. They showed that the addition of latex to a clay suspension led to the formation of bulkier structures when the latex interacted with the clay. After centrifugation, however, the interacting latex gave only slightly bulkier structures than the non-interacting latex. In the dry coatings, the effect of capillary forces on the structure was controlled by the composition of the coating suspensions: a denser structure formed when the latex content increased and slightly bulkier structures formed when the latex interaction with clay increased. The most important result of Larrondo and Lepoutre (1992) is that the volume fractions of maximum packing in the

dry coatings containing non-interacting latex correlated quite well with the values obtained from the flow curves. On the other hand, the values obtained in coatings containing an interacting latex were much higher than those given by the flow curves, suggesting that the bulky structures formed in the aqueous suspensions collapse upon drying.

Similar results were obtained when the pH changes. The FCC slightly decreases with a decrease in pH of the coating color because the zeta potential of the pigment changes with pH (Watanabe and Lepoutre, 1982). The effect of pigment type and blending on the FCC and SCC was evaluated (Lee et al. 1994b; 1995) and it was shown that blocky particles such as GCC showed higher solid volumes in FCC and decreased the shrinkage of the coating layer between the FCC and SCC.

Multispeckle-diffusing wave spectroscopy (MS-DWS) is one of the methods that can evaluate the consolidation process of the coating layer. The principle of this method is to measure the interfering backscattered waves derived from the Brownian motion of the particles or porous structure of the coating layer. Several studies used this principle to evaluate the viscoelastic properties of pullulan solutions and latex suspension (Hemar and Pinder 2006; Narita et al. 2013) and the film formation of paint and latex suspensions (Brunel et al. 2007; Brun et al. 2008; Durand et al. 2010; Lee et al. 2013). The process of latex film formation during drying is shown in Fig. 1-3 as a function of drying time. The particulate dispersion gives high speckle rates when all particles are

well dispersed because active Brownian motion is possible for all particles. When the particles start to contact at higher solid levels, more or less stable speckle rates are obtained until complete immobilization of all particles.

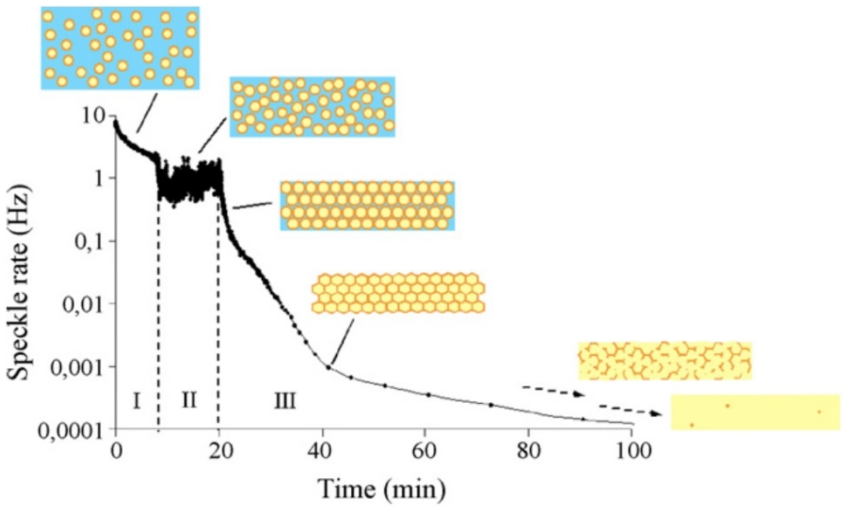

Fig. 1-3. Speckle rate of latex film during drying (Brun et al. 2008).

3.3 Stress development of coating layer

Upon drying, the wet coating layer shrinks due to the evaporation of solvent, coalescence, and cross-linking. Constrained shrinkage of the suspension on a rigid substrate develops tensile stress in the coating layer. Eventually, the coating layer is deflected by the bending moment. Further, the developed tensile stress may cause defects such as cracking, delamination, and curling in the coating layer. Thus, understanding the stress development is important for minimizing drying defects.

The stress development of the wet coating layer changes due to various factors including material property, formulation of the suspension, and drying condition. The drying stress has been explored in various particulate systems (Chiu et al. 1993; Chiu and Cima 1993; Lewis et al. 1996; Kiennemann et al. 2005; Guo and Lewis 1999; Martinez and Lewis 2002; Kim et al. 2009; 2010; 2011; Lim et al. 2015; Laudone et al. 2004; Wedin et al. 2004; 2005). In the coating layer composed of non-deformable particles, the capillary force due to its porous structure develops the drying stress. After stress development due to the capillary force, the drying stress is relaxed and reaches a stress-free state. Thus, stress development in the non-deformable particle system depends on the pore structure and surface tension of the solvent (Lim et al. 2015; Wedin et al. 2004; 2005).

On the other hand, stress development of a polymer solution shows very different behavior than the non-deformable particle system. There is no stress due to the capillary force because it forms a continuous phase and the drying stress increases with the evaporation of the solvent. A high-Tg polymer shows higher drying stress than a low-Tg polymer because shrinkage of the polymer film beyond the solidification point increases with the Tg (Wedin et al. 2005).

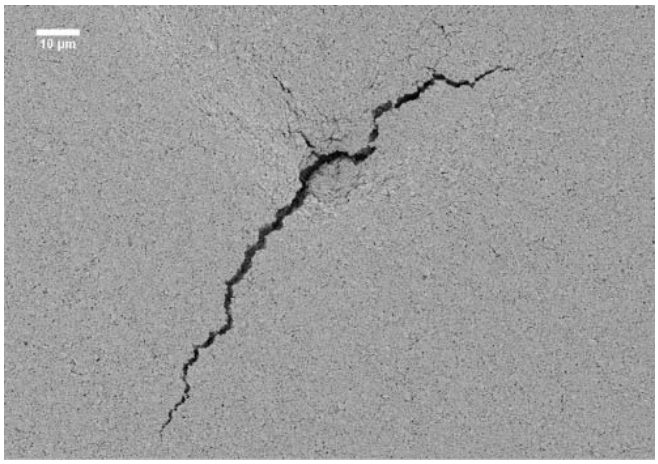

Fig. 1-4. Cracking in coating layer during drying.

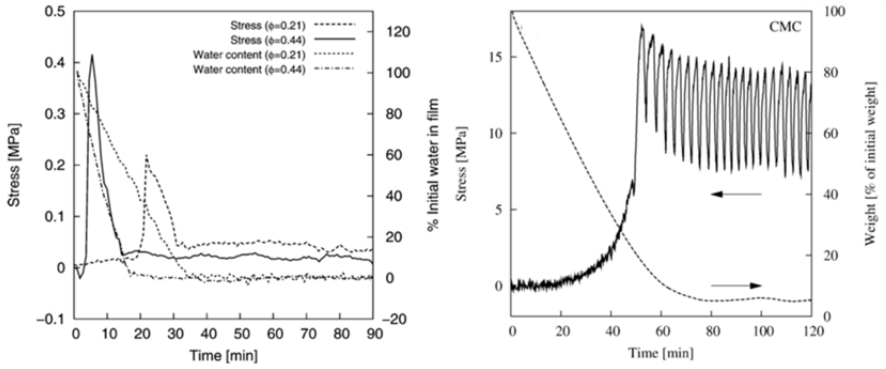

Fig. 1-5. Drying stress non-deformable particle (calcium carbonate) and polymer (carboxymethyl cellulose) film (Wedin et al. 2005).

The coating layer containing non-deformable particles and binder changes the behavior of the stress development upon drying. In this system, residual stress is introduced because the binder can bridge between the non-deformable particles and form a film in the coating layer (Kiennemann et al. 2005; Kim et al. 2009; 2010; 2011; Lim et al. 2015; Wedin et al. 2004; 2005). The amount of binder is important in stress development. Higher binder content increases the drying stress because more binder can make more bridges between the non-deformable particles (Lim et al. 2015); thus, the shrinkage of the coating layer increases beyond the solidification point (Ludone et al. 2004). Several studies report that residual drying stress increased with the addition of a binder (Martinez and Lewis 2002; Lim et al. 2015).

The film forming behavior of the binder is critical in the stress development of the coating layer. When the drying temperature is enough to lead to film formation of the binder, a high-Tg binder increases the drying stress of the coating layer. When the drying temperature is not high enough to lead to film formation, stress relaxation develops in the coating layer (Wedin et al. 2004). A soluble polymer like starch increases the drying stress compared to the latex binder at the same coating formulation (Laudone et al. 2004). Starch shrinks much more than the latex particle due to its low degree of crosslinking between polymer chains.

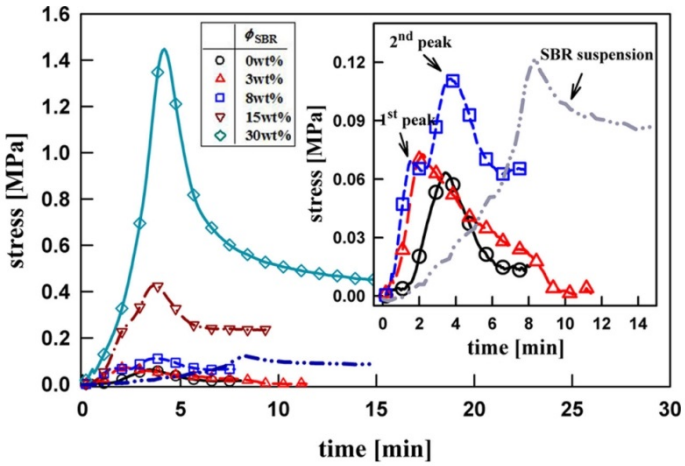

Fig. 1-6. Drying stress of graphite and latex system in accordance with latex content (Lim et al. 2015).

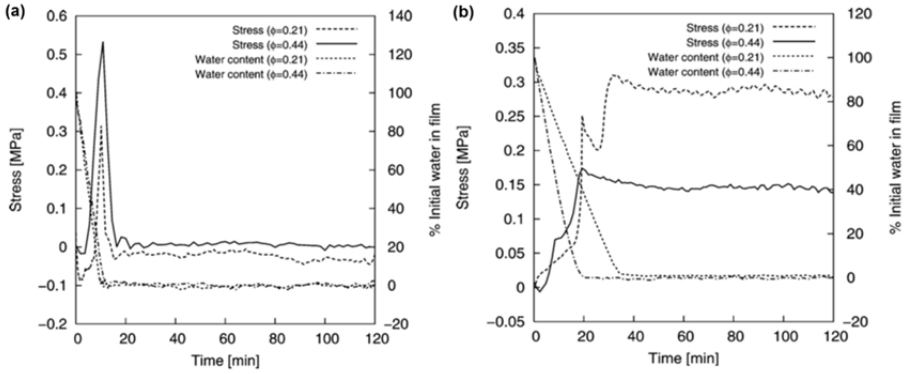

Fig. 1-7. Drying stress depending on latex deformability (Wedin et al. 2004). (a) rigid latex (high Tg), (b) soft latex (low Tg).

3.4 Absorption characteristics and mottle of coated paper

Absorption characteristics of the coated paper mainly affect printability. Back trap mottle, which is one of the most frequent defects in coated paper, is attributed to the non-uniform absorption of ink into coated paper. Back trap mottle generally occurs at the second printing nip in a multi-color printing system. When the paper, printed at the first printing nip, passes under the second printing nip, an ink layer is retransferred to the blanket roll of the second printing unit. At this moment, the non-uniform immobilization of the first printing ink causes non-uniform ink transfer to the rubber blanket of the second printing unit, causing back-trap mottle. The mechanism of the ink back trap is shown in Fig. 1-8.

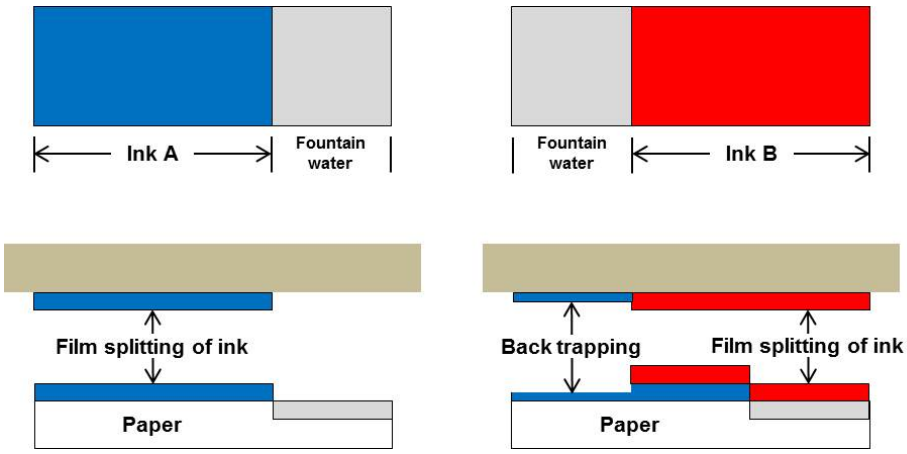

Fig. 1-8 Scheme of ink back trapping (Lee 2008).

Ink absorption on the coated paper is governed by surface characteristics, which are affected by several factors such as material properties, formulation of coating color, coat weight variation, drying condition, and calendaring. The particle size and shape of the pigment influences surface characteristics of the coated paper. Fine and coarse sized pigments cause fine and large pores in the coating layer, respectively (Risio and Yan 2006; Ridgway and Gane 2007). The particle size distribution is also a factor affecting the surface structure of the coated paper by influencing pigment packing. A broad particle size distribution gives low porosity and pore density because it gives tight packing of the pigment (Al-Turaif and Bousfield, 2005; Risio and Yan 2006; Larsson et al. 2007; Vidal 2008). Therefore, pigment blending can be a method to form the desired coating structure (Lee 1992; Lee 1994a; Hiorns et al. 2003; Preston et al. 2007; McCoy 1998; Pöhler et al. 2006; Kim and Lee 2001). Porosity and pore density of the coating layer are reduced by an increase in binder content due to the pore filling tendency of binders (Pan et al. 1996; Lafon and Trannoy 2006; Gane et al. 2009; Songok et al. 2012).

Surface variation of the coating base stock results in local coat weight variation and the variation in coat weight is known as the principal cause of print mottle. Several mechanisms such as binder migration, consolidation of coating layer, and calendaring have been reported to cause non-uniform ink absorption; these are influenced by the coat weight variation. Binder migration causes non-uniform surface porosity because of increased sealing of the coating surface at high coat weight regions upon drying, which arises from

higher latex particle migration from the bulk to the surface of the coating layer in the high coat weight region than in the low coat weight region (Hagen 1989).

Non-uniform shrinkage of the coating layer has been suggested to cause non-uniform porosity in the coating layer surface (Groves et al, 1993; Engström, 2008). Deformation of filter cake, which is considered a viscoelastic composite, is rate dependent. The shrinkage of filter cake is faster in the low coat weight region than at high coat weight. The deformation of the filter cake is more in the high coat weight region than at low coat weight. The difference of deformation depending on the coat weight variation led to non-uniform porosity in the coating layer surface (Groves et al, 1993; Engström, 2008). A closed area, which has fewer pores absorbing printing ink, is introduced in the low coat weight region by calendaring. Non-uniform distribution of the closed area is linked to print mottle (Chinga and Helle, 2003). Ozaki et al. (2008) confirm the importance of uniform coating layer thickness because low coat weight variation leads to uniform ink absorption of the coated paper.

Ragnarsson et al. (2013) investigated the cause of porosity variation by measuring the change in reflectance of the coated paper before and after calendaring. When carboxymethyl cellulose and dextrin are used with styrene-butadiene (S/B) latex, the porosity variation is associated with calendaring. When oxidized starch is used with S/B latex, however, back-trap mottle is caused by consolidation of the coating layer during drying.

Several methods to evaluate absorption uniformity of coated paper have been reported. Shen et al. (2005) introduced a liquid-bridge probe test to evaluate absorption uniformity by analyzing the absorption amount as a function of absorption time. Purfeerst and Van Gilder (1991) reported a modified Vandercook press test. First, an unpigmented low-tack ink is applied on the coated paper. The applied ink tack increased with the increase of absorption time. After a delay, cyan ink is printed on the ink layer. Uniformity of the trapped cyan ink depends on the absorption uniformity of the low-tack ink.

Chapter 2

Rheological Properties, Drying Kinetics and Pore Characteristics of the CNF and CMC Coating Layers

1. Introduction

Thickener is the one of the most important additives in a paper coating formulation because it controls the rheological and water-holding properties of the coating color that are critical for optimization of the coating process. CMC has been used as a traditional thickener to increase the viscosity and water retention of the coating color. Recently, synthetic thickeners are widely used to control the rheology of the coating color. The principal properties of CMC and synthetic thickeners as rheological modifiers lie in their water-holding capability deriving from their hydrophilic character and flocculating action toward pigment particles, especially for clay particles, in the coating color. In particular, it is known that synthetic thickeners have a high affinity for pigment particles; therefore, they form bridges between the pigment particles. The interparticular bridge, however, is temporary and disrupted by exposure to high shear. However, the bridges reform when the shear strain disappears, which helps to improve surface coverage of the coating color.

Recently, there are attempts to use CNF as a thickener in the coating color because of its gel-like structure and shear-thinning behaviors (Dimic et al. 2013). Several studies reported the rheological properties of coating colors containing CNF. The viscosity and viscoelastic behaviors of the coating color prepared with CNF as an additive were analyzed under various evaluation conditions to predict spreading, leveling, and dewatering of the coating color. It has been shown that the effect of CNF is different from that of CMC since it

is not a water-soluble polymeric additive. Most previous studies on CNF have examined the effect of CNF on the rheological properties of the coating color. As shown by Larrondo and Lepoutre (1992), the information obtained from measurements made on the coating suspension cannot always be used to predict the properties of the dry coatings. This suggests that a systematic study to correlate the suspension property with dry coating property is necessary. Thus, there is a clear need to study on the effect of CNF on the drying stress development and structure formation of coating layers, and to correlate it with the suspension property.

The principal aim of this chapter is to investigate the effect of CNF on drying kinetics such as particle diffusion and structure-forming point. The microstructure of a coating color containing CNF was evaluated using a stress-controlled rheometer to see the role of CNF on the suspension property. Drying kinetics of the coating layer was investigated using the MS-DWS technique that measures the Brownian motion of individual particles in the suspension, thereby deriving structural changes of the coating color in both the suspension and the drying state. Furthermore, the pore structure of the dried coating layer was analyzed. Finally, the mechanism of structure formation by CNF was suggested.

2. Experimental

2.1 Materials

Ground calcium carbonate (GCC, setacarb 77K, Omya Korea) was used as a coating pigment. Median size of the GCC was 0.78 μm and the percentage of particles below 2 μm was 98%. Styrene-butadiene (S/B) latex was provided by LG Chem. The size, glass transition temperature and gel content of the S/B latex were 123 nm, -6°C, and 82%, respectively. Carboxymethyl cellulose (CMC) with a degree of substitution of 0.78 (Finnfix 5, CP Kelco, Korea) and cellulose nanofibrils (CNF) were used as additives for coating.

CNF was prepared by grinding bleached Eucalyptus kraft pulp with a grinder (Super Masscolloider, Masuko Co.). Before grinding, the bleached Eucalyptus kraft pulp was pretreated using a laboratory Valley beater to 450 mL CSF. The average size of CNF agglomerates determined at 0.1 wt% was about 3.8 μm, and the zeta potential of CNF was -38.9 mV at pH 9. Water retention value (WRV) of CNF measured in accordance with ISO/DIS 23714 was 6.4 g of water/g of solids. The widths of most CNF were less than 50 nm while some CNF had the width of about 100 nm (Fig. 2-1). As seen in Fig. 2-1, CNF was highly flocculated because of its high length to diameter ratio.

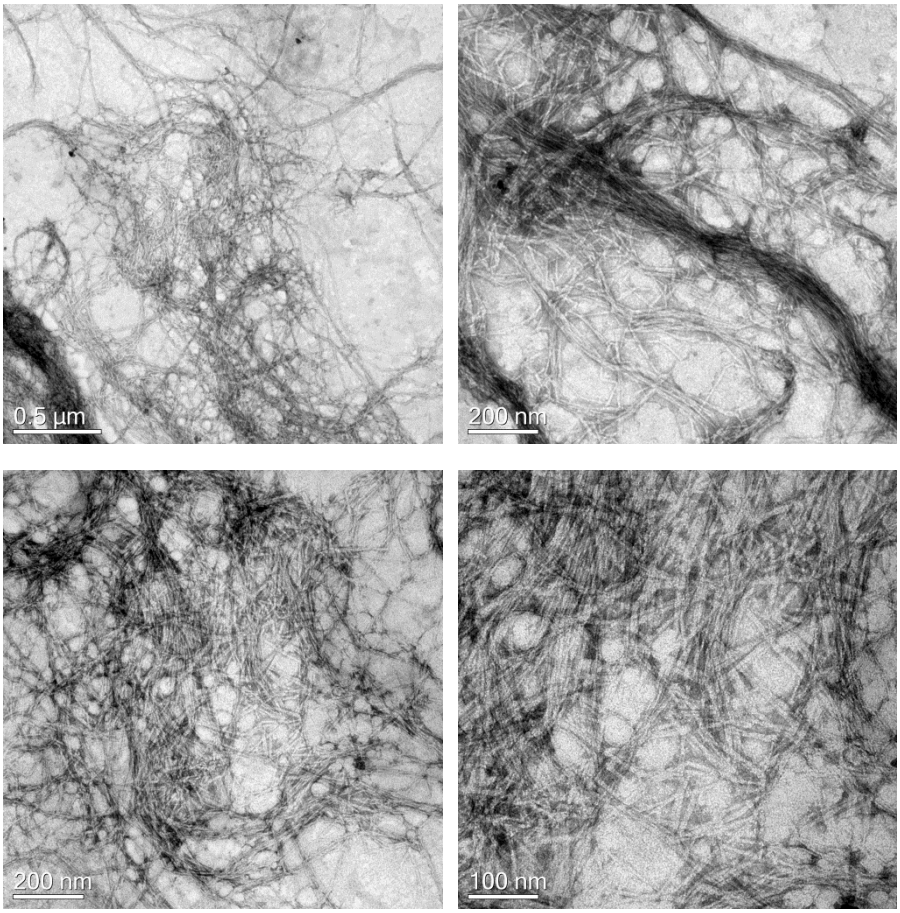

Fig. 2-1. TEM image of CNF.

2.2 Formulation and preparation of coating color

Formulations of the coating colors used in this study are shown in Table 2-1. Coating colors were prepared by mixing S/B latex with pigment slurries and then CMC and CNF were added and thoroughly mixed. Mixing was made for 30 minutes to obtain complete mixing of all ingredients. The gel structure of CNF disappeared after 5 minutes of mixing. Finally, the coating color was filtered using a 100-mesh wire and then pH of the coating color was adjusted to 9.3 with 0.1N of NaOH solution.

Table 2-1. Formulation of coating color

Formulation							
Pigment, pph	Setacarb 77K	100					
Binder, pph	S/B latex	6, 12, 18				12	
Additive, pph	CMC	-	0.1	0.3	0.1	0.5	0.1
	CNF	-	-	-	0.2	-	0.4
Solids content, %		64					
pH		9.3					

2.3 Sedimentation of coating color

Into a Falcon tube, 10 g of the coating color was transferred and centrifuged at 3000 G for 90 min for complete sedimentation. After centrifugal sedimentation, the level of sediment was recorded with a digital camera.

2.4 Low shear viscosity and dewatering of coating color

Low shear viscosity was measured using a Brookfield viscometer (Brookfield DV2T) at a rotation speed of 100 rpm. No. 3 spindle of the viscometer was used for measurement. An Åbo Akademi Gravimetric water retention device (ÅA-GWR) was used to measure the dewatering amount of coating colors under pressure. 10 mL of the coating color was poured into the cylindrical vessel placed on a membrane (mixed cellulose ester membrane filter, pore size 0.2 μm, Advantec) and blotter papers. Dewatering of the coating color was performed under the pressure of 2 bar for 60 sec. Before and after dewatering, the weight difference of the blotter paper was measured and water retention value was determined.

2.5 Rheological properties of coating color

Viscosity and microstructure of the coating color were measured using a stress-controlled rotational rheometer (CVO, Bohlin instruments) with a cone-plate geometry (R=40 mm, angle=4°). The viscosity was evaluated as a function of shear rate from 0.1-100 s^{-1}. The microstructure of the coating color was investigated with oscillatory tests by measuring storage (G') and loss modulus (G") as a function of the frequency (0.01-10 s^{-1}). Before the frequency sweep test, linear viscoelastic range of the coating color was confirmed from an amplitude sweep test in a constant angular frequency (1 s^{-1}) as a function of shear stress (0.03-10 MPa).

2.6 Drying kinetics of coating layer

Multispeckle diffusing-wave spectroscopy (MS-DWS, Horous, Formulaction) was used to investigate the drying process of coating layer. A laser light illuminated the wet coating sample, and the light was scattered by the particles in the coating sample (pigment, latex, fibbers, etc.). When the scattered light was monitored using a camera without lens, a peculiar image is shown called speckle image (Fig. 2-2). The speckle image is composed of dark and bright area by the interferences of backscattered light caused by Brownian motion of the particle in the coating sample. In other words, the motion of the particle causes the change of intensity of the speckle image.

In each speckle image, using Eq. (1), d_2 was calculated based on a standard image which is the first image captured by the camera. The d_2 was plotted as a function of time from which correlation time was determined (Fig. 2-3). Speckle rate was the reciprocal of the correlation time.

$$d_2 = \sqrt{\sum_{x=0}^{x=dimx-1} \sum_{y=0}^{y=dimy-1} (I_2(x,y) - I_1(x,y))^2} \qquad \text{Eq. (1)}$$

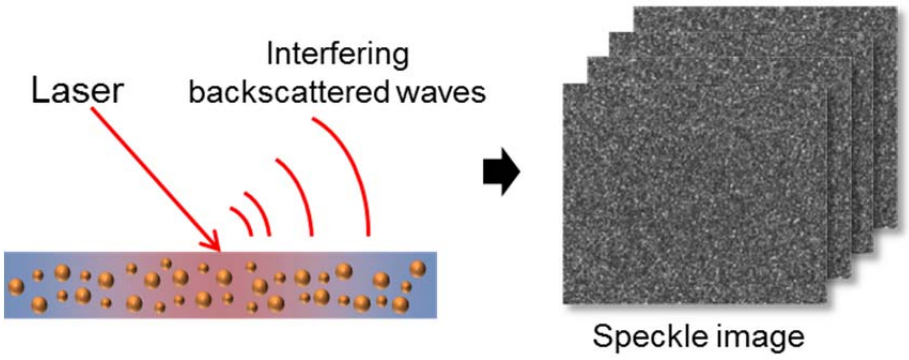

Fig. 2-2. Speckle image by interfering backscattered waves.

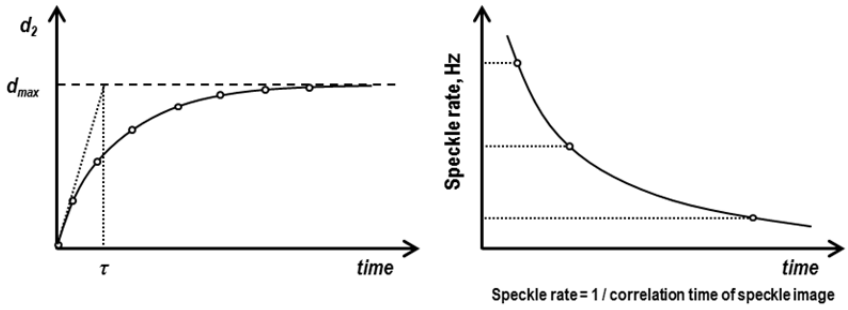

Fig. 2-3. Relationship between correlation time and speckle rate (Brun et al. 2008).

Wavelength of the laser was 655 nm, and the camera of which maximum frame rate was 30 images/sec could take images consisted of 320 x 240 pixels. Schematics of the MS-DWS instrument for the evaluation of drying kinetics is shown in Fig. 2-4.

The wet coating layer was applied using a blade doctor. The thickness of wet film was 50 μm and its area was 10 cm^2. The wet coating layer was dried in a constant temperature and humidity room (23.0±0.5°C, RH 50±3%). Weight loss during drying was measured using an analytical balance (Radwag, Poland) whose resolution was 0.1 mg. The dried wet coating layer was shown in Fig. 2-5.

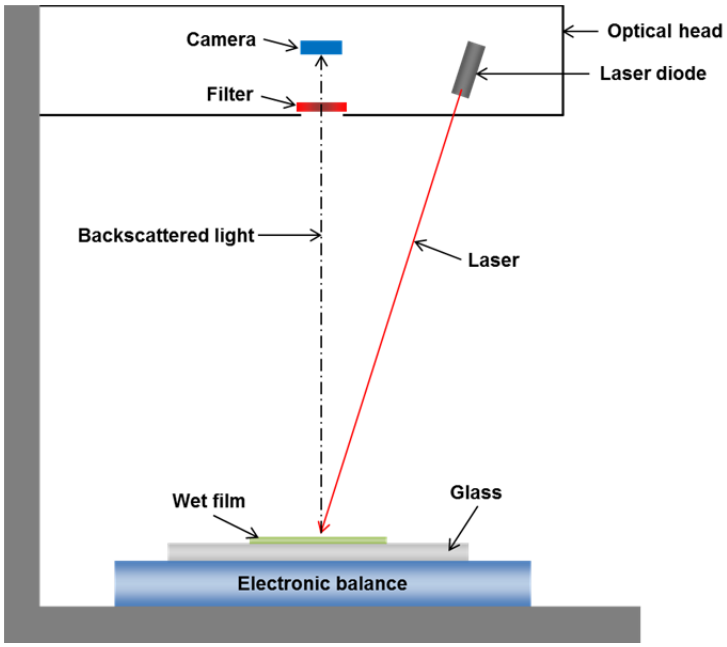

Fig. 2-4. Schematics of instrument for evaluation of drying kinetic of coating layer.

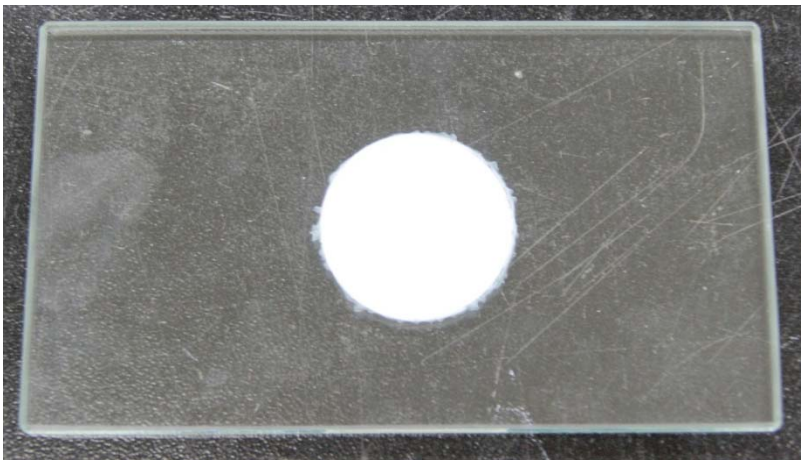

Fig. 2-5. Coating sample after MS-DWS measurement.

2.7 Pore structure of coating layer

Pore structure of the coating layer was analyzed by mercury intrusion porosimetry (Autopore Ⅳ 9500, Micromeritics Instruments Corporation). The coating layer was formed on a PET film (thickness: 100 μm) using an application bar of which gap size was 100 μm. The wet coating layer was dried at room temperature. The thickness of the dried coating was about 50 ± 5 μm. Porosity and pore size distribution of the dried coating were evaluated by measuring the intruded mercury into the pore of the coating layer. In present study, the range of the pore size investigated was from 10 nm to 1000 nm. The pore was assumed cylindrical in shape and its size was depicted as a diameter of the cylinder. Washburn equation in Eq. (2) was used to obtain the pore diameter from the external pressure data

$$P = \frac{-4\gamma\, cos\theta}{d} \quad \text{Eq. (2)}$$

where P, γ, θ and d are the external pressure, surface tension of mercury, contact angle and the pore diameter, respectively.

3. Results and discussion

3.1 Sedimentation of coating color

The effect of the formulation change on sedimentation behavior of the coating color was shown in Fig. 2-6 and 2-7. Sedimentation height increased with an increase of CMC content indicating CMC induced the flocculation of coating components in the color. The coating color containing 0.5 pph of CMC gave transparent supernatant indicating that almost no particles were present except CMC in the supernatant. On the other hands, the supernatants of other coating colors were turbid, and this suggested that incomplete sedimentation of the pigment particles occurred. This showed that flocculation of all pigment particles into large enough size to sediment was obtained when 0.5 pph of CMC was used as additive. While the addition of CMC less than 0.5 pph resulted in turbid supernatant because of the incomplete sedimentation of small pigment particles. The sedimentation height of coating colors containing CNF was similar with that of CMC 0.1, indicating that no additional flocculation of pigments was resulted with CNF. In other words, it appeared that CNF in the coating color did not cause any interaction with coating components.

The sedimentation height was different depending on the latex content in the coating color (Fig. 2-7). The sedimentation height increased with an increase of the latex content partly because the solids volume fraction of the coating

color increased with latex dosage. In addition, the increase in sedimentation volume suggested that stronger flocculation effect of CMC occurred due to larger number of latex particles present in the high latex coating color.

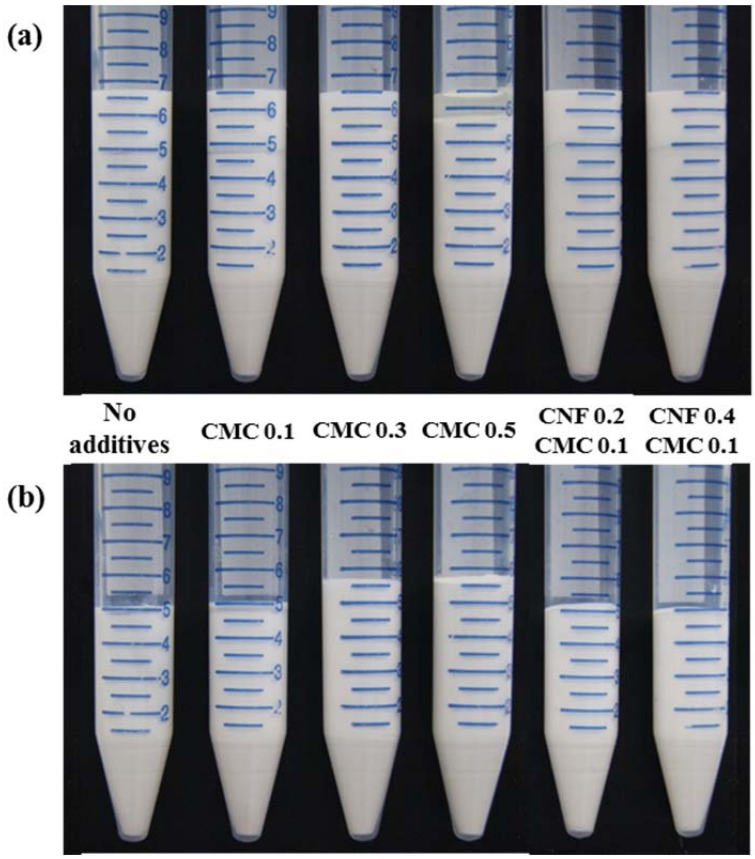

Fig. 2-6. Sedimentation behavior of coating color (latex content: 12 pph). (a): after centrifugation, (b): elimination of the supernatant to identify the sedimentation height.

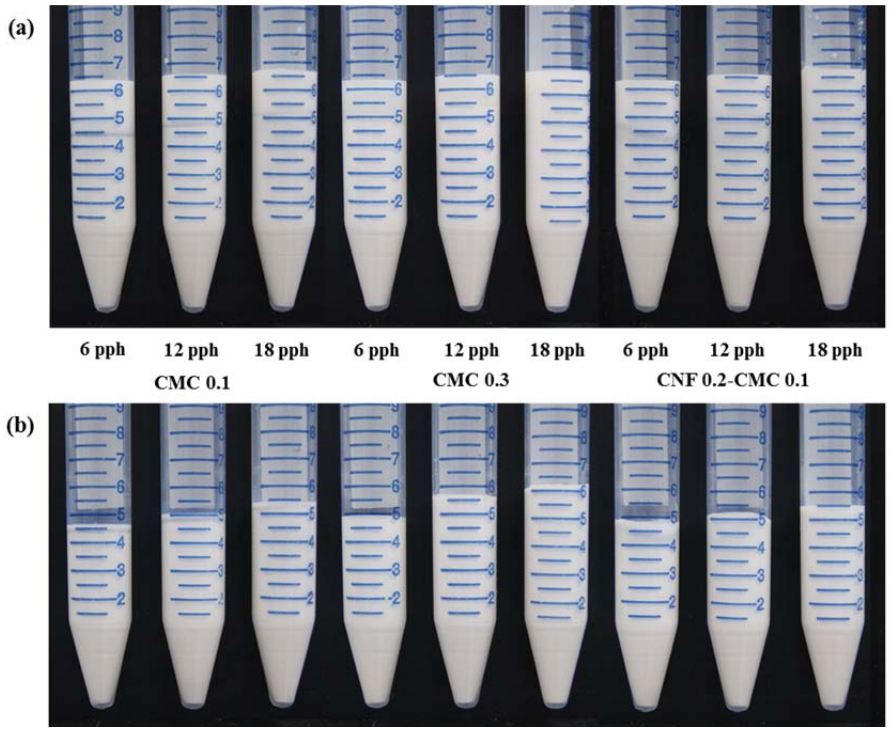

Fig. 2-7. Sedimentation behavior of coating color depending on latex content. (a): after centrifugation, (b): elimination of the supernatant.

3.2 Low shear viscosity and water retention of coating color

The low shear viscosity and dewatering amount of the coating color by CMC and CNF are shown in Fig. 2-8 and 2-9. The addition of CMC and CNF increased the viscosity of coating color. The CMC coating, however, showed much higher viscosity than the CNF coating because CMC made the coating components flocculated via depletion mechanism. This effect of depletion flocculation of coatings by CMC has been reported in several studies (Fadat et al. 1988; Mcgenity et al. 1992; Husband 1998; Wallström and Järnström 2004; Choi et al. 2015). The addition of CNF caused an increase in the low shear viscosity because CNF itself is highly viscous material. The level of viscosity increase, however, was marginal compare to the CMC since it did not cause any flocculation of pigments. In addition, the number of CNF in the coating color is far less than CMC, which limits the effect of CNF on the viscosity of coating color.

The addition of CMC decreased the dewatering amount of coating color, while the addition of CNF increased the dewatering. The effect of CMC and CNF on the dewatering of coating color will be discussed further.

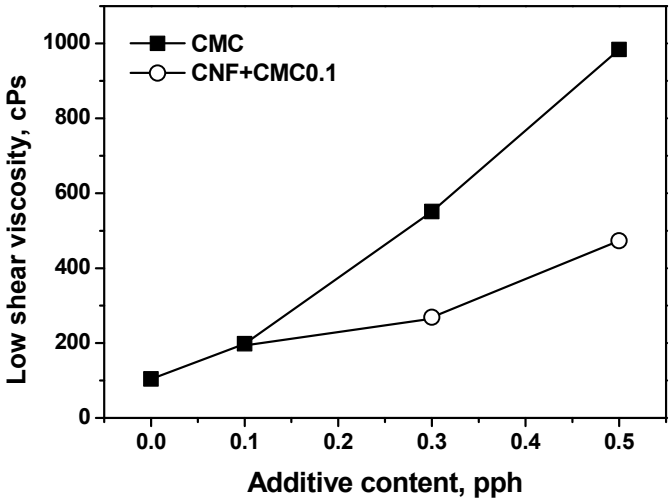

Fig. 2-8. Low shear viscosity of coating color with CMC and CNF (latex content: 12 pph).

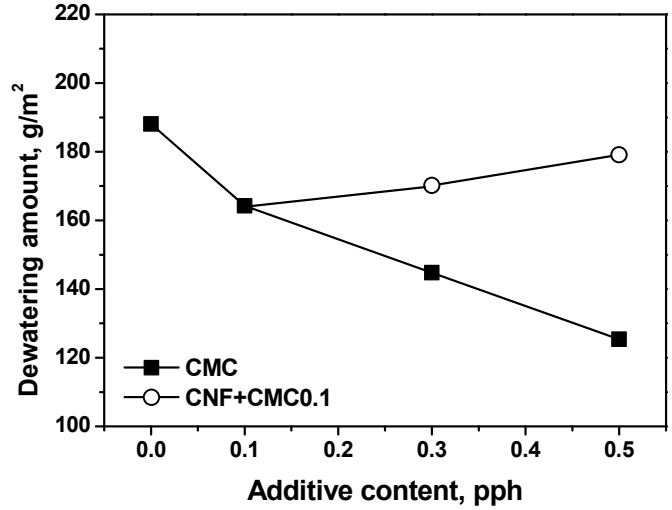

Fig. 2-9. Dewatering amount of coating color with CMC and CNF (latex content: 12 pph)

The effect of latex content on the viscosity and dewatering of coating color was shown in Fig. 2-10 and 2-11. An increase of latex content increased the solids volume fraction of the coating color by which viscosity also increased. A trend toward the decrease in dewatering amount of coating color was observed with an increase of latex content. This was attributed to the formation of more closely packed structure with an increase in latex content because the particle size of latex is substantially smaller than pigments. The addition of CNF caused reduction in water retention while it increased viscosity. This indicated that CNF caused the formation of bulkier structure of the coating after drying while its nanofibrillar structure caused restriction of shear flow of coating colors.

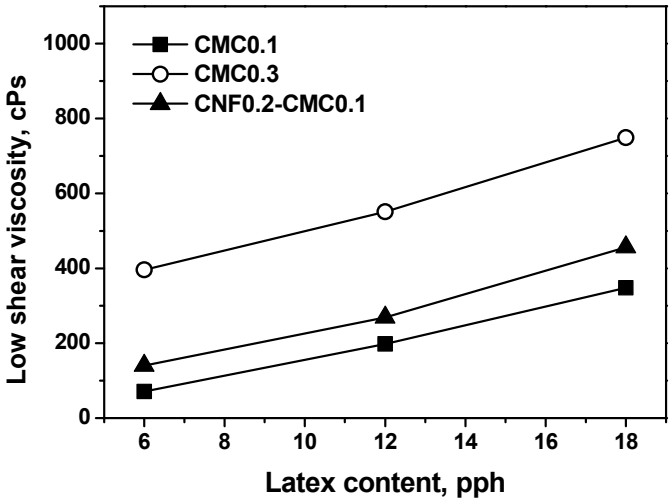

Fig. 2-10. Low shear viscosity of coating color depending on latex content.

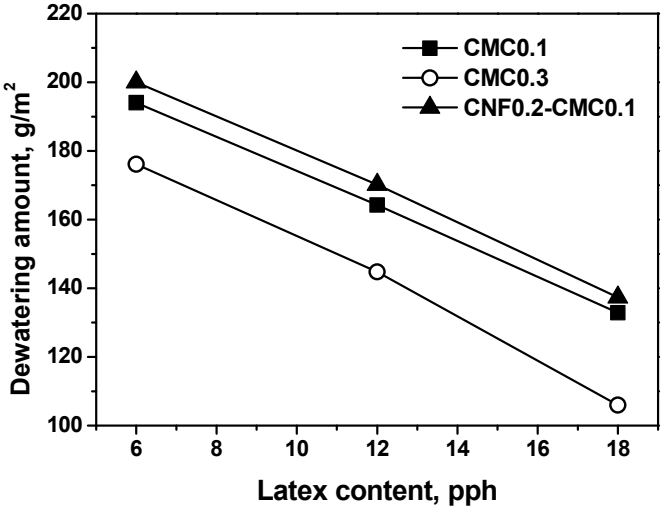

Fig. 2-11. Dewatering amount of coating color depending on latex content.

3.3 Rheological properties of coating color

The viscosity of coating color as a function of shear rate is shown in Fig. 2-12 - 2-14. Shear thinning behavior was shown for all coating colors. The dynamic viscosity of coating color by CMC and CNF was shown in Fig. 2-12 (latex content: 12 pph). The flocculation of particles in the CMC coatings gave higher viscosity compared to the CNF coatings. The viscosity of coating color containing 0.5 pph of CMC remained constant at low shear rate indicating the coating color showed a highly structured, solid-like behavior. Under the shear rate (< 0.3 s^{-1}), it was not enough to break flocculated structure.

The dynamic viscosity of coating color by latex content was shown in Fig. 2-13 and 2-14. The increase of latex content increased the viscosity of coating color. When 0.3 pph of CMC was used, the viscosity change was reduced with an increase of latex content compared to the case with 0.1 pph of CMC. This appeared that 0.3 pph CMC gave more or less complete flocculation, while 0.1 pph CMC resulted in incomplete flocculation for the coating colors. This also showed that more flocculation effect of CMC could occur with latex particles than pigment particles.

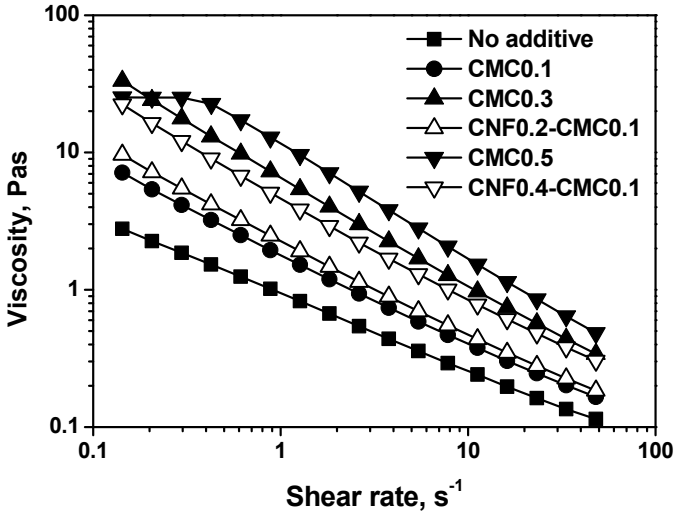

Fig. 2-12. Dynamic viscosity of coating color with CMC and CNF (latex content: 12 pph).

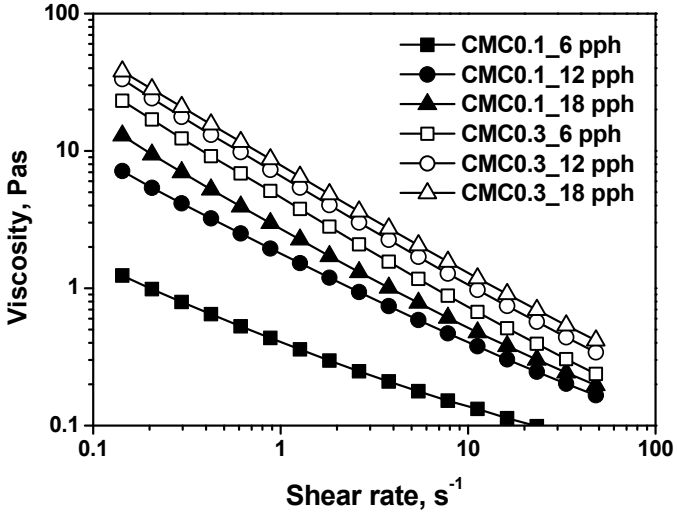

Fig. 2-13. Dynamic viscosity of coating color depending on latex content (CMC coating).

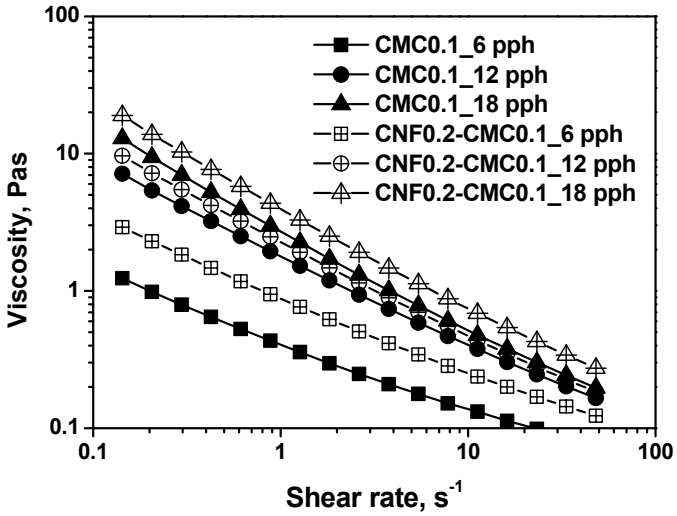

Fig. 2-14. Dynamic viscosity of coating color depending on latex content (CNF coating).

The amplitude sweep test was conducted and shown in Figs. 2-15, 2-16. Here, it is clear the presence of a linear viscoelastic region. Storage modulus (G') and loss modulus (G") of the coating color containing 12 pph of latex and CMC were depicted as a function of shear rate at a constant angular frequency (1 Hz) in Fig. 2-15 and 2-16. G' was larger than G" in the linear viscoelastic region in all coating colors, and the difference was greater when the addition rate of CMC increased indicating that CMC gave more solid-like properties for the coating color. The structure formed by CMC, however, was not strong enough to withstand high shear stress. When the structure started to break down, G' valuse greatly decreaed with increasing the shear stress. The addition of CNF to coatings increased G', however, the increment was less than CMC only coating. This indicated that CNF did not give as strong flocculation or interaction among coating components as CMC.

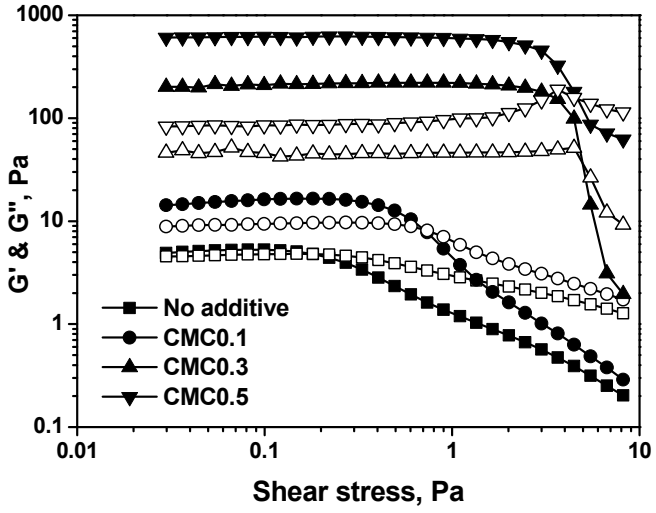

Fig. 2-15. Storage (closed symbol) and loss (open symbol) moduli of CMC coating color as a function of shear stress (latex content: 12 pph).

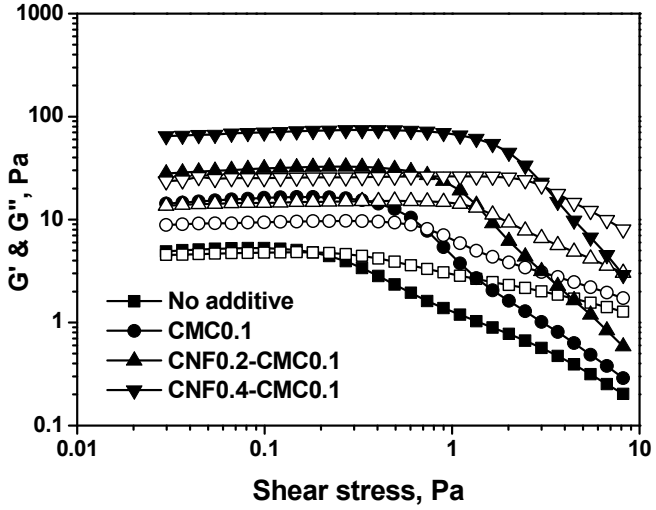

Fig. 2-16. Storage (closed symbol) and loss (open symbol) moduli of CNF coating color as a function of shear stress (latex content: 12 pph).

The G' and G" of the coating color containing different amounts of latex was depicted in Fig. 2-17 – 2-19. G' was larger than G" of the coating color except the coating color containing 6 pph of latex with 0.1 pph of CMC. The difference between G' and G" became greater with an increase of CMC content in the coating. This shows that the effect of CMC on the storage modulus is greater for latex than pigment.

Increase in latex content in coating color also increased the critical stress because of the increase of solids volume fraction and partly because of more depletion flocculation occurred. Because the density of GCC and S/B latex are 2.8 and 1 g/cm^3, respectively, the solids volume fraction of coating color containing 6, 12 and 18 pph are 41.2, 43.1 and 44.7 vol %, respectively. However, it has been shown that depletion flocculation by CMC is critical for latex, and the floc formation of latex would give stronger interaction among particles in coating colors.

The difference of G' and critical stress for coatings with latex content for coating colors containing 0.3 pph of CMC was not so great as the coatings with 0.1 pph of CMC because the flocculation of the particles occurred already strong enough among coating components with 0.3 pph CMC. Especially, when 6 pph of latex was used along with 0.3 pph of CMC, the G' and G" increased significantly compared to other conditions.

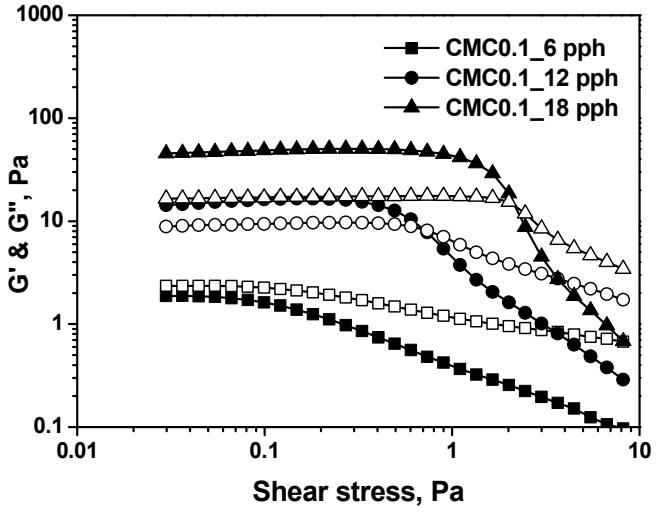

Fig. 2-17. Storage (closed symbol) and loss (open symbol) moduli of coating color as a function of shear stress in various latex content (CMC 0.1).

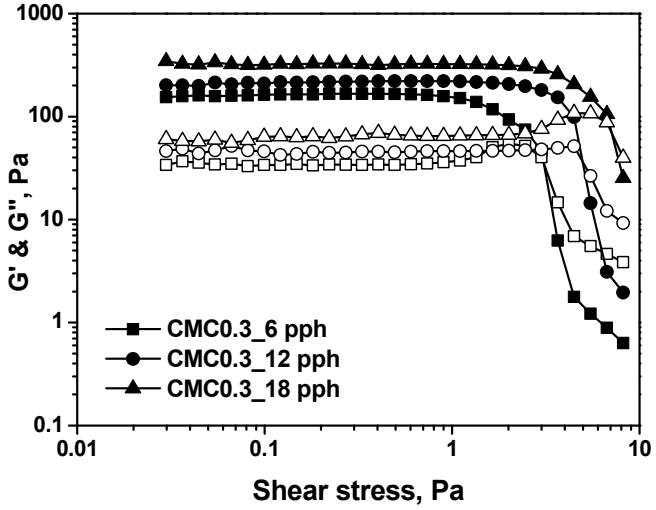

Fig. 2-18. Storage (closed symbol) and loss (open symbol) moduli of coating color as a function of shear stress in various latex content (CMC 0.3).

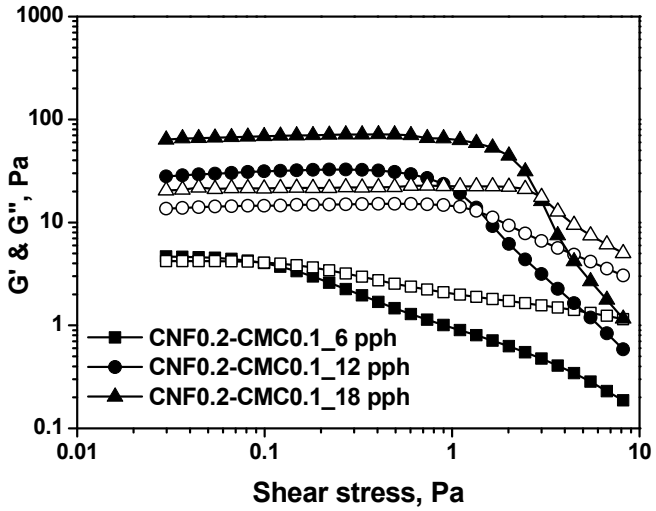

Fig. 2-19. Storage (closed symbol) and loss (open symbol) moduli of coating color as a function of shear stress in various latex content (CNF 0.2-CMC 0.1).

The microstructure of coating color was confirmed by the frequency sweep test. G' and G" of the coating color was suggested as a function of frequency with constant shear stress in Fig. 2-20 and 2-21 (latex content: 12 pph). G' and G" of the coating color were increased with an addition of CMC and CNF. G' and G" of coating color were increased with an increase of frequency except for two coatings with CMC 0.3 and CMC 0.5. The increase of G' and G" indicated weakly flocculated structure was formed in the coating color. When 0.3 and 0.5 pph of CMC were used, however, the G' and G" were constant regardless of frequency, which indicated the strongly flocculated structure was formed.

The difference of the coating color microstructure was attributed to characteristics of CMC and CNF. The flocculation of the particles was developed in CMC coating because the size and number of CMC are much smaller and larger than those of CNF. For example, when density, diameter, length, and aspect ratio of CNF were 1.5 g/cm^3, 20 nm, 4 μm and 200, the ratio of number of CMC to CNF was about 2500: 1. Thus, the small and large number of CMC can develop the depletion force in the coating color.

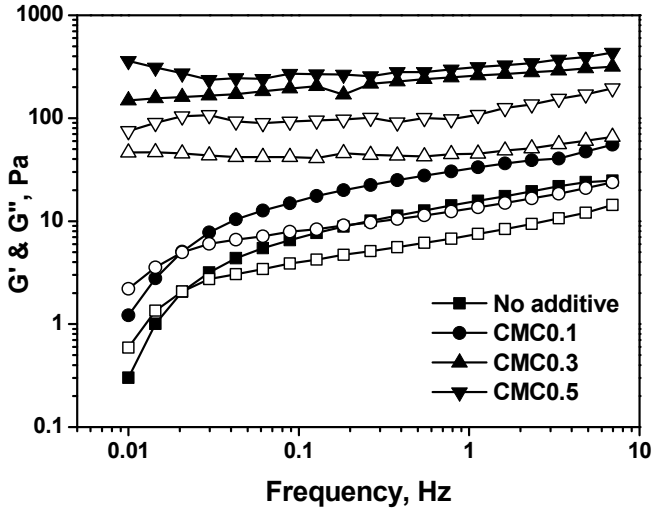

Fig. 2-20. Storage (closed symbol) and loss (open symbol) moduli of CMC coating color as a function of frequency (latex content: 12 pph).

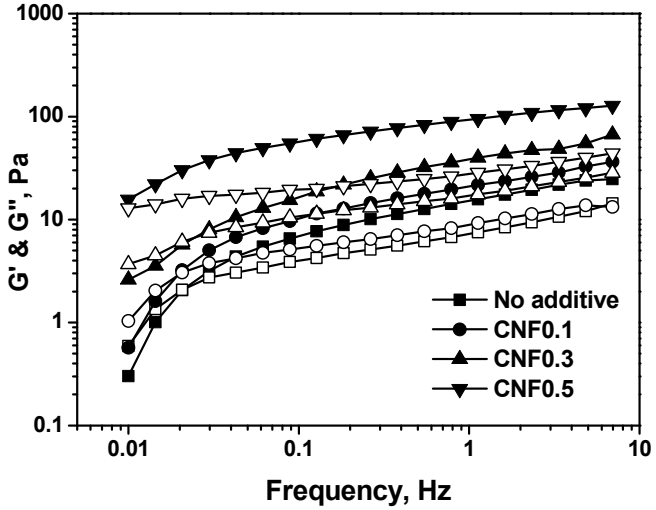

Fig. 2-21. Storage (closed symbol) and loss (open symbol) moduli of CNF coating color as a function of frequency (latex content: 12 pph).

The change of G’ and G” by latex content was presented in Fig 2-22 – 2-24. G’ and G” of the coating color were increased with an increase of latex content in all formulations. An additional CMC and CNF increased G’ and G” of the coating color compared to CMC 0.1 by increasing interaction between the coating components and the highest G’ and G” were observed in CMC 0.3. G’ and G” in CMC 0.1 and CNF0.2-CMC0.1 were increased with an increase of the frequency, which indicated that weakly flocculated formed in the coating color. G’ was higher than G” when 0.3 pph of CMC was used regardless of latex content because of the flocculation of particles.

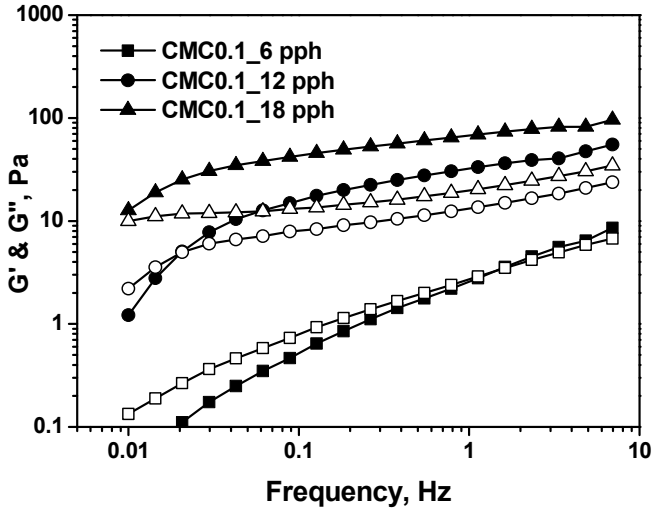

Fig. 2-22. Storage (closed symbol) and loss (open symbol) moduli of coating color as a function of frequency in various latex content (CMC 0.1).

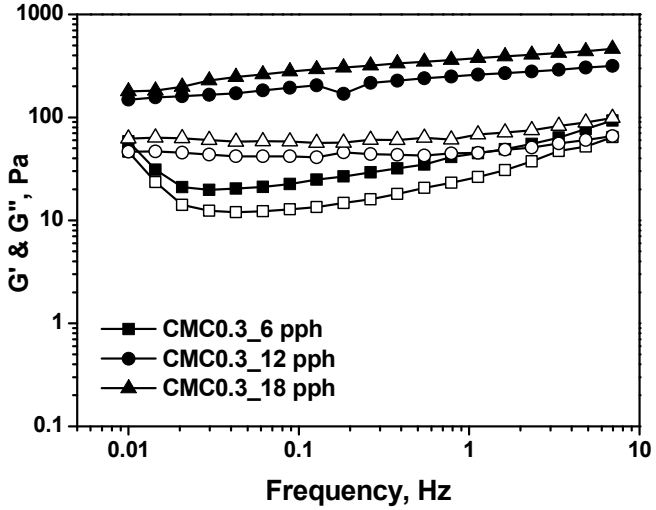

Fig. 2-23. Storage (closed symbol) and loss (open symbol) moduli of coating color as a function of frequency in various latex content (CMC 0.3).

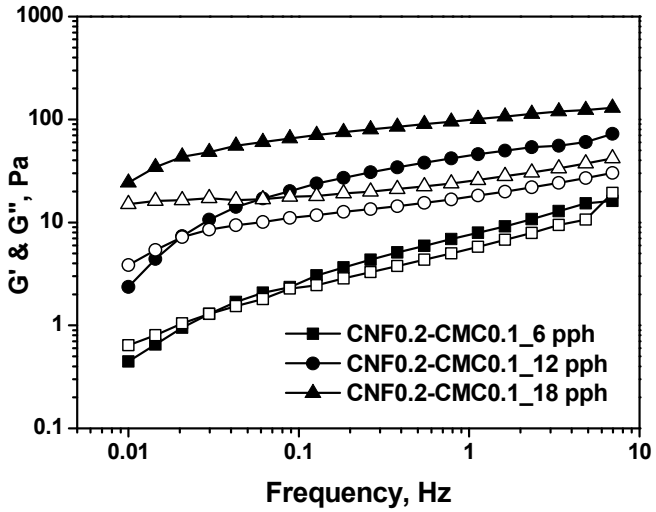

Fig. 2-24. Storage (closed symbol) and loss (open symbol) moduli of coating color as a function of frequency in various latex content (CNF 0.2-CMC 0.1).

3.4 Drying kinetics of coating layer

The drying process of the coating layer can be examined using multispeckle-diffusing wave spectroscopy (MS-DWS). From the intensity change of each pixel in the images obtained from MS-DWS the drying stage can be divided into three regimes as shown in Fig. 2-25. In regime 1, which begins just after coating color application on the glass plate, the speckle rate of the film decreased gradually by the evaporation of water and then an abrupt change in the speckle rate began that coincided with the beginning of regime 2. However, the speckle rate remained high in the regime 1 indicating fast motion of the particle in the coating layer still prevailed. The movement of the particles greatly was restricted by the neighboring particles with increasing solids volume fraction of the coating by drying in regime 2. In other words, the structure of the coating layer almost fixed in regime 2 (Burn et al. 2008). Critical time (t_c) was determined by the sudden change of the speckle rate between the regime 1 and 2. The solids content of the coating layer at the starting point of regime 3 was calculated which ranged 96 – 98%. It is impossible to distinguish the regime 3 using the MS-DWS technique.

The change of the speckle rate with CMC content was shown in Fig. 2-26. The speckle rate in the regime 1 and the t_c was decreased with an increase of CMC content. Coating colors without any additive and CMC 0.1 showed similar speckle rate in regime 1 and solids content at t_c. The solids content at t_c was 79, 77, 70 and 66 wt% when CMC content was 0, 0.1, 0.3 and 0.5 pph,

respectively. This clearly showed that CMC made early immobilization of pigment movement in coating. When CNF was used, the speckle rate in the regime 1 and the t_c was slightly decreased compared to the CMC coatings (Fig. 2-27) because of less structure forming of the CNF coatings. The solids content were 74 and 72 wt% when CNF content was 0.2 and 0.4 pph, respectively.

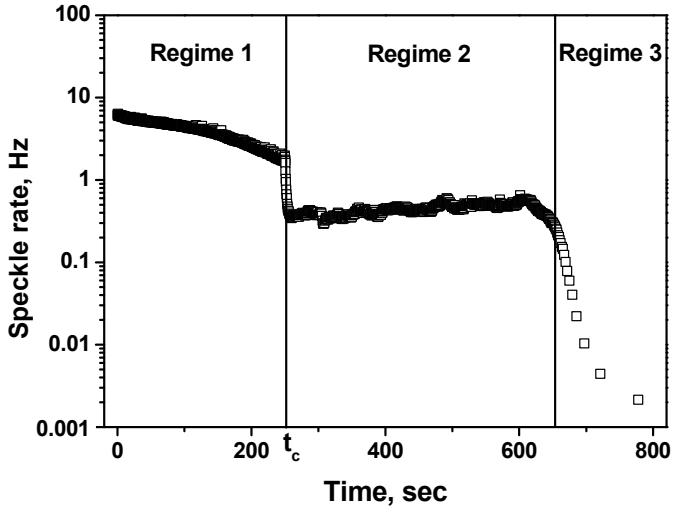

Fig. 2-25. Regimes depending on speckle rate change during drying.

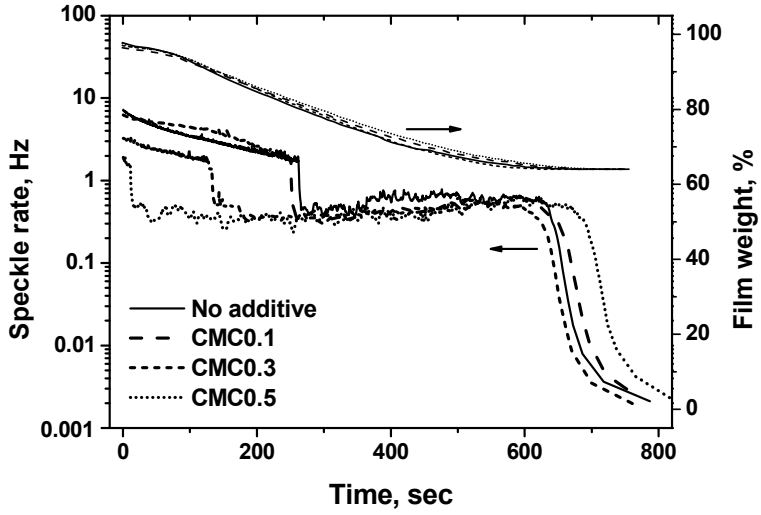

Fig. 2-26. Speckle rate and film weight as a function of drying time in CMC coatings (latex content: 12 pph).

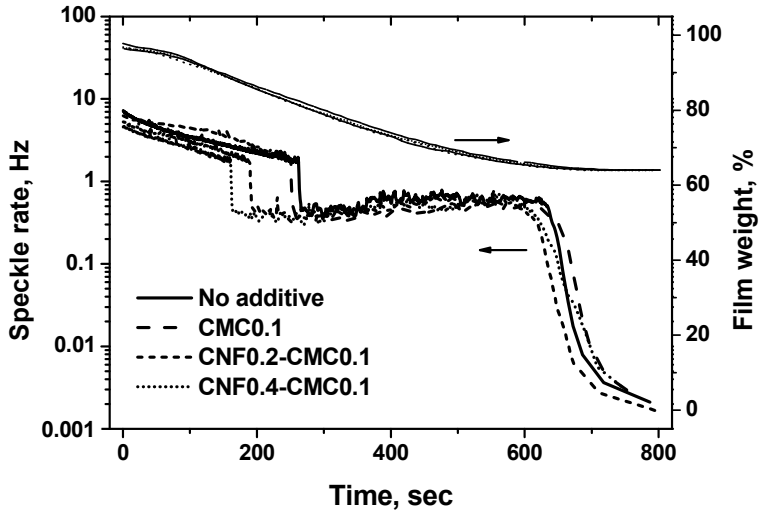

Fig. 2-27 Speckle rate and film weight as a function of drying time in CNF coatings (latex content: 12 pph).

The change of speckle rate in regime 1 and t_c can be explained by a diffusion coefficient and the flocculation of particles. Before forming capillary in the surface of coating, the particles movement is governed by Brownian motion (Zang et al. 2013). Eq. (3) is Sokes-Einstein equation

$$D = \frac{K T}{6 \pi \eta R} \qquad \text{Eq. (3)}$$

Where D is the Stokes-Einstein diffusion coefficient, K is Boltzmann constant, T is drying temperature, η is viscosity of aqueous phase and R is hydrodynamic radius of particle. CMC that was not absorbed on GCC and latex give rise to attractions between them by which the structure was formed in the coating color, which resulted in an increase of R. CMC also increases the viscosity of the aqueous phase. Thus, diffusion of pigment particles would decrease substantially with an increase of CMC addition. In other words, the movement of particles was restricted due to the increase of viscosity by CMC in the aqueous phase. In addition, the movement was also hindered by the flocculation of particles. These two effects significantly decreased speckle rate (regime 1) and t_c in the CMC coatings. On the other hands, CNF that formed gel structure in the coating color did not increase the viscosity of aqueous phase and not caused any flocculation of the particles. Thus, the speckle rate and t_c decreased slightly compared to the CMC coatings.

The different effect of CMC and CNF influenced the dewatering characteristics of the coating color. According to the modified Kozeny-

Carman equation, the average mass flow $\dot{m}$ is given as Eq. (4).The equation was used to explain the effect of CMC and CNF on the dewatering of coating color.

$$\dot{m} = \frac{f\prime\, b\, dP}{\mu_f\, \mu_l\, L} \qquad \text{Eq. (4)}$$

Where $\dot{m}$ is average mass flow, f' is filtration amount, μ_f is pore coefficient, b is flow coefficient, μ_l is path coefficient, dP is difference in pressure and L is layer thickness. Through further modification of this equation, Letzelter and Eklund (1993) suggested Eq. (5) to describe the total amount of liquid filtrated through the growing immobilized layer.

$$V = \sqrt{f^2\, A\, C\, dP\, t} \qquad \text{Eq. (5)}$$

$$C = \frac{C'}{\eta} \qquad \text{Eq. (6)}$$

where V is dewatering volume, f is cross-section area, C is structure coefficient, A is coating color coefficient, dP is actual pressure, t is time and η is viscosity of aqueous phase. Thus, the dewatering volume is proportional to the square root of time and actual pressure.

The structure coefficient depends on type of pigment and packing and coating color coefficient is related to immobilization of coating color. In present study, f, dP and t was constant during dewatering, so following relation held between dewatering amount and viscosity of aqueous phase (Eq. (7)).

$$V \sim \frac{1}{\sqrt{\eta}} \qquad \text{Eq. (7)}$$

Dimic-Misic et al. (2013) investigated the influence of CMC and CNF addition on the solids content of the immobilized layer, and found that the solids content of immobilized layer of the CMC coating was lower than that of the CNF coating. This was also shown from the sedimentation experiment and MS-DWS test. Even though the addition of CMC gave more porous filter cake, the increase in viscosity of aqueous phase decreased the dewatering amount for the CMC coating. On the other hands, more aqueous phase was filtrated through the filter cake when CMC was replaced with CNF.

CMC and CNF changed the rheological property of coating color and drying kinetics in a quite a different way. Flocculation of the coating component by depletion flocculation is the main thickening mechanism of coating color by CMC. On the other hands, water absorbing characteristic of CNF was the main thickening mechanism for the CNF coating color. The absorbed water to CNF, which decreased the amount of the aqueous phase, increased effective volume fraction of the coating color. Eq. (8) was used to calculate the

effective volume fraction considering the amount of water absorbed by CNF as solid fraction.

$$Effective\ volume\ fraction, \% = \frac{V_s + V_c}{(V_s + V_c) + (V_w - V_c)} \times 100 \qquad \text{Eq. (8)}$$

Where V_s is volume of solids, V_w is volume of water and V_c is volume of water bound with CNF. Table 2-2 shows the effective volume fraction of coating color solids with an addition of CNF. When 0.4 pph of CNF was used as an additive, the effective volume fraction was 45.4%, and this corresponded to 66 wt% of the coating color composed of GCC and S/B latex.

Table 2-2. The effective volume fraction with an addition of CNF

CMC, pph	CNF, pph	Effective volume fraction, %
0.1	0	43.1
0.1	0.2	44.3
0.1	0.4	45.4

The effect of latex content on drying process for coatings with 0.1 pph or 0.3 pph of CMC and 0.2 pph CNF and 0.1 pph CMC was presented in Fig. 2-28 – 2-30. The speckle rate in the regime 1 and the t_c decreased with an increase of latex content for coatings of CMC 0.1 and CNF 0.2-CMC 0.1. When the latex content was 6, 12 and 18 pph in CMC 0.1 coatings, the solids content at the t_c was 82, 77 and 74 wt%, respectively. It appeared that there are two reasons of speckle rate reduction for the coatings with greater amounts of latex. The first rational is that an increase of latex content resulted in higher solids volume fraction and this hindered the particles movement. The second rational is that the depletion flocculation by CMC increased with latex content, which has been reported in literature (Wharen-Show et al. 1995) It has been shown that more effective depletion flocculation by CMC occurs with latex than with pigment. When 0.3 pph of CMC was used, the speckle rate in the regime 1 and the t_c were similar regardless of latex content due to the flocculation of the coating components occurred more or less completely at this high dosage of CMC.

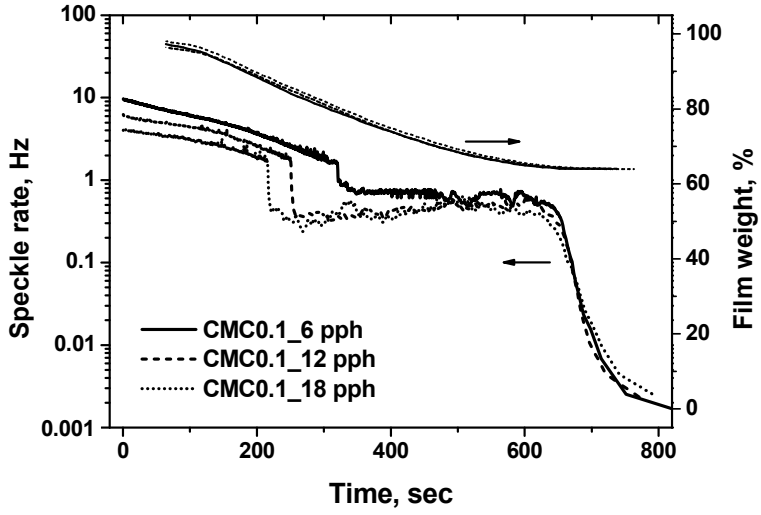

Fig. 2-28. Speckle rate and film weight as a function of drying time in various latex content (CMC 0.1).

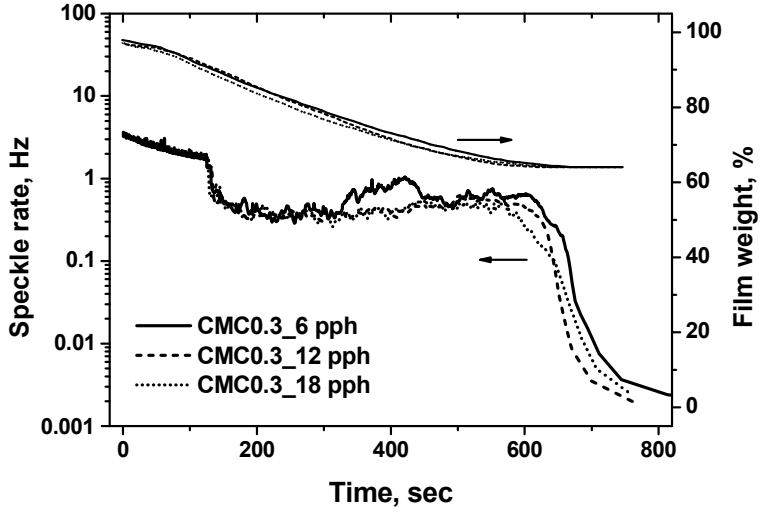

Fig. 2-29. Speckle rate and film weight as a function of drying time in various latex content (CMC 0.3).

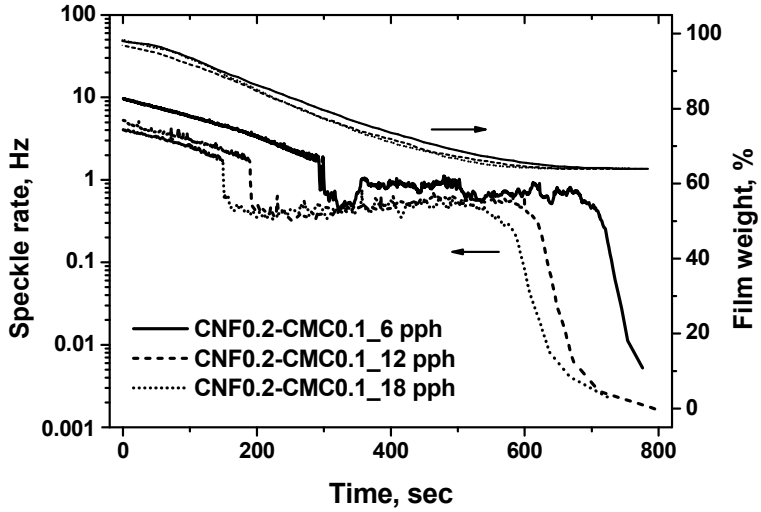

Fig. 2-30. Speckle rate and film weight as a function of drying time in various latex content (CNF 0.2-CMC 0.1).

3.5 Pore characteristics of coating layer

The total intrusion volume and porosity of the coating layers influenced by the addition of CMC and CNF were shown in Table 2-3. The characteristics of coating layer of CMC 0.1 were similar to those of the reference coating layer (No CMC and CNF). Additional use of CMC and CNF increased the intrusion volume and porosity of the coating layer, reflecting the effect of flocculation by CMC. Especially, when the thickener content increased from 0.3 to 0.5 pph, the structural change of coating layer was significantly. CMC and CNF can act as a binder due to their film forming characteristics of them. If the addition of CMC and CNF decreases the porosity of the coating layer, the film forming characteristics of these two additives greatly influence on structure formation of the coating layer. However, the porosity of the coating layer was decreased with an addition of CMC and CNF, which indicated that the film forming characteristics of them was not a main effect on the structure formation of the coating layer. The mechanism involved the structure formation of the coating layer will be discussed further

Pore size distribution of the coating layer was shown in Fig. 2-31 and 2-32. All pores were smaller than 1 μm in diameter, and most pores had the diameter ranging from 50 to 80 nm. With an addition of CMC and CNF, the pore between 60 – 80 nm increased while the pore around 50 nm in diameter decreased.

Table 2-3. Pore characteristics of coating layer with CMC and CNF

Additive content, pph	CMC		CNF + CMC 0.1	
	Total intrusion volume, mL/g	Porosity, %	Total intrusion volume, mL/g	Porosity, %
0	0.124	21.2	-	-
0.1	0.124	21.3	-	-
0.3	0.128	24.1	0.126	23.0
0.5	0.149	26.8	0.136	24.4

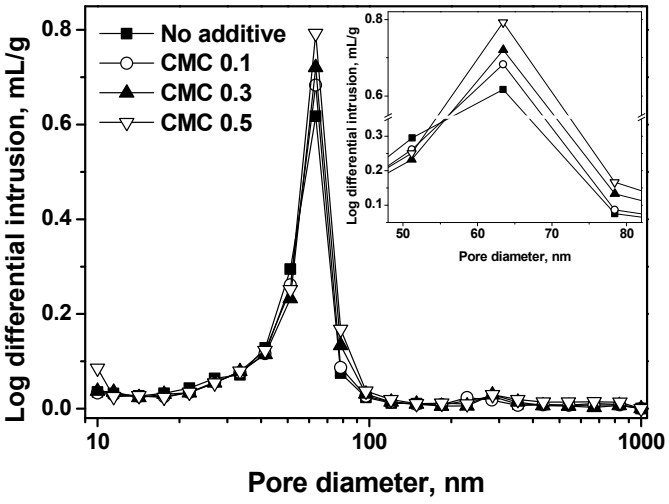

Fig. 2-31. Pore size distribution of coating layer with CMC (latex content: 12 pph).

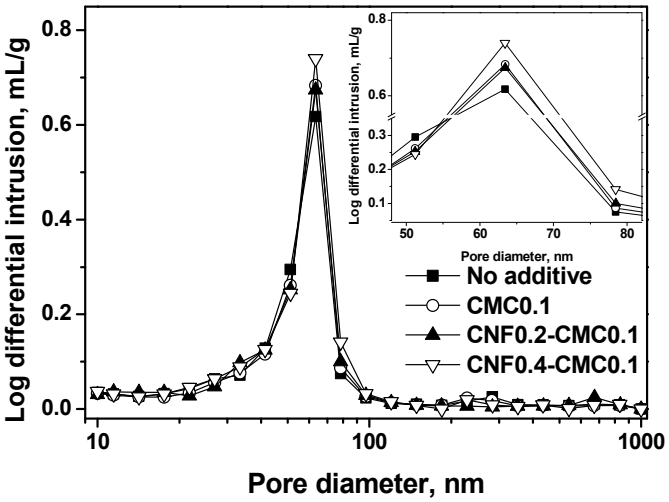

Fig. 2-32. Pore size distribution of coating layer with CNF (latex content: 12 pph).

The effect of latex content on the pore characteristics of coating layer was presented in Table 2-4. A trend toward decrease in the total intrusion volume and porosity was observed with an increase of latex content. This shows that the latex fills the voids between pigment particles. The addition of CMC 0.3 and CNF0.2-CMC0.1 gave higher the intrusion volume and porosity than that of CMC 0.1 suggesting that more loose packing of the coating components was obtained. The pore size distribution of coating layer was shown in Fig. 3-33 – 35. The increase of latex content made small pores in the coating layer because the pores were filled by the latex particles.

Table 2-4. Pore characteristics with latex content

Latex content, pph	Additive condition	Total intrusion volume, mL/g	Porosity, %
6	CMC 0.1	0.146	24.8
	CMC0.3	0.168	27.7
	CNF 0.2-CMC 0.1	0.172	28.5
12	CMC 0.1	0.124	21.3
	CMC0.3	0.128	24.1
	CNF 0.2-CMC 0.1	0.126	23.0
18	CMC 0.1	0.084	18.0
	CMC0.3	0.091	20.2
	CNF 0.2-CMC 0.1	0.094	20.1

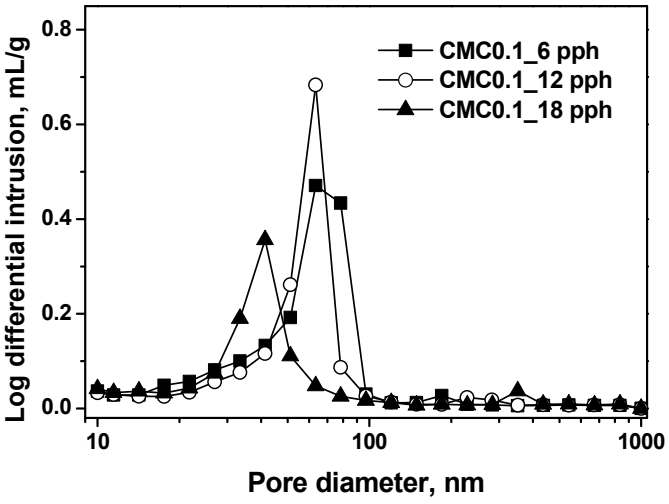

Fig. 2-33. Pore size distribution of coating layer depending on latex content (CMC 0.1).

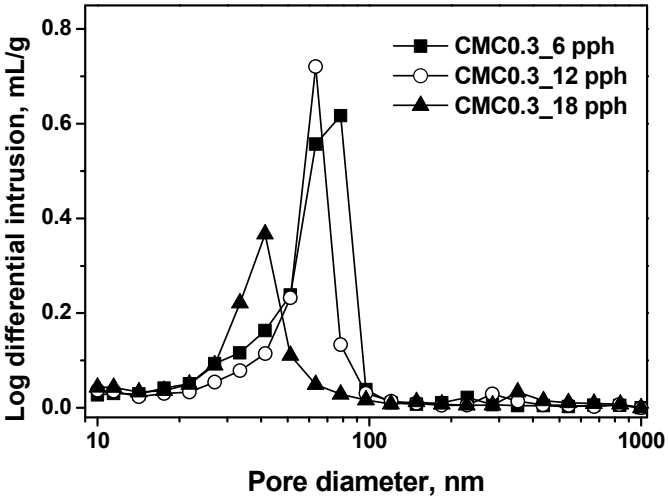

Fig. 2-34. Pore size distribution of coating layer depending on latex content (CMC 0.3).

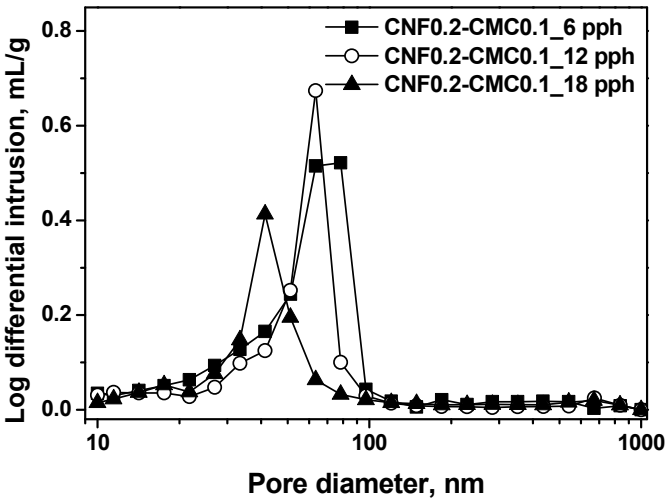

Fig. 2-35. Pore size distribution of coating layer depending on latex content (CNF 0.2-CMC 0.1).

3.6 Drying process

Fig. 2-36 showed the development of coating layer structure during drying for coatings without any additives and with CMC and CNF. The particles can move until forming the close packed structure when CMC and CNF were not used. However, CMC prevented rearrangement of the particles by flocculating particles due to its small and large number. CMC by which loose packed structure was formed in the structure forming point made coating layer porous. In addition, the large pores can be produced between the flocculation structures. The mechanism of forming porous coating by CNF differs from CMC. Although the particles in the CNF coating forms close packed structure, the voluminous characteristics of CNF that forms gel-like structure in the coating color made coating layer porous during drying.

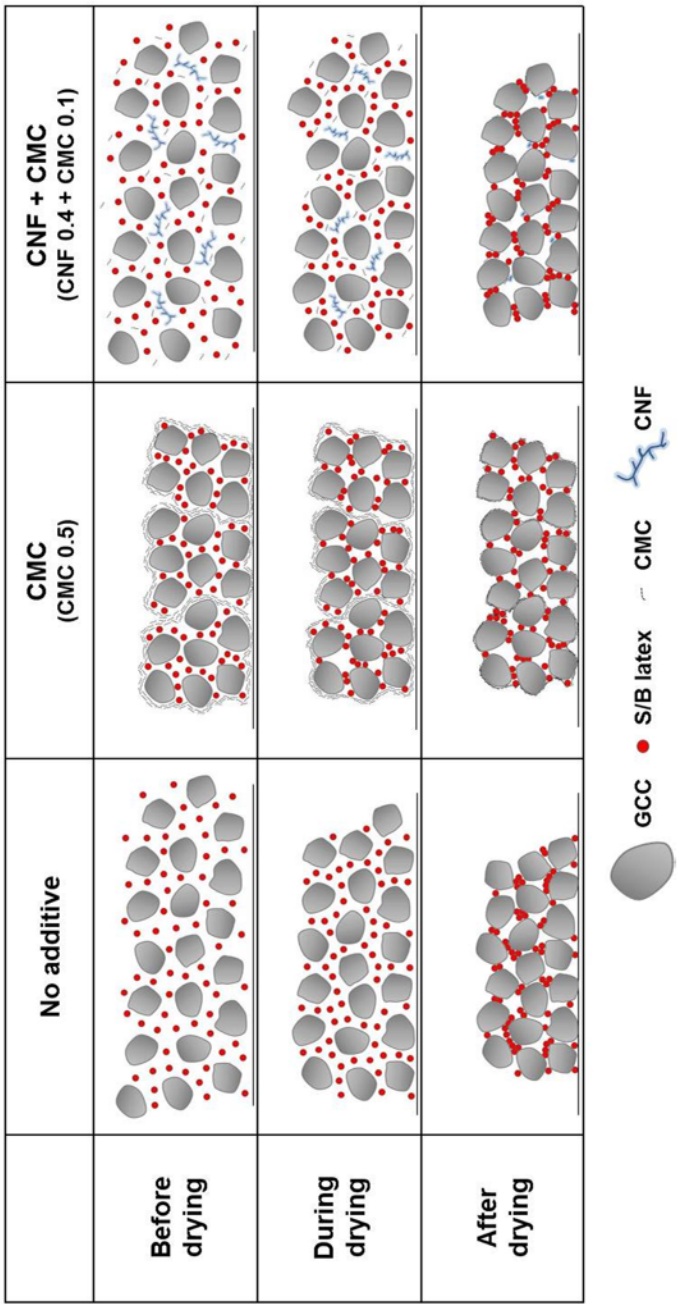

Fig. 2-36 Schematics mechanism of forming structure during drying.

4. Summary

The effects of CMC, CNF, and latex content on the rheological properties of coating color, particle diffusion, structure formation, and pore structure of the coating layer were investigated. CMC coating color showed more elastic behavior than CNF coating color because CMC tended to make flocculate particles via depletion flocculation, which results in a higher viscosity for the CMC coating than the CNF coating. On the contrary, CNF existed independently in the coating suspension in a gel-like structure. The increasing viscosity of the coating color was attributed to the increase of the effective volume fraction because of the water holding ability of CNF. The increase in latex content increased the viscosity and elastic component of the coating color by increasing the volume fraction of solids.

CMC and CNF showed different effects on the dewatering of the coating color. The dewatering amount of the coating color decreased with CMC addition due to the increase in viscosity of the aqueous phase. The dewatering amount, however, increased by adding CNF because it made the filter cake structure, which is favorable for filtrate flow. The increased latex content gave a lower dewatering amount by forming a dense filter cake structure.

Critical time decreased with addition of CMC and CNF. The CNF coating showed lower t_c and higher initial diffusion of the particles than the CMC coating because of lower structure formation. It can be seen that the solids

content of the CNF coating at t_c is higher than that of the CMC coating. The increased latex content decreased t_c and the initial diffusion of particles; however, there was no difference in the particle diffusion and structure-forming point in the flocculated condition.

CMC and CNF made the coating layer porous; however, the mechanism of structure formation was different. CMC prevented rearrangement of the particles by which a porous coating layer was formed. The voluminous characteristics of CNF made a porous coating layer. The increase of latex content gave a dense coating layer by filling the pores.

Chapter 3

Stress Development and Surface Characteristics of Coating Layer by Cellulose Nanofibrils

1. Introduction

The structure of the coating layer is formed by the evaporation of solvent along with volume reduction during drying. The constrained shrinkage of the coating layer develops tensile stress that causes coating defects such as cracking, delamination, and curling. Thus, evaluation of the drying stress can predict the mechanical properties and defects of the coating layer.

Several studies on the particle and binder system have reported on stress development in the paper coating system. Previous investigations have made efforts to confirm the effects of the coating color formulation and properties of coating components on stress development. The drying stress of a coating layer composed of calcium carbonate and latex or starch was evaluated by changing the binder content (Laudone et al. 2004). The effects of latex deformability and CMC addition on the drying stress were reported (Wedin et al. 2004); however, there have been few studies attempting to understand the effect of CNF on the drying stress.

In this chapter, it is aim to investigate the effect of formulation on the stress development and surface characteristics of the coating layer. The change in the drying stress was evaluated by the beam deflection method during drying. The surface of the coating layer was explored using FE-SEM to understand the effect of the drying stress and the drying behavior of additives on the surface characteristics of the coating layer.

2. Experimental

2.1 Materials

The information of the pigment, latex, CMC and CNF used in this chapter was presented in Chapter 2 (2.1).

2.2 Formulation of coating color

Formulation of the coating color for evaluation of effect of CMC, CNF and latex content on the stress development was shown in Table 2-1.

2.3 Evaluation of stress development during drying

Beam deflection method was applied to measure the stress development during drying. Schematic of drying stress measurement is shown in Fig. 3-1. During drying, shrinkage of the wet coating layer develops tensile stress by which the substrate is deflected. The deflection of the substrate was evaluated by the laser and position sensing detector. A silicon wafer (thickness: 530 μm; dimensions: 70 mm × 6 mm) was used as a substrate and it was gold coated in back side to enhance reflection of the laser. The coating color was applied to the substrate using a blade doctor with an area of 45 mm × 6 mm. The coating layer was dried in a chamber at controlled temperature of 23(±1)°C and relative humidity of 20(±2)%. The deflection of the substrate was converted to

drying stress using Eq. (9).

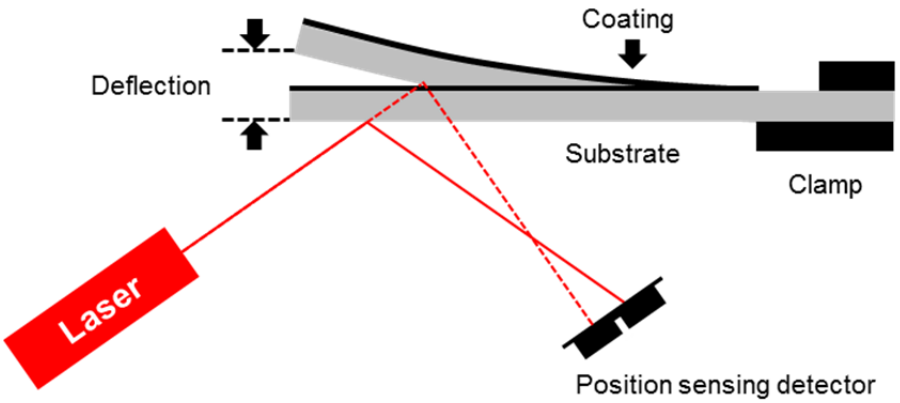

Fig. 3-1. Schematics of drying stress measurement.

$$\sigma = \frac{dE_s t_s^3}{3t_c l^2 (t_s + t_c)(1 - v_s)} + \frac{dE_c (t_s + t_c)}{l^2 (1 - v_c)} \qquad \text{Eq. (9)}$$

Where *d, E, t, l and v* are deflection, elastic modulus, thickness, coating length and Poisson ratio, respectively. Subscription s and c represent substrate and coating layer, respectively. The second term of the Eq. (9) is related to relaxation in the coating layer. However, the second term can be ignored when modulus of the coating layer is much lower than that of the substrate.

2.4 Gloss of coating layer

Gloss of the coating layer was measured with a gloss tester (L&W, Sweden). The coating layer was dried at room temperature and the thickness was about 50 ± 5 μm.

2.5 Moisture content of coating components during drying

Moisture content of the coating components was evaluated by a moisture analyzer (MX-50, A&D Company, Japan). Calcium carbonate, latex, CMC and CNF were prepared in 1 wt%. 2 g of prepared suspension or solution was dried at 80°C.

2.6 Observation of coating layer surface

Imaging of the coating layer surface was carried out using a filed-emission scanning electron microscope (FE-SEM, AURIGA, Carl Zeiss)

3. Results and discussion

3.1 Drying stress of coating layer

3.1.1 Effect of CMC

The effect of CMC content on the stress development was shown in Fig. 3-2. The drying stress increased to the first peak followed by a weak relaxation. Then the stress showed an additional increment and reached a plateau. The first peak and final drying stress increased with an increase of CMC level. Summarized maximum and final drying stress of the coating layer with CMC addition were presented in Fig. 3-3.

Several studies reported that the drying stress caused by the shrinkage of coating layer begins from the solidification point until it ends at the completion of the drying process (Wedin et al. 2005). An investigation by Laudone et al. (2004) showed that starch binder gave higher drying stress than latex because its loosely packed structure at FCC transforms to tighter packing at SCC. The MS-DWS results shown in Chapter 2, CMC addition caused a reduction in t_c and low speckle rates. This showed that the solids content at solidification point decreased with CMC addition. Thus, the total amount of water evaporated to cause coating shrinkage that starts from the solidification point and ends at the completion of drying increased with CMC addition.

In addition, the shrinkage of CMC influenced the additional increment of drying stress after the weak relaxation. A trend toward increase in the additional increment of the stress was observed with an increase of CMC content. The additional increase was about 0.1 MPa in no CMC condition. However, it was about 0.4 MPa when 0.5 pph of CMC was used. The shrinkage of CMC that was precipitated during drying was developed in CMC-rich region by which the additional increment of the drying stress was increassed with an increase of CMC level (Wedein et al. 2004).

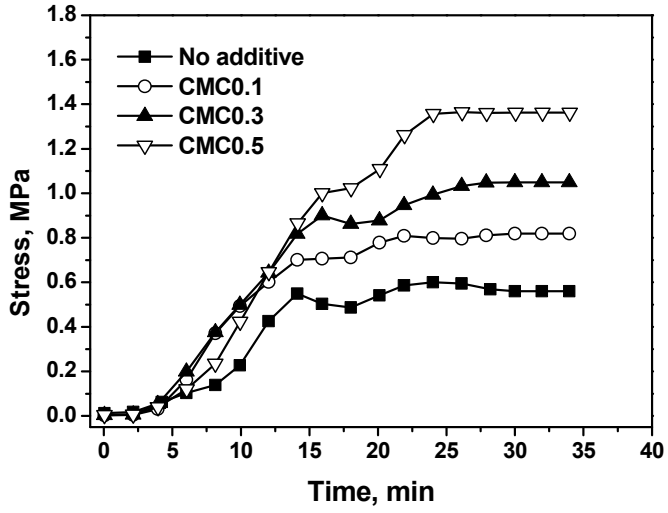

Fig. 3-2. Stress development of coating layer with CMC (latex content: 12 pph).

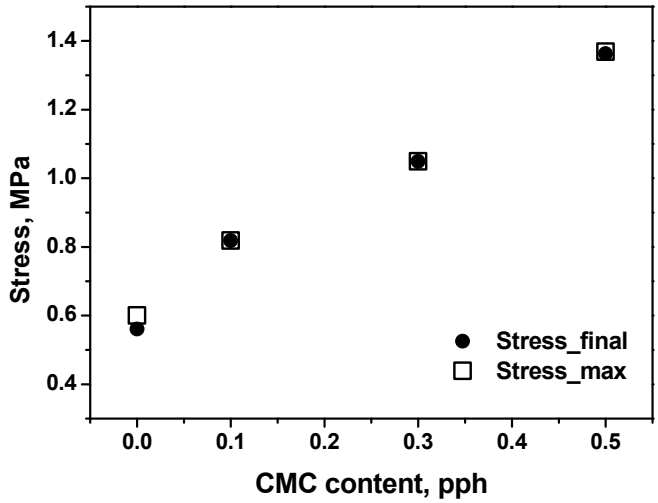

Fig. 3-3. Final and maximum drying stress of coating layer with CMC (latex content: 12 pph).

3.1.2 Effect of CNF

The effect of CNF on the drying stress of the coating layer was shown in Fig. 3-4. The first peak and final drying stress of the CNF coating were lower than those of CMC 0.1 in Fig. 3-2. CNF0.2-CMC0.1 coating gave the lowest drying stress among the formulation tested. The slight increment of the drying stress was shown in the case of CNF0.4-CMC0.1. The additional increment of the drying stress after the weak relaxation was almost similar between the additive conditions containing 0.1 pph of CMC. Summarized maximum and final drying stress are depicted in Fig. 3-5.

As discussed earlier in Chapter 2, CNF forms gel-like structure and does not flocculate particles. Even though CNF decreases the solidification point as CMC does, the coating containing CNF showed lower drying stresses than CMC 0.1 coating. Shrinkage of CNF was one of the factors affecting drying stress of the coating layer. It has been well known that cellulose fiber shrinks more in cross section than the length in which the shrinkage is only a few present. This low shrinkage of cellulose fiber in longitudinal direction would make less reduction during drying, which resulted in low tensile stress development.

The drying stress was increased when CNF content was increased from 0.2 pph to 0.4 pph in the coating color. The increase in the drying stress was related to the structural change of CNF. Ryu (2013) reported that the increase

of CNF consistency improves the association of CNF by increasing contact number between the nanofibrils. It can be inferred that the increase of CNF content restricted the stretch of nanofibrils due to the strongly associated state of CNF. This resulted in the slight increase of the drying stress even though CNF content was increased.

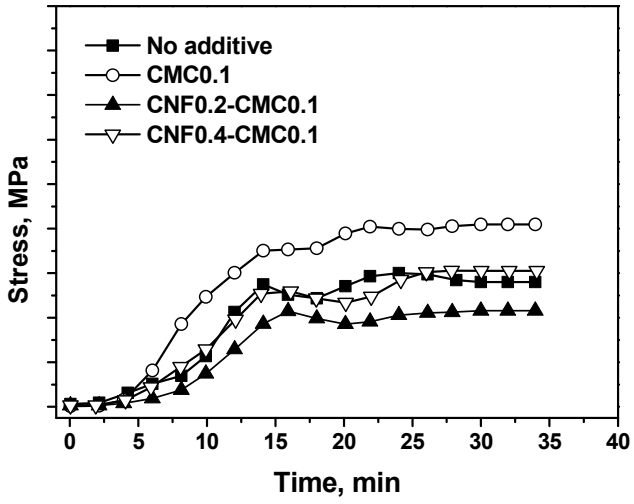

Fig. 3-4. Stress development of coating layer with CNF (latex content: 12 pph).

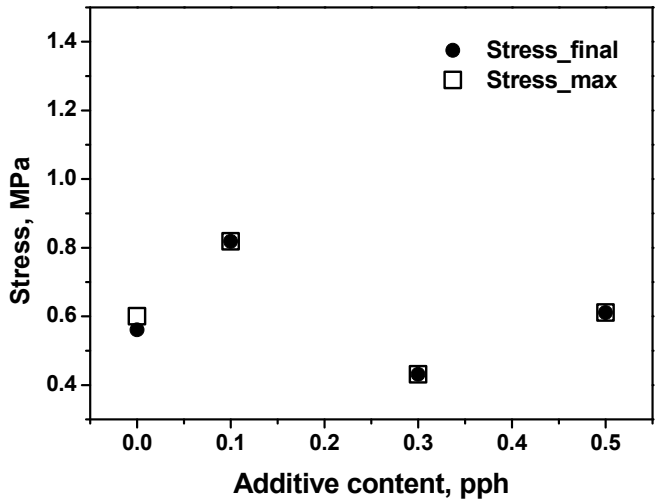

Fig. 3-5. Final and maximum drying stress of coating layer with CNF (latex content: 12 pph).

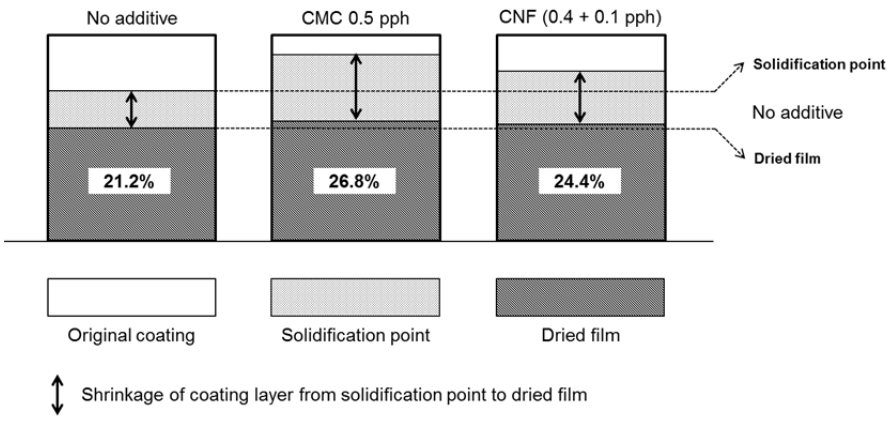

Fig. 3-6. Schematics of shrinkage of coating layer depending on CMC and CNF.

3.1.3 Effect of latex content

Change of the drying stress by latex fraction was shown in Fig. 3-7 – 3-12. The increased latex fraction increased the maximum and final drying stress of the coating layer. The drying stress of the coating layer containing CNF showed the lowest drying stress regardless of the latex content. When the latex content was 18 pph, the drying stress increased steeply and reached to the maximum stress in the CMC coatings; however, the stress was increased to the first peak followed by a weak relaxation and it showed an additional increment to the plateau in the CNF coating. The latex particle can bridge between the pigment particles in the low addition level. Further increase of the latex content filled the pores and formed a film by the coalescence of the latex particles, which increased the drying stress with an increase of the latex content.

Previous investigation (Kiennemann et al. 2005) reported that the drying stress was maximized in critical pigment volume concentration (CPVC). Several studies (Laudone et al. 2004; Kiennemann et al. 2005; Lim et al. 2015) have reported that the increase of binder content increased the drying stress over the CPVC. The similar trend of the drying stress was also shown in the present study.

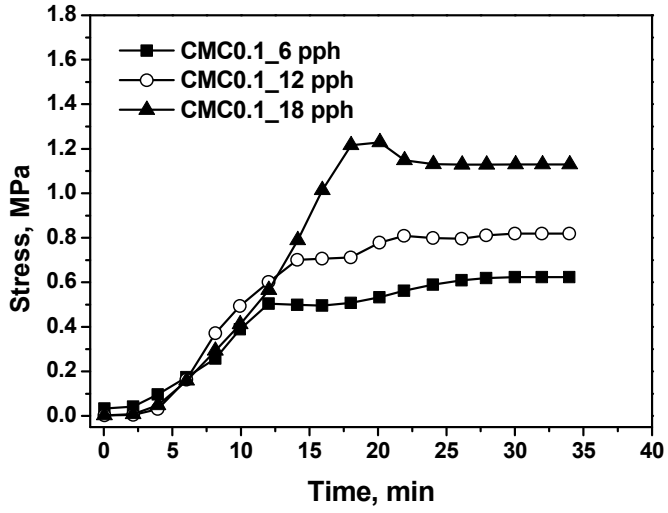

Fig. 3-7. Stress development of coating layer depending on latex content (CMC 0.1).

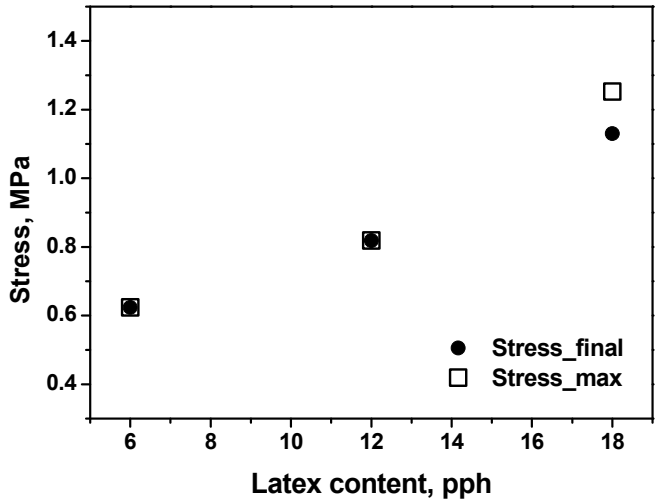

Fig. 3-8. Final and maximum drying stress of coating layer depending on latex content (CMC 0.1).

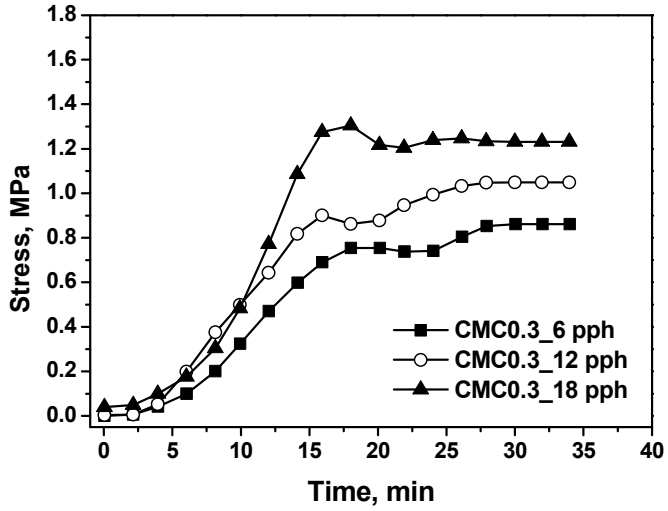

Fig. 3-9. Stress development of coating layer depending on latex content (CMC 0.3).

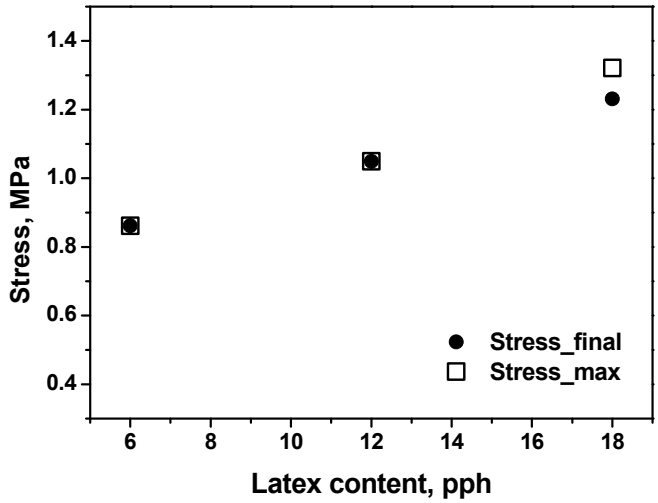

Fig. 3-10. Final and maximum drying stress of coating layer depending on latex content (CMC 0.3).

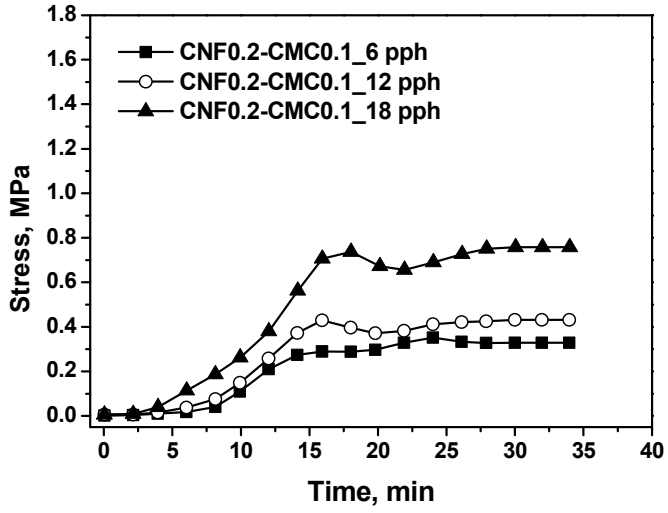

Fig. 3-11. Stress development of coating layer depending on latex content (CNF 0.2-CMC 0.1).

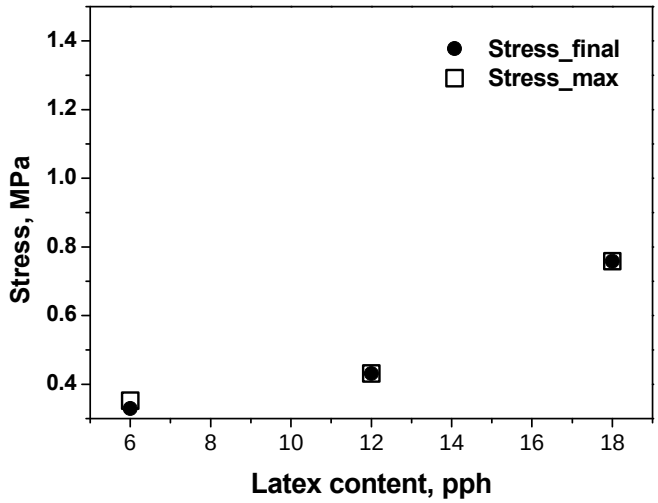

Fig. 3-12. Final and maximum drying stress of coating layer depending on latex content (CNF 0.2-CMC 0.1).

3.2 Surface characteristics of coating layer

3.2.1 Surface morphology of coating layer

Different types of defect were developed in the coating surface by CMC and CNF. Most coating surface was non-defected area (Fig. 3-13(a)). Small and large cracks were shown in CMC 0.5 because of the high drying stress (Fig. 3-13(b) and (c)). Craters that came from collapsing CNF during drying were observed in CNF 0.4-CMC 0.1 (Fig. 3-13(d)).

Changes of the coating surface depending on latex content were shown in Fig. 3-14. The decrease in pores was observed with an increase of the latex content because the excessive latex particles formed the film in coating surface and filled the pores.

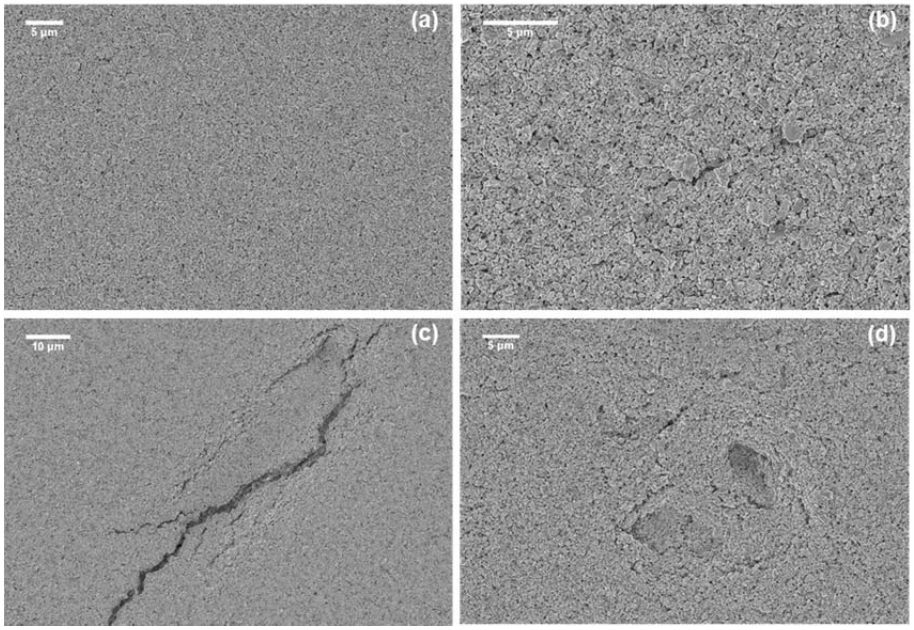

Fig. 3-13. Surface of coating layer depending on CMC and CNF. (a) CMC 0.1, (b), (c) small and large crack in CMC 0.5 and (d) collapsed defect in CNF 0.4-CMC 0.1.

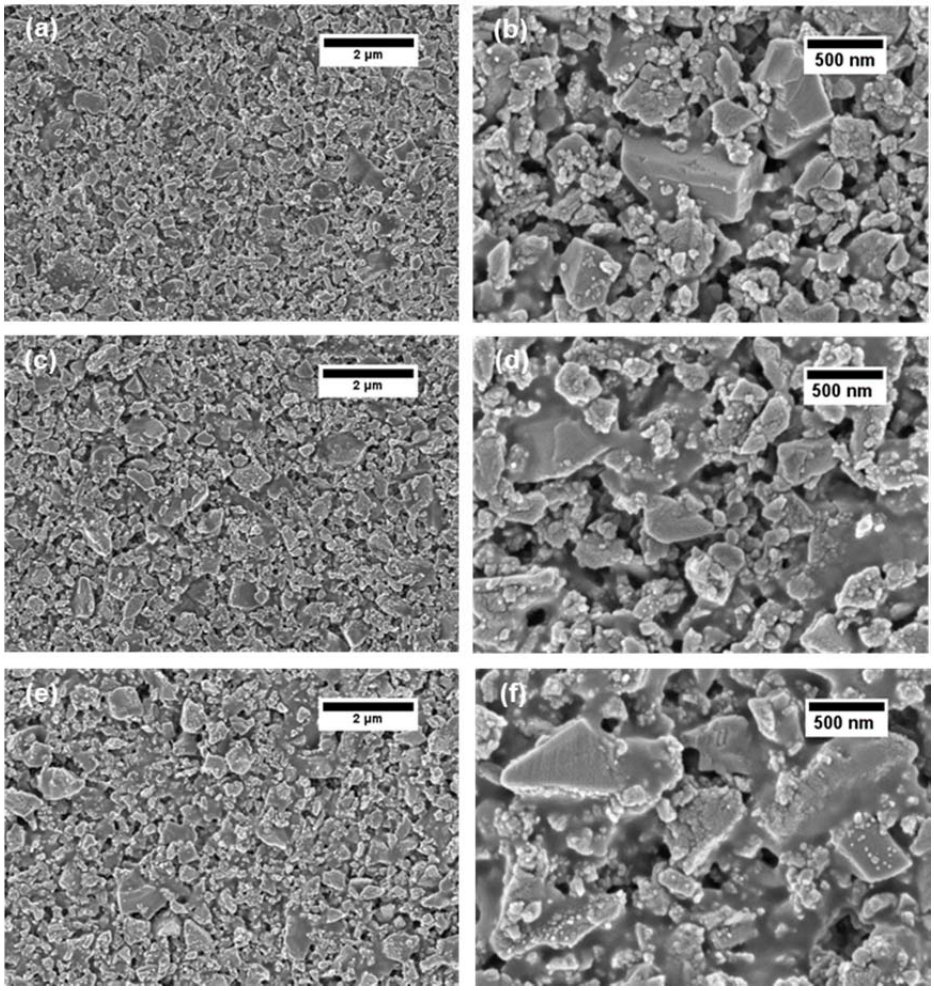

Fig. 3-14. Surface of coating layer depending on latex content. (a), (b) latex: 6 pph, (c), (d) latex: 12 pph and (e), (f) latex: 18 pph.

3.2.2 Gloss of coating layer

The effects of CMC, CNF and latex content on the gloss of the coating layer were shown in Fig. 3-15 and 3-16. A trend toward decrease in the gloss was observed with an increase of CMC and CNF content. The decrease of the gloss in the CNF coating was much more than in the CMC coating at the same thickener content. The gloss of coating layer was reduced with an increase of latex content (Fig. 3-16). The coating layer containing 0.1 pph of CMC showed the highest gloss regardless of latex content. More shrinkage of the coating layer caused the decrease in gloss with an increase of latex content.

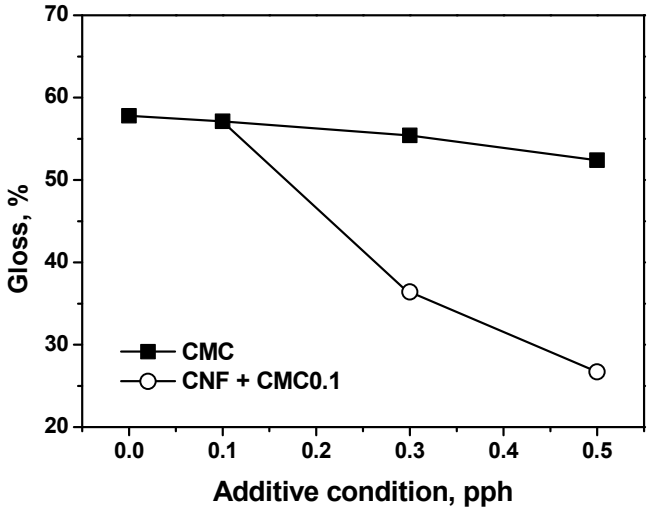

Fig. 3-15. Gloss of coating layer depending on CMC and CNF (latex content: 12 pph).

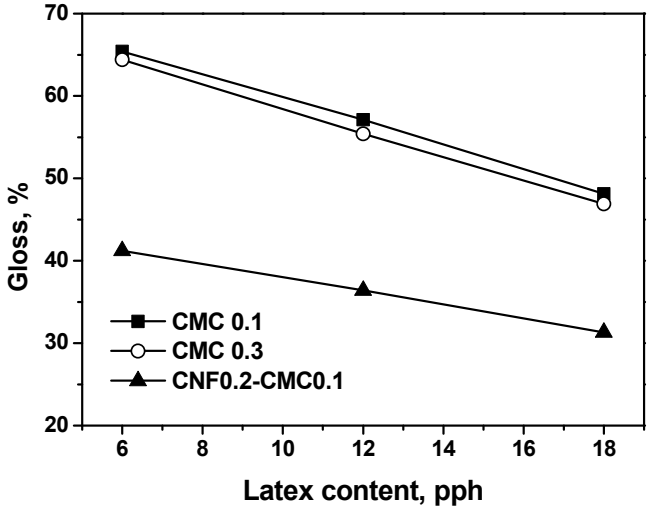

Fig. 3-16. Gloss of coating layer depending on latex content.

The gloss of the coating layer was slightly decreased with an addition of CMC. Several studies reported that the more shrinkage between FCC and SCC showed lower gloss of the coating layer (Watanabe and Lepoutre 1982). In Chapter 2, the decrease in the solids content at t_c with CMC addition led to more shrinkage of the coating layer by which the rough surface was formed. There is a chance that latex migration can improve the gloss by forming the film on the surface of the coating layer. Zang et al. (2010) reported that addition of CMC prevented latex migration from bulk to the surface of the coating layer. The decrease in the gloss was not only the increase of coating layer shrinkage but also decrease of the migration of latex particles. Considering the drying temperature (25℃), however, the latex migration is not regarded as the main influence on the decrease of gloss.

The gloss reduction in the CNF coating was explained by the water holding behavior of CNF. The film weight change of the coating components that were used in this study was observed during drying. The initial solids content was 1% and drying temperature was 80℃. The calcium carbonate, latex, and CMC showed a similar trend of the weight change during drying (Fig. 3-17). The weight change of CNF, however, was slower than other components because of the water absorbing characteristics. The characteristics formed rough surface by introducing non-uniform moisture content.

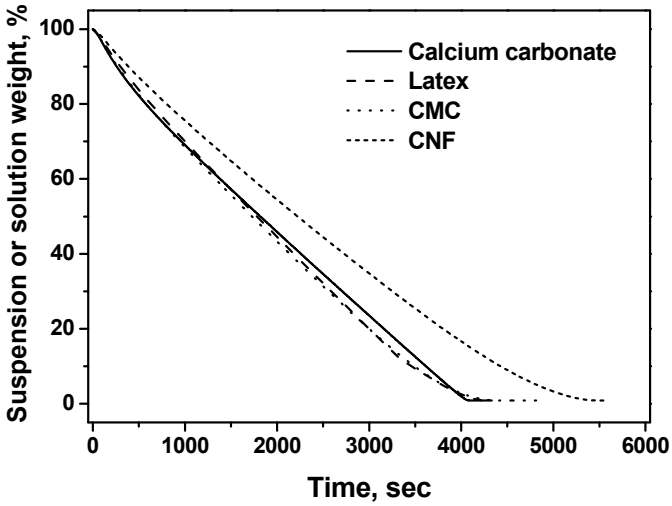

Fig. 3-17. Change of weight loss of coating components during drying.

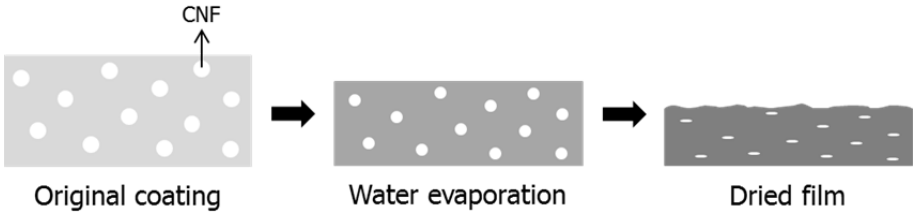

Fig. 3-18. Gloss reduction of coating layer by CNF.

4. Summary

The drying stress and surface characteristics of the coating layer were investigated. The drying stress was influenced by the shrinkage of the coating layer after the solidification point and the characteristics of the thickeners. The flocculated CMC coating reached the solidification point at lower solids content than CNF coatings. The drying stress was thus increased by addition of CMC. In addition, CMC that was precipitated during drying influenced the additional increment of drying stress with shrinkage of the CMC-rich region. The shrinkage of the CNF coating was lower than that of the CMC coating and its low shrinkage characteristics relaxed the stress developed. The drying stress of the coating layer was increased with an increase in latex content due to the coalescence of latex particles.

Small and large cracks were seen in the CMC coating due to the high drying stress. CNF caused craters in the coating layer because of the collapsing coating layer above CNF. The decrease in gloss was much higher in the CNF coating than in the CMC coating because of non-uniform shrinkage of the coating layer due to the water absorbing characteristics of CNF. The increased latex content gave a lower gloss to the coating layer.

Chapter 4

Effect of Cellulose Nanofibrils on Surface and Absorption Characteristics of Coated Paper

1. Introduction

The prime purpose of the paper coating is to improve appearance and printability of the paper. This purpose can be achieved by forming a smooth and microporous coating structure on the base paper. From the materials point of view, the coating pigment and binder govern the structure of the coating layer because they are the main components of the coating formulation. Many studies have attempted to understand the effect of the pigment and binder on the coating structure (Al-Turaif and Bousfield, 2005; Risio and Yan 2006; Larsson et al. 2007; Preston et al. 2007; McCoy 1998). In Chapter 2, it was shown that a small amount of CMC and CNF changed the structure of the coating layer, through different mechanisms.

There was an attempt to apply CNF on the coating color and coated paper (Salo et al. 2015). They investigated the optical properties and roughness of coated paper when CMC and CNF were used as thickeners. CNF coating gave a higher mobility than CMC coating, and formed a smooth and glossy surface because CNF did not introduce flocculation between the coating components. However, the effect of CMC and CNF on printability has not been reported. Kumar et al. (2016) reported that the process condition of CNF application influenced the quality of the paper. The uniform surface was formed by using CMC and applying high shear conditions.

Evaluation of ink absorption characteristics such as absorption rate and uniformity of the coated paper is important to predict the printability of coated paper. Ink absorption test (SCAN 70:09) has been widely used, as it is the easiest method to evaluate the absorption characteristics of coated paper. Several studies that evaluated absorption characteristics using this method (Groves et al. 1993; Saito et al. 1992; Lee et al. 1997) have been reported. However, this method has limitations in predicting the absorption characteristics of coated paper under real printing conditions. In the ink absorption test, the ink absorption time is much longer and the amount of applied ink is much larger than that employed in real printing. This difference often results in unexpected and unrealistic evaluation of the printability of coated papers. Thus, there is a clear need for a new method to predict the absorption characteristics of coated papers that simulate the results under real printing conditions more effectively and accurately through a simple experiment. It would also be interesting to see what effect CNF has on the printability of coated papers.

The aim of this chapter is to investigate the effect of CNF on the properties of coated paper including the optical, structure, and absorption characteristics. In order to evaluate the absorption characteristics of the coated paper and ink back trapping, a novel technique was used.

2. Experimental

2.1 Materials

Base paper (woodfree paper) of 117(±2) g/m^2 was supplied from Moorim paper (Korea). The information on the pigment, latex, CMC and CNF used in this chapter was presented in Chapter 2 (2.1). Coarse ground calcium carbonate (Hydrocarb 60, OMYA Korea) was used as a pre-coating pigment in double-coated paper. Particles below 2 μm was 61%. S/B latex for pre-coating was provided by LG Chem, and its average particle diameter was 180 nm. The glass transition temperature and gel content of the latex were -19°C and 85%, respectively.

For vehicle absorption test, vehicle for offset ink comprised of aromatic naphtha, and an offset ink (Magenta, tack value: 12) were used. The aromatic naphtha was used to control viscosity of the vehicle.

2.2 Formulation of coating color

Formulation of the coating color to manufacture coated paper was presented in Table 4-1. Formulation for double coated paper was shown in Table 4-2.

Table 4-1. Formulation of coating color

Formulation			
Pigment pph	Setacarb 77K	100	
Binder, pph	S/B latex	12	
Additive, pph	CMC	0.1, 0.3, 0.5	0.1
	CNF	-	0.2, 0.4
Solids content, %		64	
pH		9.3	

Table 4-2. Formulation for double coated paper

		Pre	Top			
Pigment pph	Hydrocarb 60	100	-			
	Setacarb 77K	-	100			
Binder, pph	S/B latex	10	12			
Additive, pph	CNF	0.2	0	0.1	0.2	0.3
	CMC	-	0.4	0.3	0.2	0.1
Solids content, %		65	64			
pH		9.3				

2.3 Coating on base paper and coat weight of coated paper

The prepared coating color was applied onto the base paper with a laboratory bar coater (GIST, Korea). The coated paper was dried and calendered using a hot air dryer (120°C, 120 s) and calendered using a laboratory soft-nip calender (2 times) at the calendering pressure of 130 kgf/cm. Coat weight of the coated paper was presented in Table 4-2. As seen here, there were some variations in coat weights depending on the coating formulation even though the same coating rod was used.

Table 4-3. Coat weight of coated paper (g/m^2)

Rod No.	#2	#4	#6	#8	#10
CMC 0.1	7.3	12.5	17.3	21.7	24.8
CMC 0.3	8.8	11.8	15.9	19.9	23.0
CMC 0.5	6.8	12.1	16.2	20.2	23.4
CMC 0.1 CNF 0.2	7.6	12.4	16.6	21.0	23.6
CMC 0.1 CNF 0.4	7.5	12.7	16.4	21.2	24.3

The double coating of the paper was made with a Maiyo coater at 100 m/min. The paper was dried using hot air and IR radiation drying at 130°C and 100°C, respectively. The coated paper was calendered using the laboratory soft-nip calender (2 times). The coat weight of pre- and top-coating was about 10 g/m^2.

2.4 Gloss and roughness of coated paper

Gloss and roughness of the coated paper were measured using the Gloss tester (L&W, Sweden) and Parker Print Surface (L&W, Sweden), respectively.

2.5 Ink absorption ratio

Ink absorption ratio of the coated paper was evaluated in accordance with SCAN-P 70:09. Ink absorption ratio was determined by the brightness of the coated paper before and after the ink absorption (Eq. (10)). R_∞ and R_s are the brightness before and after ink absorption, respectively. Croda ink was used as a model ink. Ink absorption time was 2 min.

$$Ink\ absorption\ ratio, \% = \frac{R_\infty - R_S}{R_\infty} \times 100 \qquad \text{Eq. (10)}$$

2.6 Vehicle absorption test

The vehicle absorption test was used to depict the phenomenon of ink back trapping in the offset printing system. Schematic diagram how the vehicle absorption test was made is shown in Fig. 4-1. The viscosity controlled vehicle and magenta ink were distributed onto the first and second blanket roll, respectively. At the first printing nip, the vehicle distributed uniformly on the first blanket roll was applied onto the coated paper. The transferred vehicle to the paper was allowed to absorb for 5 or 10 sec by controlling the rotation of

the backing cylinder, and then the magenta ink was applied onto the vehicle layer at the second printing nip.

After the vehicle absorption test, the coated paper sample was left in a constant temperature and humidity room at least for 24 hrs and then the printing image was converted the digital image using a scanner (Epson Perfection V33, EPSON; resolution: 1200 dpi). The image was converted to 8-bit gray scale image (0-255) to evaluate the uniformity of the vehicle absorption. The uniformity was analyzed using a STFI-mottling Expert v1.31 software. The coefficient of variation (COV) with spatial wavelength (1– 8 mm) was used to calculate mottle index using an Eq. (11).

$$Mottle\ index = \sqrt{{COV_{1-2}}^2 + {COV_{2-4}}^2 + {COV_{4-8}}^2} \qquad \text{Eq. (11)}$$

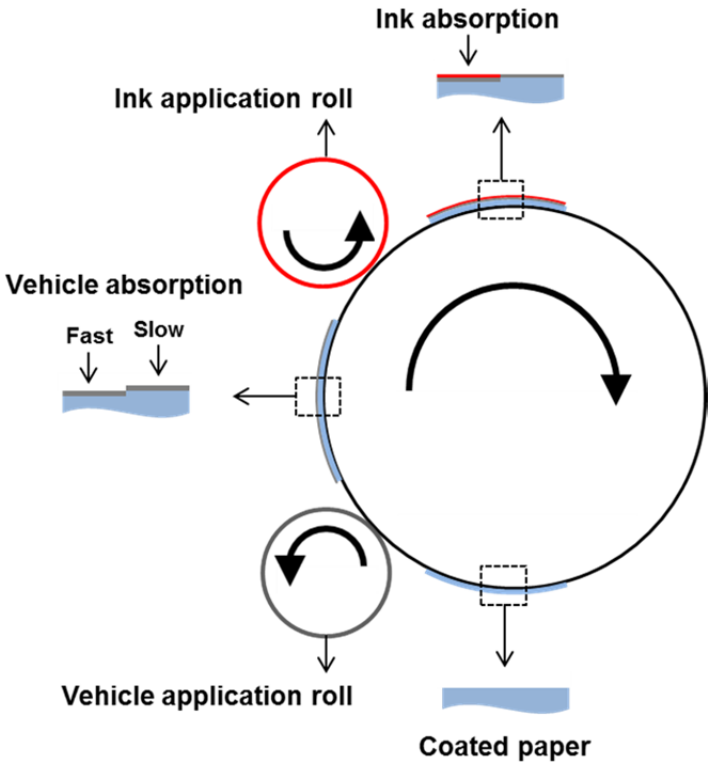

Fig. 4-1. Schematics of vehicle absorption test.

2.7 Observation of coated paper using FE-SEM

Cross-section images of the coated paper were obtained using a focused ion beam (FIB) imaging with FE-SEM (AURIGA, Carl Zeiss). The obtained image was trimmed for the image processing, and converted to 8-bit gray scale image. After the adjustment of the brightness and contrast, the image was filtered to detect the edge using the Roberts filter. Then surface profile was extracted manually. The procedure is depicted in Fig. 4-2.

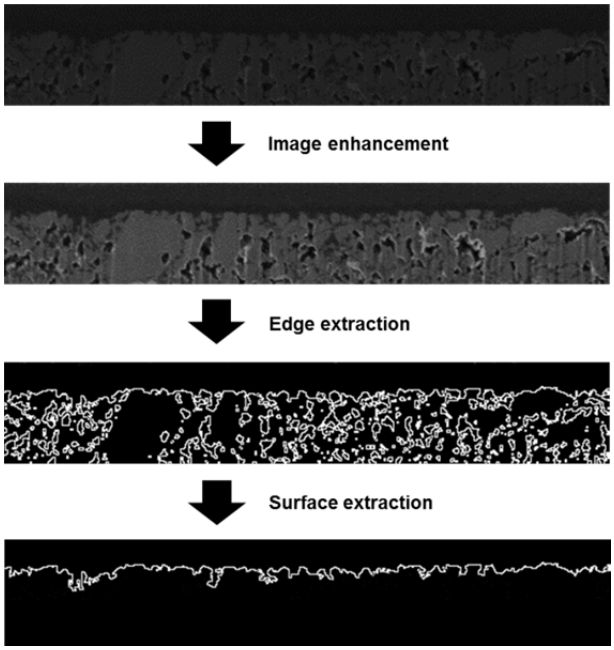

Fig. 4-2. Procedure of image processing for extraction of coated paper surface.

3. Results and discussion

3.1 Gloss and roughness of coated paper

The effect of CMC on the gloss and roughness of the coated paper was shown in Fig. 4-3 and 4-4. Gloss and smoothness increased with the increase of the coat weight due to the improvement of coating coverage. The gloss decreased slightly with increasing CMC content when the coat weight was over 10 g/m^2. Watanabe and Lepoutre (1982) reported that rough surface formed when the shrinkage of coating layer increased between FCC and SCC. MS-DWS results in Chapter 2 showed that the shrinkage between FCC and SCC increased with an increase of CMC content. Fig. 4-3 and 4-4 showed that the gloss and roughness showed not much correlation each other. Coated paper containing 0.1 pph of CMC showed the highest roughness in spite of the highest gloss.

The effect of CNF on the gloss and roughness of the coated paper was shown in Fig. 4-5 and 4-6. Even though the roughness of the coated paper was decreased with an increase of the coat weight, the gloss was not improved in the coated paper containing CNF. The gloss of coated paper containing 0.2 pph of CNF was increased when the coat weight was increased from 8 to 12 g/m^2. In addition, 0.4 pph of CNF decreased the gloss with an increase of the coat weight. The gloss was much lower in the CNF coating than the CMC coating because of the gel-like structure and water absorbing characteristics of

CNF. These properties caused non-uniform shrinkage of the coating layer during drying by introducing non-uniform moisture distribution. As the coat weight was increased, the decrease in the gloss was caused by promoting non-uniform shrinkage of the coating layer.

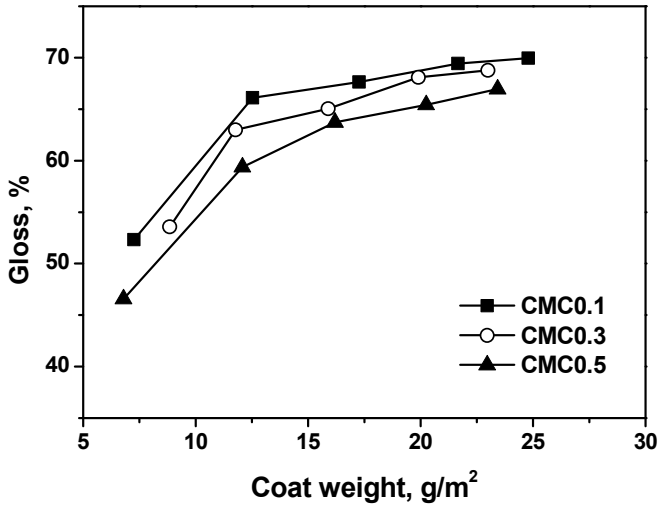

Fig. 4-3. Gloss of coated paper with CMC (latex content: 12 pph).

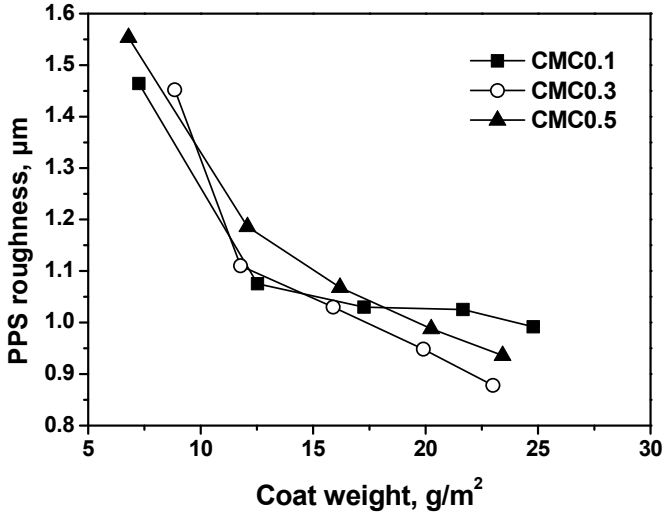

Fig. 4-4. Roughness of coated paper with CMC (latex content: 12 pph).

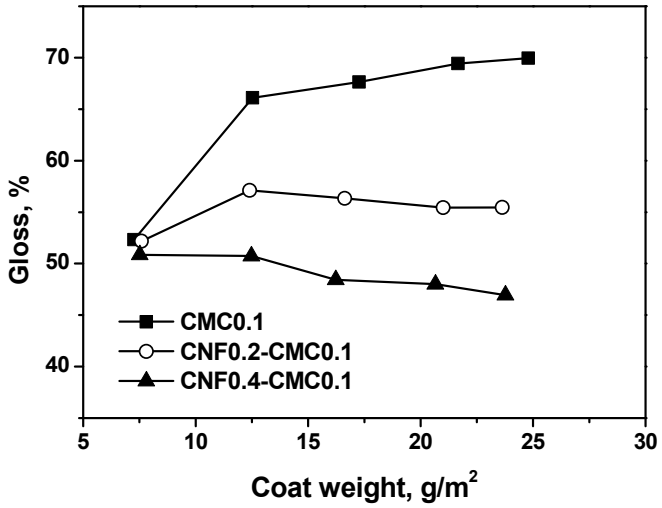

Fig. 4-5. Gloss of coated paper with CNF (latex content: 12 pph).

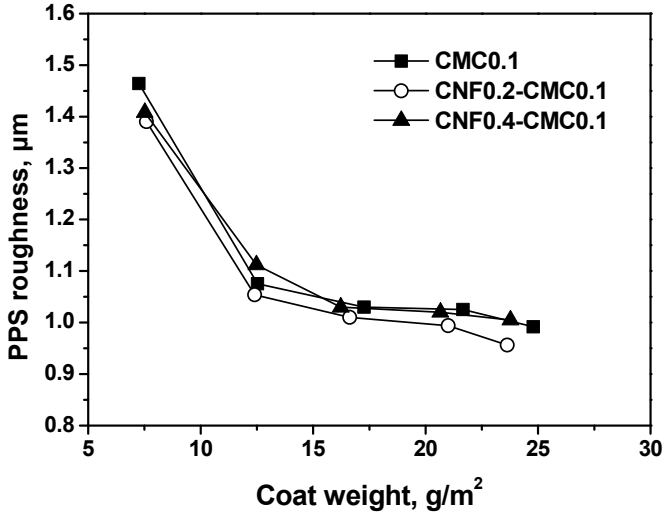

Fig. 4-6. Roughness of coated paper with CNF (latex content: 12 pph).

3.2 Ink absorption ratio

The ink absorption ratio of coated paper by CMC and CNF was shown in Fig. 4-7 and 4-8. The ink absorption ratio was increased as the coat weight was increased from 7 to 12 g/m^2. It was attributed to increase of thickness of the coating layer that can absorb ink. The ratio was decreased when the coat weight was over the 12 g/m^2. The migration of the latex particles from bulk to surface caused sealing of the surface pores, which reduced the ratio. This result was in close agreement with that of Lee et al. (1997).

CMC 0.3 and 0.5 showed slightly higher ink absorption ratio than that of CMC 0.1; however, the difference between them was not great. One of causes for this result was relatively long absorption time (2 minute). The time was enough to for ink penetrate into the coated paper minimizing the difference of absorption characteristics between the CMC coatings.

The CNF coating showed much higher ink absorption ratio than the CMC coating. The more porous coating layer was formed in the CNF coating than in the CMC coating. Low shrinkage of CNF decreased the shrinkage of the coating layer, which formed the porous coating layer.

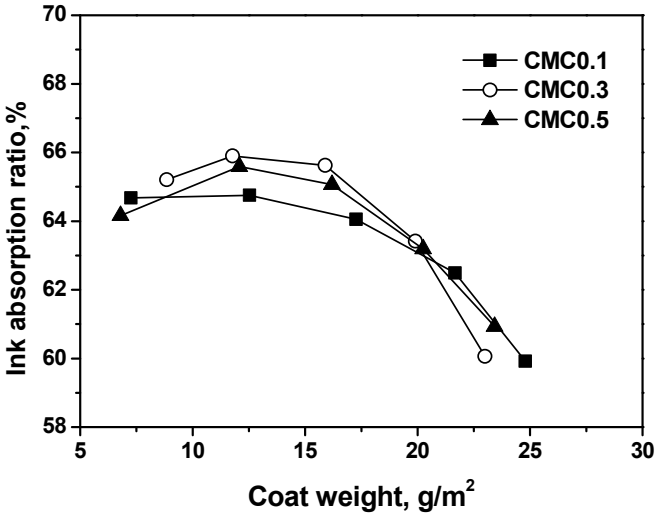

Fig. 4-7. Ink absorption ratio of coated paper depending on CMC (latex content: 12 pph).

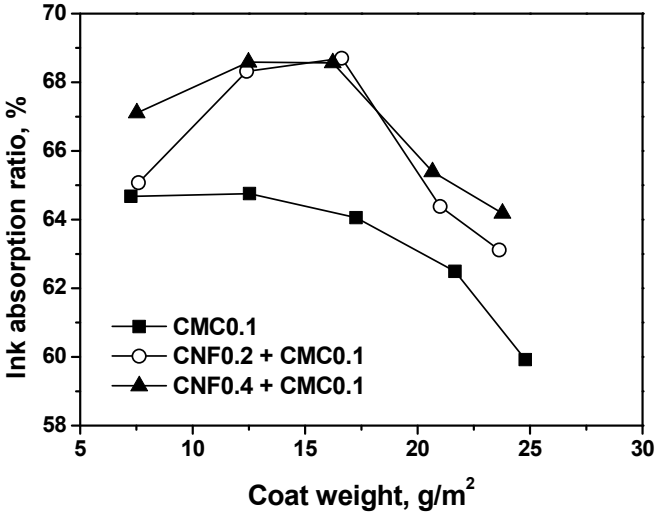

Fig. 4-8. Ink absorption ratio of coated paper depending on CNF (latex content: 12 pph).

3.3 Absorption uniformity of coated paper

The scanned images after printing with the red ink on a RI printing tester are shown in Fig. 4-9. Printing with red ink was made 5 or 10 second after of the vehicle application. During this time, the applied vehicle penetrates into the coating layer. If there was not enough void structure in the coating layer to absorb the applied vehicle, incomplete absorption left some vehicle on the coating surface, which would interfere the transfer of printing ink. The transferred ink density increased with an increase of absorption time from 5 to 10 sec. This indicated that more ink was transferred from the second roll to the surface of coated paper because increased absorption time increased the vehicle penetration into the coating layer and decreased the repellency of the printing ink. If the vehicle substituted with another ink, this experiment mimics the trapping of the ink onto the inked surface.

The cross-sectional images after the vehicle absorption test are shown in Fig. 4-10 (coat weight: 15 g/m^2). The thicknesses of the vehicle and ink layer were different depending on the absorption time. The average thickness of the vehicle layer decreased, while the thickness of the ink layer increased with an increase of the absorption time. The increase of absorption time from 5 to 10 sec gave thinner vehicle layer and much thicker ink layer.

Fig. 4-10 indicated that most film splitting in 2nd printing nip occurred in the ink layer. The amount of the transferred ink from 2nd printing nip depended on

the absorption of the vehicle layer. The white areas that were shown in Fig. 4-9 were inferred that the ink was not transferred because of low absorption rate of the vehicle in this area. Thus, the difference of the color density was caused by the degree of the vehicle absorption rate of the coated paper.

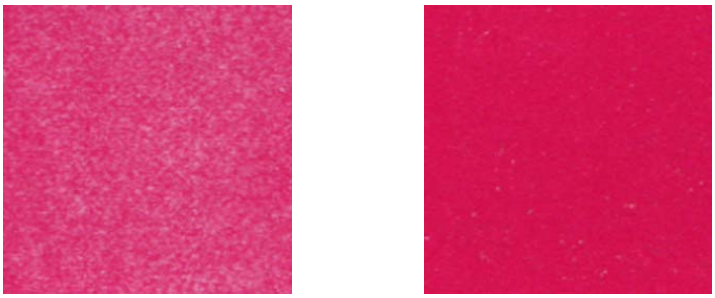

Fig. 4-9. Image after vehicle absorption. (a): 5 sec and (b): 10 sec between 1st and 2nd roll.

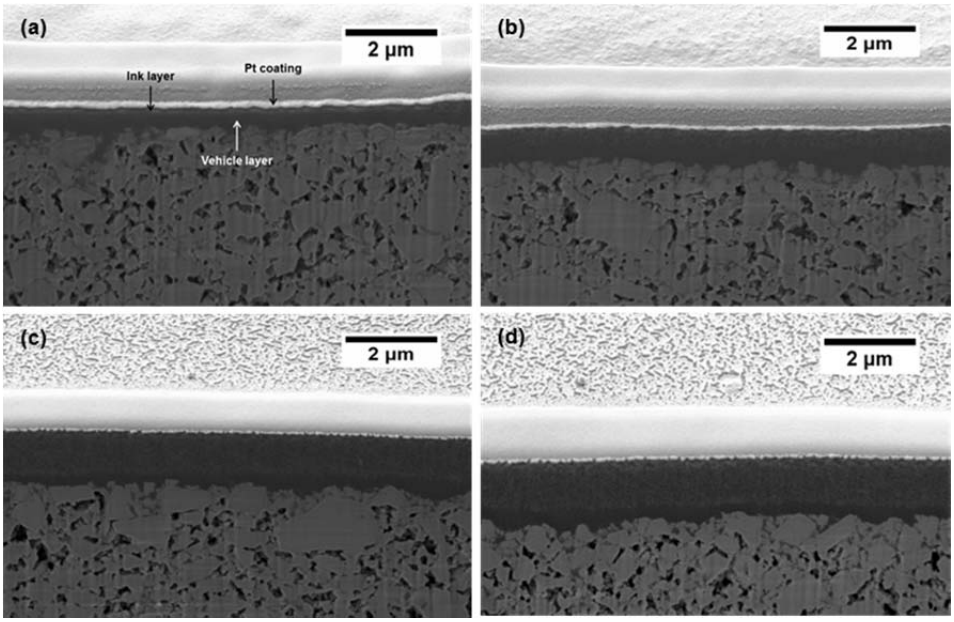

Fig. 4-10. Cross-sectional image of coated paper after vehicle absorption test. (a), (b): 5 sec and (c), (d): 10 sec between 1st and 2nd roll.

The mottle index of the coated paper by the absorption time was presented in Fig. 4-11 and 4-12. The scanned images after the vehicle absorption test were shown in Fig. 4-13 and 4-14. A trend toward the increase in the mottle index was observed with an increase of the coat weight. In general, the mottle of coated paper is improved with an increase of the coat weight due to higher coverage of the coating layer. In this study, however, the trend of the mottle index exhibited opposite results because this method maximized the ink density by the absorption rate of the vehicle layer. Therefore, to apply this method, the mottle index of the sample has to be compared in similar coat weight.

The mottle index was clearly reduced with an increase of the absorption time. The more ink was transferred from 2nd roll to the surface of the vehicle layer because the consolidation of the vehicle was accelerated with an increase of the time. The increase of CMC content in 12.0 and 16.5 g/m^2 of coat weight decreased the mottle index; however, the mottle index was similar regardless of the CMC content in 24.0 g/m^2 of the coat weight when the absorption time was 5 sec.

The replacement of CMC with CNF further decreased the mottle index because the CNF coating led to faster consolidation than the CMC coating. The higher ink density in the CNF coating than in the CMC coating can be confirmed in Fig. 4-13 and 4-14.

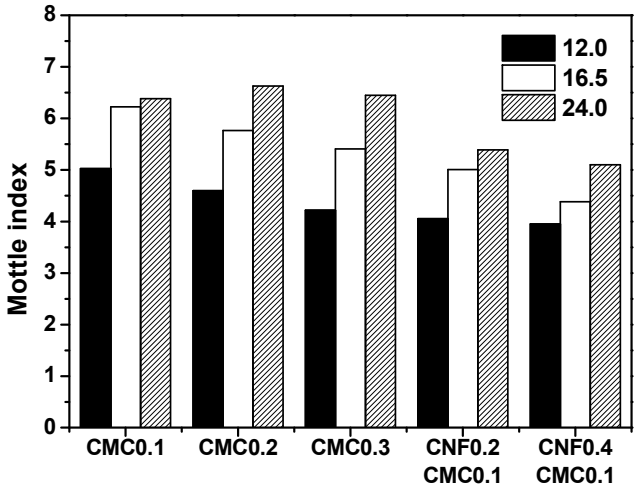

Fig. 4-11. Mottle index after vehicle absorption test (5 sec between 1st and 2nd roll).

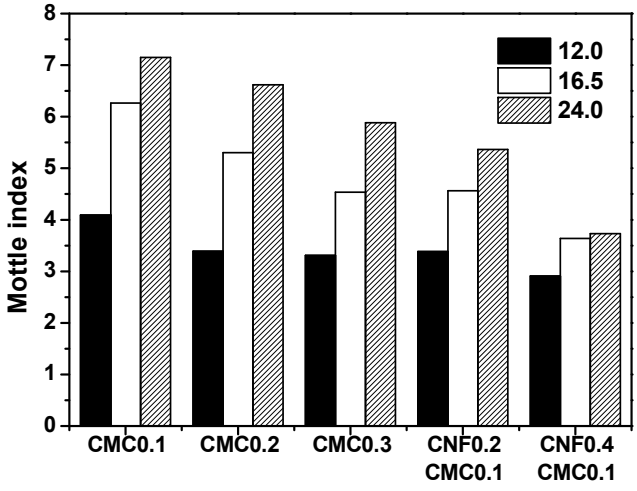

Fig. 4-12. Mottle index after vehicle absorption test (10 sec between 1st and 2nd roll).

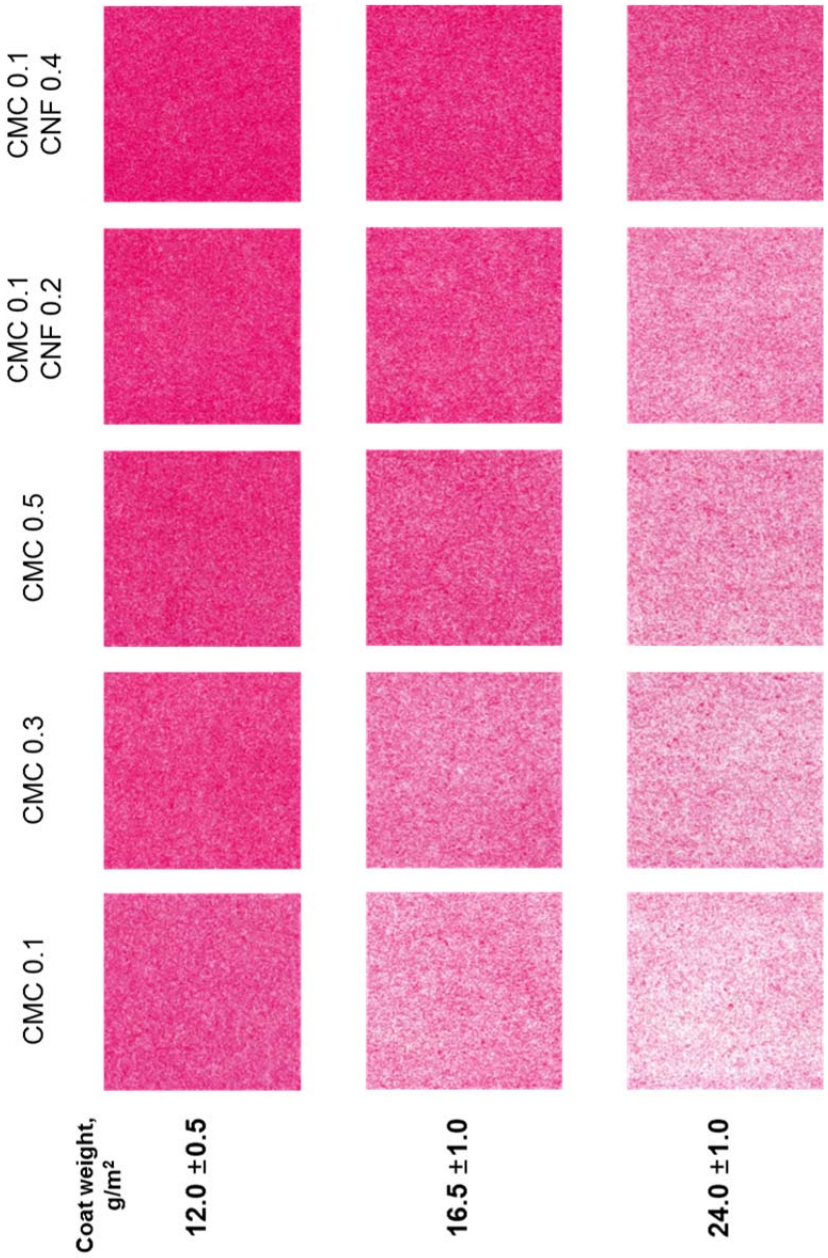

Fig. 4-13. Surface image after vehicle absorption test (5 sec between 1st and 2nd roll, image size : 0.5 in × 0.5 in).

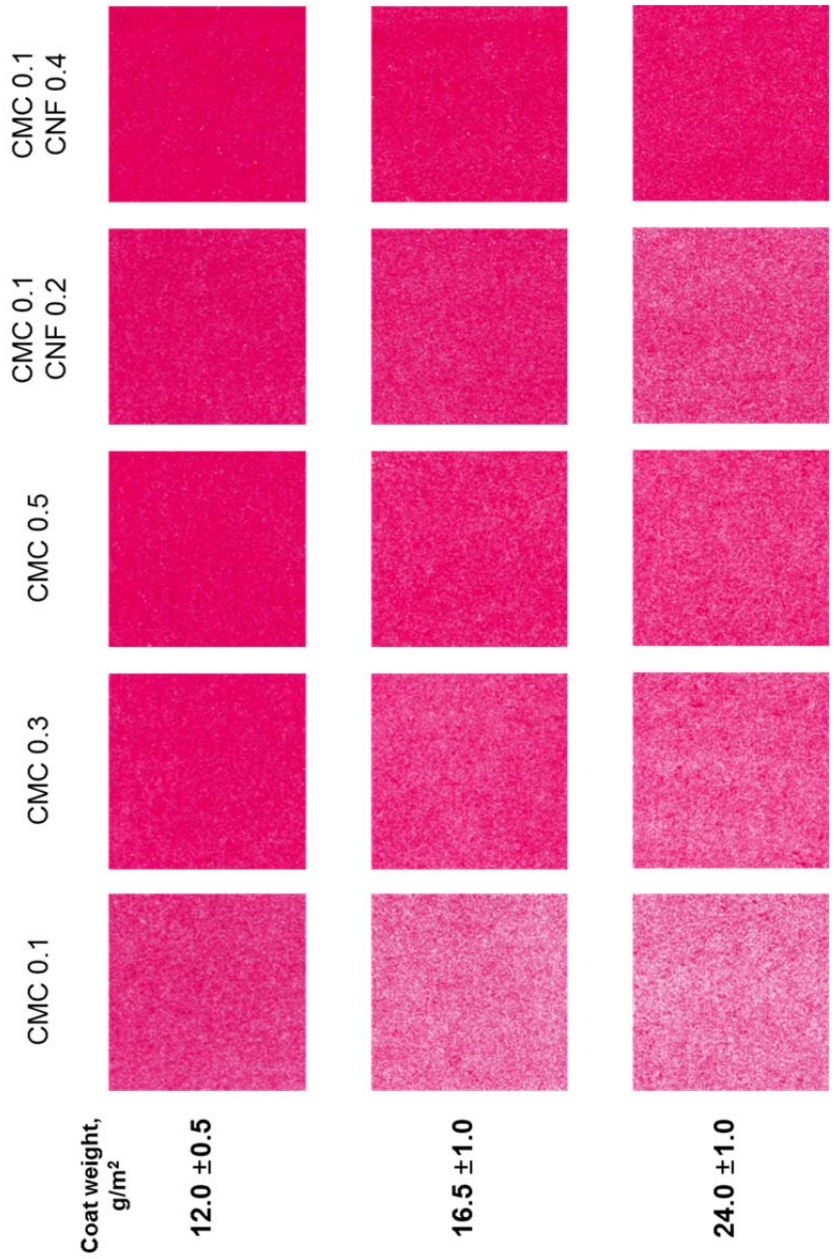

Fig. 4-14. Surface image after vehicle absorption test (10 sec between 1st and 2nd roll, image size : 0.5 in × 0.5 in).

3.4 Surface characteristics of coated paper

The surface of the coated paper before and after calendaring was shown in Fig. 4-15 and 4-16. Closed areas that were sealed by the latex particle were observed before the calendaring when 0.1 pph of CMC was used (Fig. 4-15(b)). Coarser surface of the coated paper was shown in CMC 0.5 compared to CMC 0.1 (Fig. 4-15(c) and (d)). When CNF was used, the carters that were developed by the collapsing of CNF were also shown in Fig. 4-15(f).

Most closed areas were introduced by the calendaring because the locally low coat weight region was compressed more than high coat weight region (Fig. 4-16). The result was in close agreement with that of Chinga and Helle (2003). The closed areas were observed in all coating conditions; however, the areas were rare in CMC 0.5.

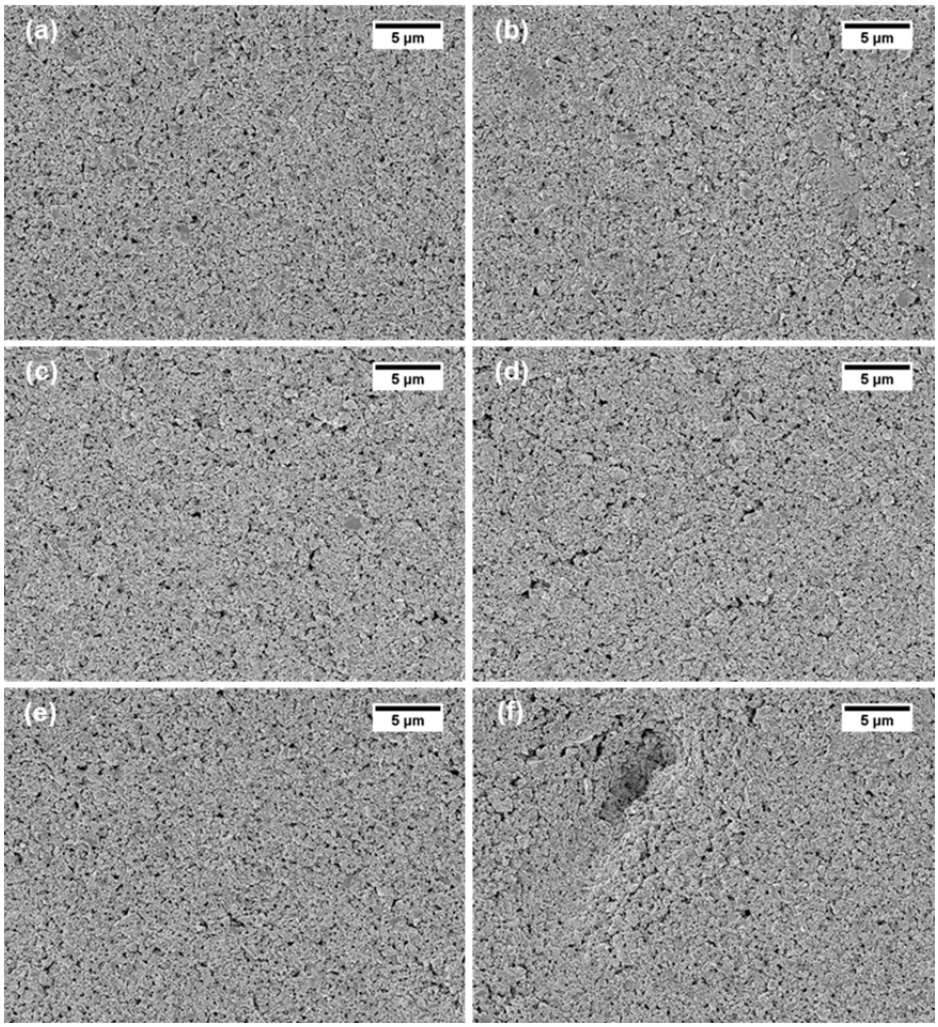

Fig. 4-15. FE-SEM images of coated paper before calendering. (a), (b): CMC 0.1, (c), (d): CMC 0.5 and (e), (f): CNF 0.4-CMC 0.1.

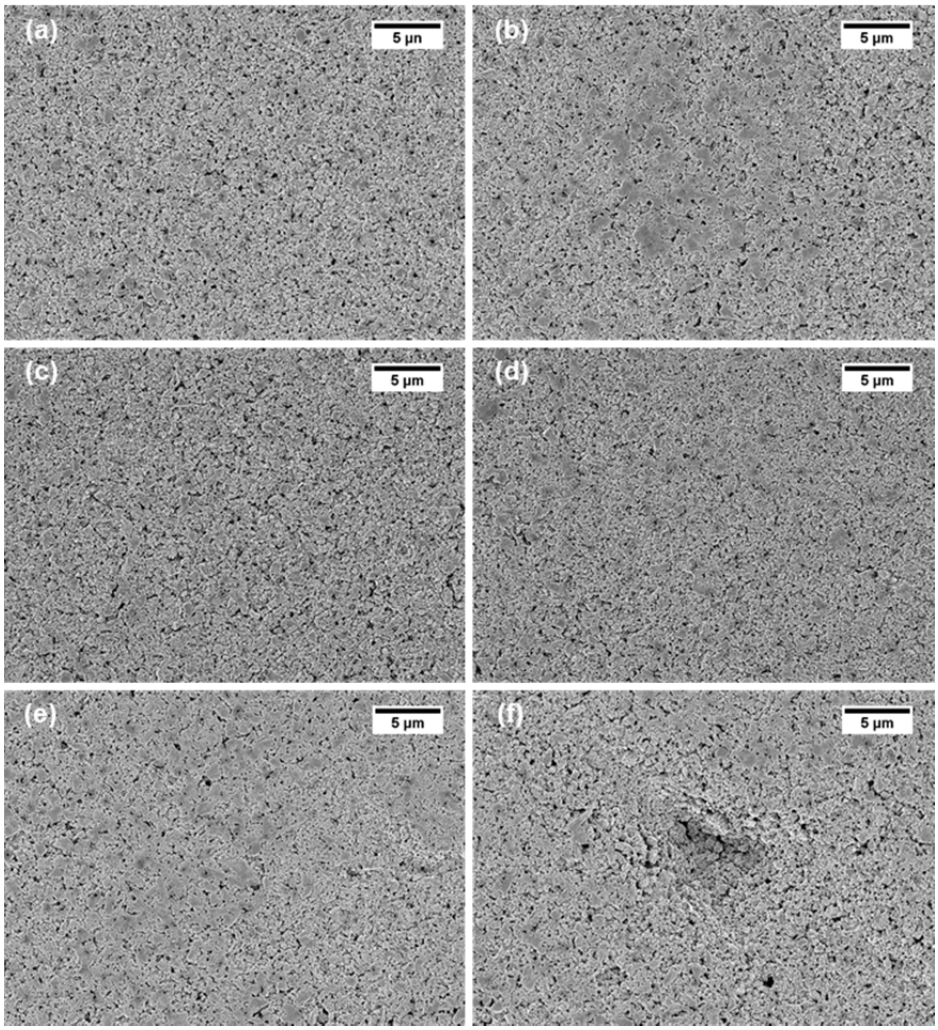

Fig. 4-16. FE-SEM images of coated paper after calendering. (a), (b): CMC 0.1, (c), (d): CMC 0.5 and (e), (f): CNF 0.4-CMC 0.1.

The surface profile in the cross-sectional image was shown in Fig. 4-17. The addition of CMC and CNF made the coating surface rough by forming shallow and deep pores. More rough surface and deep pores were shown in increased CMC and CNF addition level. Thus, the consolidation of the vehicle layer was accelerated and the color density was increased by an addition of CMC and CNF.

The CNF coating showed much faster consolidation of vehicle layer than the CMC coating at the same additive content in similar coat weight (Fig 4-13 and 4-14). In the CNF coating, many deep pores, which accelerated the consolidation of the vehicle, were shown compared to the CMC coating.

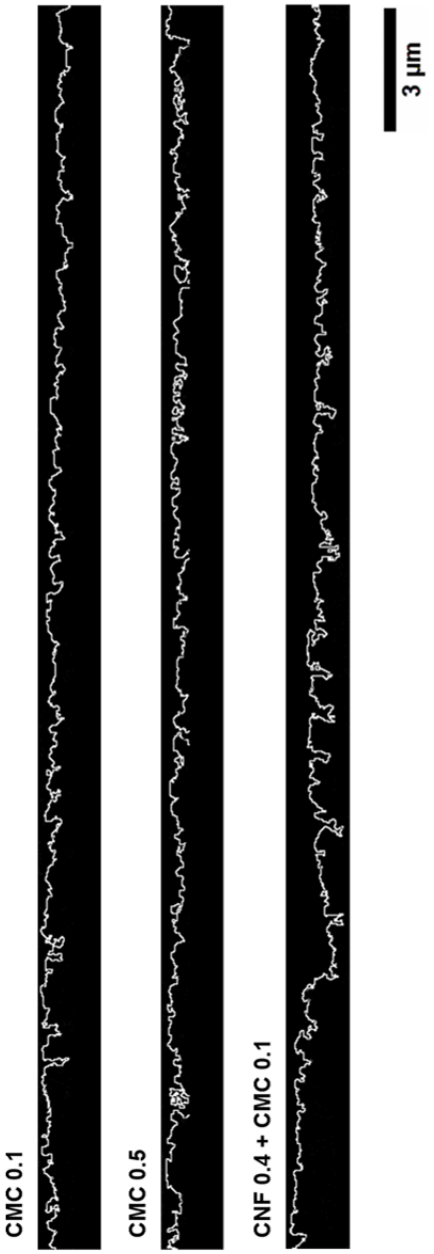

Fig. 4-17. Surface profile in cross-sectional images.

3.5 Double-coated paper

In this part, to overcome the defects in coating layer containing CNF, coat weight was controlled to minimize the non-uniform shrinkage, and high shear coating was applied to collapse the gel-like structure of CNF. Dimic et al. (2013) reported that the gel structure of CNF was collapsed in high shear rate condition (> 1000 s^{-1}).

The properties of the coating color that were used to manufacture the coated paper were given in Table 4-4. The trend of the low shear viscosity and dewatering amount were similar to that of previous results in Chapter 2. The gloss and roughness of the double-coated paper were presented in Table 4-5. A slightly decrease in the gloss of the coated paper was shown when CNF was used. The roughness was similar between the thickener conditions. It was identified that the coated paper that was made in high shear rate condition improved the uniformity of the coated paper because the shear rate condition was enough to destroy the gel-like structure of CNF.

Table 4-4. Properties of coating color for top-coating

Coating color properties				
CNF	0	0.1	0.2	0.3
CMC	0.4	0.3	0.2	0.1
Low shear viscosity, cPs	1368	1086	804	618
Dewatering amount, g/m^2	134.3	141.8	167.2	170.1

Table 4-5. Gloss and roughness of double-coated paper

	Before calendaring				After calendaring			
CNF	0	0.1	0.2	0.3	0	0.1	0.2	0.3
CMC	0.4	0.3	0.2	0.1	0.4	0.3	0.2	0.1
Gloss, %	51.6	51.1	50.3	46.3	70.7	70.3	69.5	68.6
Roughness, μm	-	-	-	-	0.76	0.78	0.78	0.77

The mottle index of the double-coated paper was suggested in Table 4-6. In the double-coated paper, the effect of CNF on the absorption rate of the coated paper was also identified (Fig. 4-18). The replacement of CMC with CNF decreased the index by accelerating fast vehicle consolidation. The surface of the double-coated paper was shown in Fig. 4-19. The defected area was still developed in the surface; however, the size was reduced due to breaking down the gel-like structure and uniform distribution of CNF in the high shear rate coating condition.

Table 4-6. Mottle index of double-coated paper

Thickener condition	CNF 0 CMC 0.4	CNF 0.1 CMC 0.3	CNF 0.2 CMC 0.2	CNF 0.3 CMC 0.1
Mottle index	12.1	11.7	10.7	10.3

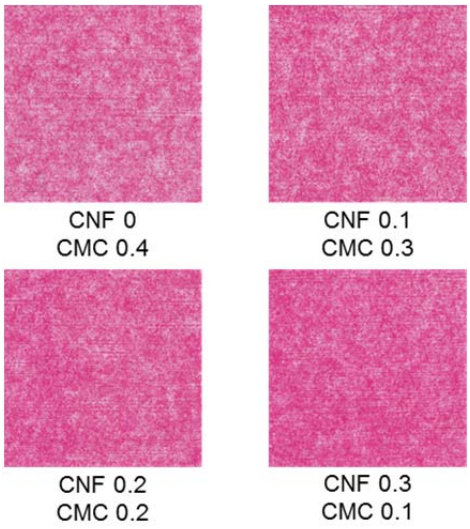

Fig. 4-18. Surface image after vehicle absorption test in double-coated paper (absorption time: 5 sec).

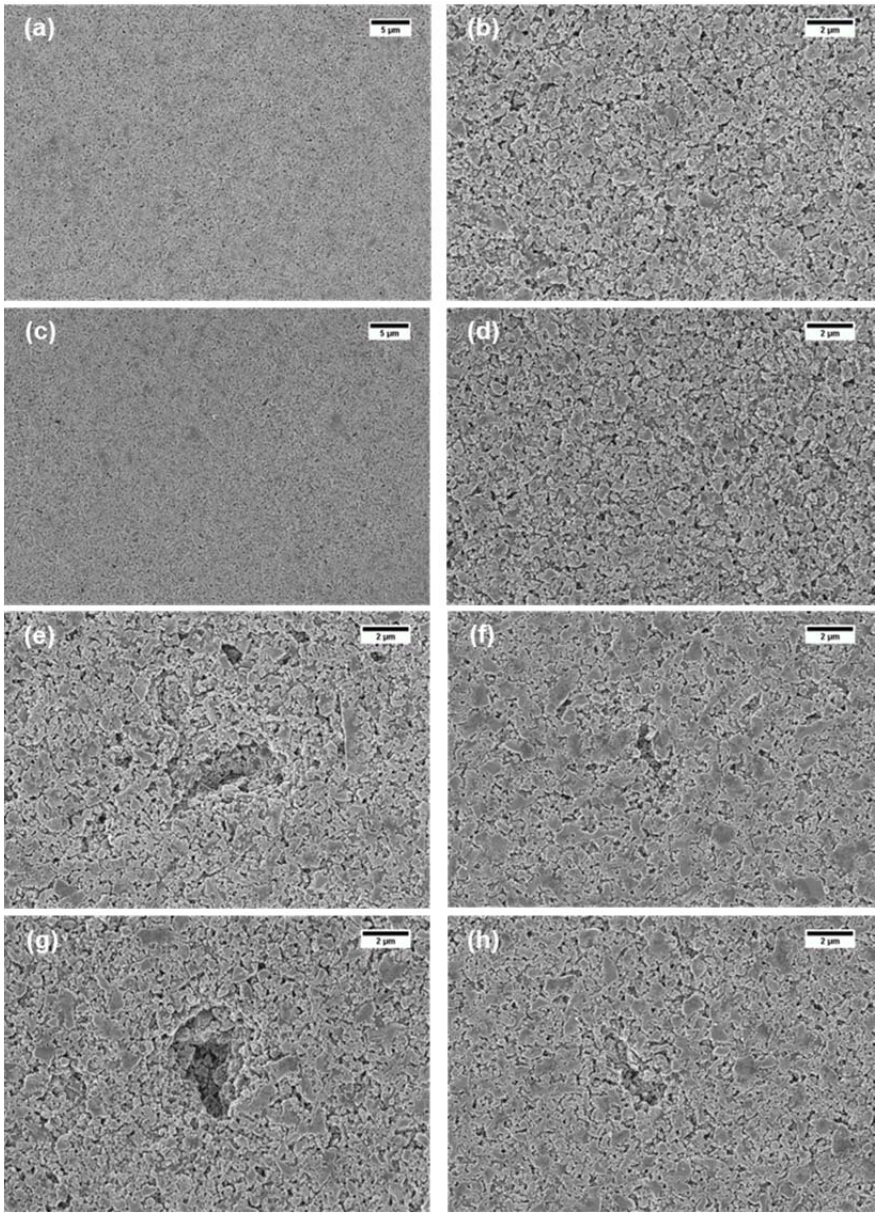

Fig. 4-19. Surface of double-coated paper. (a), (b): CMC0.4, (c), (d): CNF0.2-CMC0.2, (e) - (h): surface defects.

4. Summary

The effect of CMC and CNF on coated paper was investigated. The gloss, roughness, and ink absorption characteristics were evaluated. Increasing the coat weight improved the coverage of the base paper, which decreased the roughness and increased the gloss of the coated paper when using CMC coatings. However, when CNF was used, increasing the coat weight did not lead to improving the gloss because of the rough coating surface. The absorption rate of coated paper was improved by adding CMC and CNF. The absorption rate was faster in coated paper containing CNF than in those containing CMC due to the rough and deep pores of CNF coating. However, there were many defects introduced by the addition of CNF due to the gel-like structure of CNF.

The coated paper that was manufactured under high shear coating conditions diminished the defects of the coating layer by collapsing the gel-like structure of CNF. Even though CNF content increased, the gloss and roughness of the coated paper were similar. The ink absorption rate and uniformity of the coated paper improved by the addition of CNF

Chapter 5

Overall Conclusions

In this study, the rheological properties of coating color, drying kinetics, drying stress, structure of CNF coating layer, and its application on coated paper were investigated. CNF affected the rheological properties of coating color through a different mechanism than CMC. CMC flocculated the coating components, resulting in higher viscosity and elastic component. CNF formed a gel-like structure and showed lower viscosity and elastic component than CMC.

Particle diffusion was decreased by adding CMC because CMC behaves as a solute, increasing the viscosity of the aqueous phase. The small molecular size of CMC flocculated the particles. The initial particle diffusion was much higher in the CNF coating than in the CMC coating because CNF did not influence the viscosity of the aqueous phase and flocculate the particles. The different effects on the aqueous phase by CMC and CNF changed the water retention of the coating color. Increasing the viscosity of the aqueous phase reduced the dewatering of the coating color even though a porous filter cake was formed by CMC. CNF made the filter cake porous as well as CMC; however, it did not affect the viscosity of the aqueous phase.

The CMC coating reached the solidification point faster than the CNF coating because the structured CMC coating formed a loosely packed structure, which results in forming a porous coating layer. The porosity of the CNF coating also increased. The porous coating layer was formed by the voluminous characteristics of CNF even though the CNF coating can form a

closely packed structure.

The stress development in the coating layer was measured using the beam deflection method to investigate the level of drying stress and shrinkage of the coating layer. The drying stress of the coating layer increased with time in all coating formulations. Flocculation in the CMC coating increased the shrinkage of the coating layer after the solidification point. In addition, the precipitated CMC that formed the film in the CMC-rich region contracted during drying, which caused additional increase in stress. The less structured the CNF coating decreased the shrinkage relative to the CMC coating. Furthermore, the low shrinkage characteristics of cellulose in the longitudinal direction decreased tensile stress development in the coating layer.

The latex content changed the stress development during drying. The increase of the latex fraction increased the drying stress by increasing the volume fraction of solids, which led to a faster solidification point. This resulted in the increase of shrinkage from the solidification point to the dried film. Furthermore, the film formed by the coalescence of latex particles increased the drying stress.

CMC and CNF changed the gloss and defects of the coating layer. The decrease in gloss of the coating layer was much higher in CNF coating than in CMC coating because CNF was dried at the end of the drying process. The water absorbing ability of CNF showed slower water loss than other materials

such as GCC, latex, and CMC. The increased latex content decreased the gloss of the coating layer due to the increase of shrinkage. The surface defects in CMC and CNF coatings were different. Small and large cracks were seen in the CMC coating due to the high drying stress during drying. Craters were seen in the CNF coating due to collapse of the coating layer above CNF, not because of the drying stress.

The properties of coated paper such as gloss, roughness, absorption rate, and surface characteristics were evaluated to investigate the effect of CMC and CNF. All thickener conditions showed that increasing the coat weight decreased the roughness of the coated paper; however, the gloss of coated paper was not improved in all conditions. Even though the coat weight was increased, the gloss of coated paper containing CNF reduced. The water absorbing properties of CNF introduced local non-uniform shrinkage of the coating layer.

The absorption characteristics of coated paper were evaluated by the ink absorption test and the modified Vandercook press test by controlling the absorption time. According to the ink absorption test, the absorption ratio of the coated paper increased with the addition of CMC and CNF. CNF had a greater effect on ink absorption and showed a higher absorption ratio than CMC. The results agreed with the modified Vandercook press test that is designed to evaluate the short time absorption rate.

Coating defects that developed due to the collapsing CNF were seen in the coated paper. To diminish the defects, the coated paper was manufactured at high shear rate by changing the coating method. The size of defects reduced and the gloss and roughness were similar. The ink absorption rate and uniformity also increased by introducing CNF.

The effect of CNF on the coating color, drying process, and coating layer qualities was investigated compared to CMC. It is of great interest to use CNF as an additive because it affected the coating color and coating layer through a different mechanism than CMC. The small amount of CNF addition made the coating layer porous, which increased the absorption rate of the coated paper without changing the material properties.

References

Al-Turaif, H. and Lepoutre, P., Evolution of surface structure and chemistry of pigmented coatings during drying, Prog Org Coat 38(1): 43-52 (2000).

Al-Turaif, H. and Bousfield, D.W., The influence of pigment size distribution and morphology on coating binder migration, Nord Pulp Pap Res J 20(3): 335-339 (2005).

Brun, A., Dihang, H. and Brunel, L., Film formation of coatings studied by diffusing-wave spectroscopy, Prog Org Coat 61(2-4): 181-191 (2008).

Brunel, L., Brun, A., Snabre, P. and Cipelletti, L., Adaptive speckle imaging interferometry: a new technique for the analysis of microstructure dynamics, drying processes and coating formulation, Opt Express 15(23): 15250-15259 (2007).

Bruun, S.E., Papermaking Science and Technology, Lehtinen, E., Book 11, Fapet Oy, Filand, pp 240-290 (2000).

Chinga, G. and Helle, T., Relationship between the coating surface structural variation and print quality, J Pulp Pap Sci 29(6): 179-184 (2003).

Chiu, R.C., Garino, T.J. and Cima, M.J., Drying of granular ceramic films: 1, Effect of processing variables on cracking behavior, J Am Ceram Soc 76(9): 2257-2264 (1993).

Chiu, R.C. and Cima, M.J., Drying of granular ceramic films: 2, drying stress and saturation uniformity, J Am Ceram Soc 76(11): 2769-2777 (1993).

Choi, E.H., Kim, C.H., Youn, H.J. and Lee, H.L., Influence of PVA and CMC on the properties of pigment coating colors and their effects on curtain stability, Bioresources 10(4): 7188-7202 (2015).

Chonde, Y., Roper, J. and Salminen, P., A review of wet coating structure: pigment/latex/cobinder interaction and its impact on rheology and runability, TAPPI Coating fundamental symposium preceeding, TAPPI press (1995).

Dimic-Misic, K., Gane, P.A.C. and Paltakari, J., Micro and nanofibrillated cellulose as a rheology modifier additive in CMC-containing pigment-coating formulations, Ing Eng Chem Res 52(45): 16066-16083 (2013).

Dimic-Misic, K., Ridgway, C., Maloney, T., Paltakari, J. and Gane, P., Influence of pore structure of micro/nanofibrillar cellulose in pigmented coating formulations, Transp Porous Media 103(2): 155-179 (2014).

Du, Y., Zang, Y-H. and Sun, J., The effects of water soluble polymers on paper coating consolidation, Prog Org Coat 77(4): 908-912 (2014).

Durand, M., Molinier, V., Feron, T. and Aubry, J.M., Iossorbide mono- and di-alkyl ethers, a new class of sustainable coalescents for water-borne paints, Prog Org Coat 69(4): 344-351 (2010).

Engström, G., Forming and consolidation of coating layers and their impact on coating and print uniformity – an overview, Second International Papermaking and Environment Conference (2008).

Engström, G., Ström, G. and Norrdahl, P., Studies of the drying process and its effect on binder migration and offset mottle, Tappi J 70(12):45-53 (1987).

Fadat, G., Engström, G. and Rigdahl, M., The effect of dissolved polymers on the rheological properties of coating colours, Rheol Acta 27(3): 289-297 (1988).

Gane, P.A.C., Salo, M., Kettle, J.P. and Ridgway, C.J., Comparison of young-laplace pore size and microscopic void area distributions in topologically similar structures: a new method for characterizing connectivity in pigmented coatings, J Mater Sci 44(2): 422-432 (2009).

Grön, J., Papermaking Science and Technology, Lehtinen, E., Book 11, Fapet Oy, Filand, pp 692-724 (2000).

Groves, R., Penson, J.E. and Ruggles, C., Styrene-butadiene latex binders and coating structure, TAPPI Coating Conference: 187-205 (1993).

Guo, J.J. and Lewis, J.A., Aggregation effects on the compressive flow properties and drying behavior of colloidal silica suspensions, J Am Ceram Soc 82(9): 2345-2358 (1999).

Hagen, K.G., Using infrared radiation to dry coating, Tappi J 72(5): 77-82 (1989).

Hemar, Y. and Pinder, D.N., DWS microrheology of a linear polysaccharide, Biomacromolecules 7(3): 674-676 (2006).

Hiorns, T. and Nesbitt, T., Particle packing of blocky and platy pigments – a comparison of computer simulations and experimental results, TAPPI Advanced Coating Fundamental Symposium proceeding, TAPPI press (2003).

Husband, J., Adsorption and rheological studies of sodium carboxymethyl cellulose onto kaolin: effect of degree of substitution, Colloids Surf A 134(3): 349-358 (1998).

Jason, A.P., Stress evolution in solidifying coating, A thesis for the degree of Ph.D, The University of Minnesota (1998).

Kiennemann, J., Chartier, T., Pagnoux, C., Baumard, J.F., Huger, M. and Lamerant, J.M., Drying mechanisms and stress development in aqueous alumina tape casting, J Eur Ceram Soc 25(9): 1551-1564 (2005).

Kim, C.K. and Lee, Y.K., Studies on the pore of coating layer and printability – Effect if pigment shape on pore of coating layer, KTAAPI 33(1):53-61 (2001).

Kim, S., Sung, J.H., Chun, S., Ahn, K.H. and Lee, S.J., Adsorption-stress relationship in drying of silica/PVA suspensions, J Colloid Interface Sci 361(2): 497-502 (2011).

Kim, S., Sung, J.H., Hur, K., Ahn, K.H. and Lee, S.J., The effect of adsorption kinetics on film formation of silica/PVA suspension, J Colloid Interface Sci 344(2): 308-314 (2010).

Kim, S., Sung, J.H., Lim, S. and Ahn, K.H., Drying of the silica/PVA suspension: Effect of suspension microstructure, Langmuir 25(11): 6155-6161 (2009).

Kumar, V., Elfving, A., Koivula, H., Bousfield, D. and Toivakka, M., Roll-to-

roll processed cellulose nanofiber coatings, Ind Eng Chem Res 55(12): 3603-3613 (2016).

Lafon, M.O. and Trannoy, M., Influence of drying temperature on the morphology of latex at the surface of pigment – consequences on the paper properties, TAPPI Advanced Coating Fundamentals Symposium proceeding, TAPPI press (2006).

Larrondo, L.E. and Lepoutre, P., Approaches for characterizing interactions in paper coating suspensions, J Colloid Interface Sci 152(1): 33-40 (1992).

Larsson, M., Vidal, D., Engström, G. and Zou, X., Paper coating properties as affected by pigment blending and calendaring, Tappi J 6(8):16-22 (2007).

Larsson, M., Vidal, D., Engström, G. and Zou, X., Impact of calendaring on coating structure, Nord Pulp Pap Res J 22(2):267-274 (2007)

Laudone, G.M., Matthews, G.P. and Gane, P.A.C., Observation of shrinkage during evaporative drying of water-based paper coatings, Ind Eng Chem Res 43(3): 712-719 (2004).

Lee, H.L., Coating structure and ink absorption properties of coated papers affected by coating formulation – Coating structure, KTAAPI 24(1):5-18 (1992).

Lee, H.L., A controlling factor in light scattering coefficient of the coating layer, KTAAPI 26(2):36-43 (1994a).

Lee, H.L., FCC and structuring characteristics of coating pigment blends, KTAPPI 26(4):25-32 (1994b).

Lee, H.L., Shin, D-S. and Che, D-L., Development of paper coating technologies to prevent print mottle – analysis of coating structure and shrinkage behavior of coating layer during drying by critical solids concentration measurement, KTAAPI 27(3):34-41 (1995).

Lee, H.L., Print mottle : causes and solutions from paper coating industry perspective, KTAPPI 40(5): 60-69 (2008).

Lee, H.L., Shin, D.S and Chung, J.K., Development of paper coating technologies to prevent print mottle (Ⅲ) – Evaluation of ink absorption properties of coated papers and prediction of print mottle, KTAPPI 29(3):60-68 (1997).

Lee, J.Y., Hwang, J.W., Jung, H.W., Kim, S.H., Lee, S.J., Yoon, K. and Weitz, D.A., Fast dynamics and relaxation of colloidal drops during the drying process using multispeckle diffusing wave spectroscopy, Langmuir 29(3): 861-866 (2013).

Lepoutre, P., The structure of paper coatings: an update, Prog Org Coat 17(2): 89-106 (1989).

Letzelter, P. and Eklund, D., Coating color dewatering in blade coaters, Tappi J 76(5): 63-68 (1993).

Lewis, J.A., Blackman, K.A., Ogden, A.L., Payne, J.A. and Francis, L.F., Rheological property and stress development during drying of tape-cast ceramic layers, J Am Ceram Soc 79(12): 3225-3234 (1996).

Lim, S., Kim, S., Ahn, K.H. and Lee, S.J., Stress development of Li-ion battery anode slurries during the drying process, Ind Eng Chem Res 54(23): 6146-6155 (2015).

Martinez, C.J. and Lewis, J.A., Shape evolution and stress development during latex-silica film formation, Langmuir 18(12): 4689-4698 (2002).

McCoy, J.W., Metallographic preparation of coated papers for backscattered electron imaging of coating structure in cross-section, TAPPI Coating/Papermakers conference proceeding, TAPPI press (1998).

McGenity, P., Gane, P., Husband, J. and Engley, M., Effects of interaction between coating color components and rheology, water retention and runability, TAPPI Coating Conference: 133-152 (1992).

Narita, T., Mayumi, K., Ducouret, G. and Hebraud, P., Viscoelastic properties of poly(vinyl alcohol) hydrogels having permanent and transient cross-links studied by microrheology, classical rheometry, and dynamic light scattering, Macromolecules 46(10): 4174-4183 (2013).

Nazari, B. and Bousfield, D.W., Cellulose nanofibers influence on properties and processing of paperboard coatings, Nord Pulp Pap Res J 31(3): 511-520 (2016).

Ozaki, Y., Bousfield, D.W. and Shaler, S.M., Characterization of coating layer structural and chemical uniformity for samples with backtrap mottle, Nord Pulp Pap Res J 23(1): 8-13 (2008).

Pan, S.X., Davis, H.T. and Scriven, L.E., Substrate effects on binder migration in drying porous coatings, TAPPI Coating Conference proceeding, TAPPI press (1996).

Persson, T., Järnström, L. and Rigdahl, M., Effect of method of preparation of coating colors on the rheological behavior and properties of coating layer and coated paper, Tappi J 80(2):117-124 (1997).

Pöhler, T., Juvonen, K. and Sneck. A., Coating layer microstructure and location of binder – results from SEM analysis, TAPPI Advanced Coating Fundamental Symposium proceeding, TAPPI press (2006).

Preston, J.S., Hiorns, A.G., Parsons, D.J. and Heard, P.J., Design of coating structure for flexographic printing, TAPPI Coating & Graphic arts conference proceeding, TAPPI press (2007).

Purfeerst, R.D. and Van Gilder, R.L., Tail-edge picking, back-trap mottle and fountain solution interference of model latex coatings on a six-color press predicted by laboratory tests, TAPPI Coating Conference proceeding, TAPPI press (1991).

Ragnarsson, M., Engström, G. and Järnström, L., Porosity variations in coating layers – impact on back-trap mottle, Nord Pulp Pap Res J 28(2): 257-263 (2013).

Resch, P., Bauer, W. and Hirn, U., Calendering effects on coating pore structure and ink setting behavior, Tappi J 9(1):27-35 (2010).

Ridgway, C.J. and Gane, P.A.C., Effect of latex and pigment volume concentrations on suspension and consolidated particle packing and coating strength, J Pulp Pap Sci 33(2): 1-8 (2007).

Risio, S.D. and Yan, N., Characterizing the pore structures of paper coatings with scanning probe microscopy, Tappi J 5(3): 9-14 (2006).

Roper, J., Papermaking Science and Technology, Lehtinen, E., Book 11, Fapet

Oy, Filand, pp 635-658 (2000).

Ryu, J., Fundamental properties of nanofibrillated cellulose in suspension and mat state, PhD thesis, Seoul National University (2013).

Saito, Y., Matsubayashi, H., Takagishi, Y., Miyamoto, K. and Kataoka, Y., Novel approach to study coating structure, Pan Pacific Pulp and Paper Technology Conference proceeding (1992)

Salo, T., Dimic-Misic, K., Gane, P. and Paltakari, J., Application of pigmented coating colours containing MFC/NFC: Coating properties and link to rheology, Nord Pulp Pap Res J 30(1): 165-178 (2015).

Sandås, S.E. and Salminen, P.J., Pigment-cobinder interactions and their impact on coating rheology, dewatering and performance, Tappi J 74(11):179-187 (1991).

Shen, Y., Bousfield, D.W., Van Heiningen, A. and Donigian, D., Linkage between coating absorption uniformity and print mottle, J Pulp Pap Sci 31(3): 105-108 (2005).

Songok, J., Bousfield, D., Ridgway, C., Gane, P, and Toivakka, M., Drying of porous coating: Influence of coating composition, Ind Eng Chem Res 51(42):13680-13685 (2012).

Vidal, D., Effect of particle size distribution and packing compression on fluid permeability: a comparison of experiments and monte-carlo/lattice-boltzmann simulations, TAPPI Advanced Coating Fundamental Symposium proceeding, TAPPI press (2008).

Watanabe, J. and Lepoutre, P., A mechanism for the consolidation of the structure of clay-latex coatings, J Appl Polym Sci 27(11): 4207-4219 (1982).

Wallström, A. and Järnström, L., The relation between viscoelastic properties of suspensions based on paper coating minerals and structures of the corresponding coating layers, Nord Rheo Conf: 215-218 (2004).

Wedin, P., Lewis, J.A. and Bergstrom, L., Soluble organic additive effects on stress development during drying of calcium carbonate suspensions, J Colloid Interf Sci 290(1): 134-144 (2005).

Wedin, P., Martinez, C.J., Lewis, J.A., Daicic, J. and Bergstrom, L., Stress development during drying of calcium carbonate suspensions containing carboxymethyl cellulose and latex particles, J Colloid Interf Sci 272(1): 1-9 (2004).

Whalen-Shaw, M.W. and Gautam, N., A model for the colloidal and rheological characteristics of clay, latex, CMC formulations, TAPPI Coating conference proceeding, TAPPI press (1995).

Zang, Y-H., Du, J., Du, Y., Wu, Z., Cheng, S. and Liu, Y., The migration of styrene butadiene latex during the drying of coating suspensions: When and how does migration of colloidal particles occur?, Langmuir 26(23): 18331-18339 (2010).

초 록

도공층 구조는 도공지의 광학적 특성 및 인쇄성과 같은 품질을 결정하는 중요한 인자로 도공안료, 바인더 그리고 첨가제 및 도공액 조성에 주로 영향을 받는다. 일반적으로는 도공액 고형분의 대부분을 차지하는 도공안료와 바인더가 도공층 구조를 크게 변화시키지만, 소량의 첨가제 또한 입자간 상호작용 및 도공층 구조에 영향한다. 본 연구는 도공액에 증점효과를 부여할 수 있는 것으로 알려진 셀룰로오스 나노피브릴(CNF)이 도공액 및 도공층 특성에 미치는 영향을 기존에 범용적으로 사용되고 있는 카르복시메틸 셀룰로오스(CMC)와 비교 평가하여 구명하였다.

물을 흡착하여 겔과 같은 형태의 CNF 를 도공액에 첨가 시 CMC 가 사용된 도공액에 비하여 탄성적인 특성이 감소하였는데 이는 CNF 가 도공액 주성분간의 구조형성에 영향하지 않았기 때문이다. 이러한 CNF 의 특성은 도공액의 aqueous phase 의 점도를 상승시키지 않으므로 도공층 건조과정 중 도공안료와 바인더의 움직임이 활발하고 임계지점에서의 고형분이 높으며 조밀하게 팩킹된 도공층 구조를 형성하였다. 반대로 용해된 CMC 는 도공액의 aqueous phase 점도를 상승시키고 주성분간의 응집을 유발하여 입자의 움직임을 크게 제한하였다. 또한 임계지점에 빠르게 도달하여 고형분 함량이 낮았으며 벌키하게 팩킹된 구조를 형성하였다. 즉, CNF 와 CMC 는 서로 다른 메커니즘으로 다공성의 도공층을 형성시켰다. CNF 가 사용된 도공층에서는 CNF 가 물을 흡착하여

큰 부피를 차지함으로써 다공성의 구조를 형성하였으나 CMC 가 사용된 경우 도공액 주성분간의 응집으로 인하여 다공성의 도공층이 형성되었다.

도공층 건조과정에서의 발생되는 응력 또한 CNF 와 CMC 의 사용에 따라 영향받았다. CMC 의 함량이 증가함에 따라 건조응력이 상승하였으나 CNF 가 적용된 경우 건조응력은 감소하였다. CMC 의 경우 입자간의 응집으로 인하여 느슨한 팩킹구조를 형성하기 때문에 임계지점에서 건조필름까지의 도공층 수축이 증가하여 건조응력이 상승하였다. 그러나 CNF 는 CMC 에 비하여 조밀한 팩킹 구조를 형성하여 임계지점에서부터의 도공층의 수축이 감소하고 길이 방향으로 수축률이 낮은 셀룰로오스 자체의 특성으로 인하여 건조응력이 감소하였다.

물을 흡착하는 CNF 는 건조과정 후반부에 수축하여 도공층의 광택을 저하시켰으며 이는 CNF 가 적용된 도공지에도 관찰되었다. 도공량을 줄이고 높은 전단조건에서 도공지를 제작함으로써 CNF 의 적용에 따른 광택저하를 최소화할 수 있었다. 실제 인쇄공정을 모사한 잉크 흡수속도 및 흡수 균일성 평가 결과 CNF 의 사용에 따라 도공지의 흡수속도 및 흡수 균일성이 향상되었으며 이는 수축성이 적은 CNF 가 다공성의 도공층 형성에 기여하였기 때문이다.

주요어 : 공극구조, 건조응력, 잉크흡수, 유변학적 성질, 셀룰로오스 나노피브릴, 카르복시메틸 셀룰로오스

학 번 : 2012-30314